ROLE OF AQUAPORIN-4 WATER CHANNELS IN CEREBRAL EDEMA AFTER
ISCHEMIC STROKE

by

Elton Rodrigues Migliati

A Dissertation Submitted to the Faculty of the

GRADUATE INTERDISCIPLINARY PROGRAM IN PHYSIOLOGICAL SCIENCES

In Partial Fulfillment of the Requirements
For The Degree of

DOCTOR OF PHILOSOPHY

In the Graduate College

THE UNIVERSITY OF ARIZONA

2006

THE UNIVERSITY OF ARIZONA
GRADUATE COLLEGE

As members of the Dissertation Committee, we certify that we have read the dissertation prepared by Elton Rodrigues Migliati
entitled Role of Aquaporin-4 Water Channels in Cerebral Edema after Ischemic Stroke.
and recommend that it be accepted as fulfilling the dissertation requirement for the Degree of Doctor of Philosophy

_____ Date: _____
Andrea J. Yool, Ph.D.

_____ Date: _____
Leslie S. Ritter, Ph.D.

_____ Date: _____
William D. Stamer, Ph.D.

_____ Date: _____
Scott J. Sherman, Ph.D.

_____ Date: _____
Paul F. McDonagh, Ph.D.

Final approval and acceptance of this dissertation is contingent upon the candidate's submission of the final copies of the dissertation to the Graduate College.

I hereby certify that I have read this dissertation prepared under my direction and recommend that it be accepted as fulfilling the dissertation requirement.

_____ Date: _____
Dissertation Director: Andrea J. Yool, Ph.D.
_____ Date: _____
Dissertation Director: Leslie S. Ritter, Ph.D.

STATEMENT BY AUTHOR

This dissertation has been submitted in partial fulfillment of requirements for an advanced degree at the University of Arizona and is deposited in the University Library to be made available to borrowers under rules of the Library.

Brief quotations from this dissertation are allowable without special permission, provided that accurate acknowledgment of source is made. Requests for permission for extended quotation from or reproduction of this manuscript in whole or in part may be granted by the copyright holder.

SIGNED: Elton Rodrigues Migliati

ACKNOWLEDGEMENTS

DEDICATION

This work would never being possible without my wife, Renata. I dedicate this dissertation to her: for her support, encouragement, and for always believing that I could do it; for her true love and for her unconditional friendship. She is the air we hope after a very long dive and the rest we need after a long trip. This work is also dedicated to my son Diogo, who opened a complete new perspective of life.

TABLE OF CONTENTS

TABLE OF CONTENTS-Continued

LIST OF ILLUSTRATIONS

LIST OF ILLUSTRATIONS continued

LIST OF TABLES

LIST OF TABLES continued

ABSTRACT

Stroke is the third leading cause of death and disability in US. Cerebral edema is a major consequence of brain ischemia. Despite the importance of cerebral edema, no effective pharmacological treatments have been developed.

Previous research indicates that the aquaporin-4 channel facilitates water movement during cerebral edema formation. Mice lacking the normal expression of aquaporin-4 have decreased cerebral edema, reduced infarct formation and improved neurological outcome induced for classic models of cerebral edema (**1**, **2**, **3**). To our knowledge, no compounds that effectively block water permeability through aquaporin-4 have been discovered.

My hypothesis is that an aquaporin-4 blocker would significantly decrease the cerebral edema formation after ischemic stroke in mice. My objective was to identify and characterize a novel aquaporin-4 blocker using Xenopus *laevis*. I also proposed that dystrophin deficient mice, a mouse strain that has a decreased expression of aquaporin-4 channels would have a decrease formation of cerebral edema after transient ischemic stroke when compared with a strain matched controls.

I found that bumetanide, a well-described Na^+, K^+, Cl^- cotransporter inhibitor, reversibly and dose dependently inhibited water permeability through aquaporin-4 channels. These results indicated that the protective effect of bumetanide seen in rats after ischemic stroke (**4**) might be through a combined effect on aquaporin-4 channels and the Na^+, K^+, Cl^- cotransporter.

In order to identify the relative amount of protection conferred from the aquaporin-4 channels compared to the Na^+, K^+, Cl^- cotransporter, I characterized the dystrophin deficient mouse after ischemic stroke. I found that dystrophin-deficient mice had a decrease in the formation of cerebral edema after transient brain ischemia when compared with strain-matched controls. Dystrophin-deficient mice had an increased mortality and seizure-like activity after transient brain ischemia. One hypothetical mechanism might be that increased plasma potassium is associated with a presumably decreased ability to buffer potassium after neuronal stimulation, due to its lack of aquaporin-4 and potassium channels ($K_{ir4.1}$) at the end feet of astrocytes. Because of these additional effects, I concluded that the *mdx* mouse is not an ideal model for the study of a protective effect of an aquaporin-4 blocker after ischemic stroke.

CHAPTER 1. INTRODUCTION: AQUAPORIN-4 WATER CHANNELS AS A POSSIBLE TARGET FOR THE TEATMENT OF CEREBRAL EDEMA AFTER ISCHEMIC STROKE.

The brain is the origin of thoughts and action and controls the organism. Hence, it can be considered the most important of all organs (**5**). Although this is a philosophic consideration, the brain might truly be the last frontier in studies of the body's physiology. Great effort has been directed to the understanding of its normal physiology and the mechanisms of cerebral diseases. Ischemic stroke is one of the most important diseases of the central nervous system in modern society. A major consequence of the ischemic stress is the formation of cerebral edema. In the following chapter, we will discuss brain water physiology, pathophysiology of cerebral edema and how a pharmacological inhibition of a key player in cerebral edema, aquaporin-4 water channel, might be an important tool in stroke therapy.

Significance

Stroke is a devastating disease; with a mortality rate near 30%, it is the third leading cause of death in the United States when considered separately from heart disease (**6**, **7**). It affects about 700,000 Americans every year; from the total number of strokes approximately 500,000 are first attacks and 200,000 are recurrent attacks. Either as an underlying cause of death or a contributing factor stroke is associated with 273,000

deaths annually (**5**). About 50% of those deaths occurred out of hospital. The estimated direct cost of stroke for 2006 is 57.9 billion dollars (**8**).

Of all strokes, 88% are ischemic, 9% are intracerebral hemorrhages, and 3% are subarachnoid hemorrhages. Ischemic stroke results from a transient or permanent reduction in cerebral blood flow that is restricted to the territory of a major brain artery. Ischemic stroke is frequently caused by the occlusion of a cerebral artery either by an embolus or by local thrombosis (**7**).

Despite advances in stroke management, the propensity of ischemic brain tissue to develop edema and swelling remains the major cause of death in patients with large infarctions, particularly for those occurring within the middle cerebral artery territory and cerebellum (**9**). The mortality of progressive cerebral edema after middle cerebral artery strokes approaches 80% (**10**). Brain edema is one of the major determinants of whether patients survive beyond the first few hours after stroke (**7**). It must be acknowledged that besides hypothermia, most edema treatments have proven to be of limited value for the majority of patients with massive stroke edema. It is believed that an efficient treatment for cerebral edema will significantly reduce the fatal cases of stroke.

Recent research has suggested that a membrane water channel, aquaporin-4, might be involved in the formation of cerebral edema and an aquaporin-4 blocker would be a beneficial treatment for cerebral edema after ischemic stroke (**1**). To our knowledge, no compounds able to block aquaporin-4 channels have been described previously.

Brain Barriers

Water homeostasis in the mammalian central nervous system is directly influenced by the presence of selectively permeable barriers (**9**). The central nervous system is protected at the interface between blood and tissue by three main barrier layers: the endothelium of brain capillaries (blood brain barrier), the epithelia of the choroid plexus and the arachnoid epithelium of the meninges. Early studies on the barriers of the nervous system were conducted almost entirely on in *vivo* and in *situ* preparations (**12**) and later studies introduced by Ferenc Joó utilized methods to isolate cerebral capillaries (**13**) which enabled the examination of the mechanisms responsible for barrier function at the cellular and molecular levels, particularly for the blood-brain barrier (**14**).

The blood brain barrier differs from other capillary beds because it is impermeable to water and water-soluble compounds larger than 500 Daltons. Contrasting the blood brain barrier, all other tissues have a high water and solute flow through spaces between the endothelial cells of blood vessels (paracellular flow), and only plasma proteins and blood cells are large enough to be retained in the vascular space. Paracellular flow occurs in the capillaries of the peripheral circulation because the endothelial cells are not connected by tight junctions; paracellular flow pathway do not exist in the cerebral vascular endothelial cell lining (**15**) because the endothelial cells at the blood brain barrier are connected by tight junctions. As a consequence of the limited paracellular flow during a single passage through the cerebrovascular bed essentially no sodium is exchanged between the blood and the tissue, whereas up to 50% of the sodium leaves the blood during a single passage through muscle capillaries and a similar amount

returns from the interstitial space to the blood (**11**). The major significance of the selective characteristic of the blood brain barrier is the negligible water transport from in the cerebral capillaries.

Blood-Brain Barrier

Paul Ehrlich, in 1885, originally observed an effect consistent with the presence of blood-brain barrier. He noted that water-soluble dyes injected at the peripheral circulation stained all organs but not the central nervous system and spinal cord (**16**). Ehrlich's student, Goldmann, showed that when water-soluble dyes were injected into the cerebrospinal fluid they stained all cell types in the brain but failed to penetrate in the periphery (**16**). Therefore, it was clear that the central nervous system was isolated from the peripheric circulation by what is now know as the blood brain barrier.

Anatomical Description of the Blood-Brain Barrier

Our current understanding of the structure of the blood-brain barrier was built based on the work of Reese, Karnovsky, and Brightman done in the late 1960s (**17**, **18**). Ultrastructural and permeability characteristics of capillaries were studied using horseradish peroxidase (molecular weight 40,000), as an ultrastructural tracer in *vivo*, and colloidal lanthanum as a trace in *vitro*. A tracer is a compound used to reveal the location of cells and transport pathways. Horseradish peroxidase was visualized through electron

microscopy in the mouse brain microcirculation. Continuous capillaries have a sealed epithelium and were named as maculae ("spot") occludentes if permeable to horseradish peroxidase and zonulae ("zone") occludentes if not permeable. Fenestrated capillaries (as their name implies "window") have openings that allow larger molecules to diffuse. The tracers appear to permeate the fenestrated capillaries. The blood-brain barrier is characterized by the presence of tight cell-cell junctions and lack of fenestrations.

The tightness of intercellular junctions of the brain endothelial cells impose a resistance to water filtration generated by hydrostatic or osmotic pressure gradients. The junctional proteins at the blood brain barrier include adherens junctions (**19**), tight junctions (**20**, **21**, **22**), and possibly gap junctions (**23**, **24**, **25**, **26**). Both water filtration through tight junction complexes (paracellular route) and diffusion of water through the lipid bilayer of the endothelial cell membranes (transcellular route) are comparatively small (**27**). The tightness of intercellular junctions of the blood brain barrier expressed by their electrical resistance (R), and defined as Ω/cm^2, is about 1130-2000 Ω/cm^2, whereas in the choroid plexus this value is about 73 Ω/cm^2 (**28**). Pathological conditions that affect the blood brain barrier integrity are responsible for inducing cerebral edema. Ischemic stroke is a good example of a pathological condition that causes cerebral edema and will be the major focus of this work. **Figure 1.1** illustrates the major protein components of endothelial cell junctions and its localization. Together with the endothelial cells, basal lamina, pericytes, astrocytes and neurons are other cellular components of the blood brain barrier.
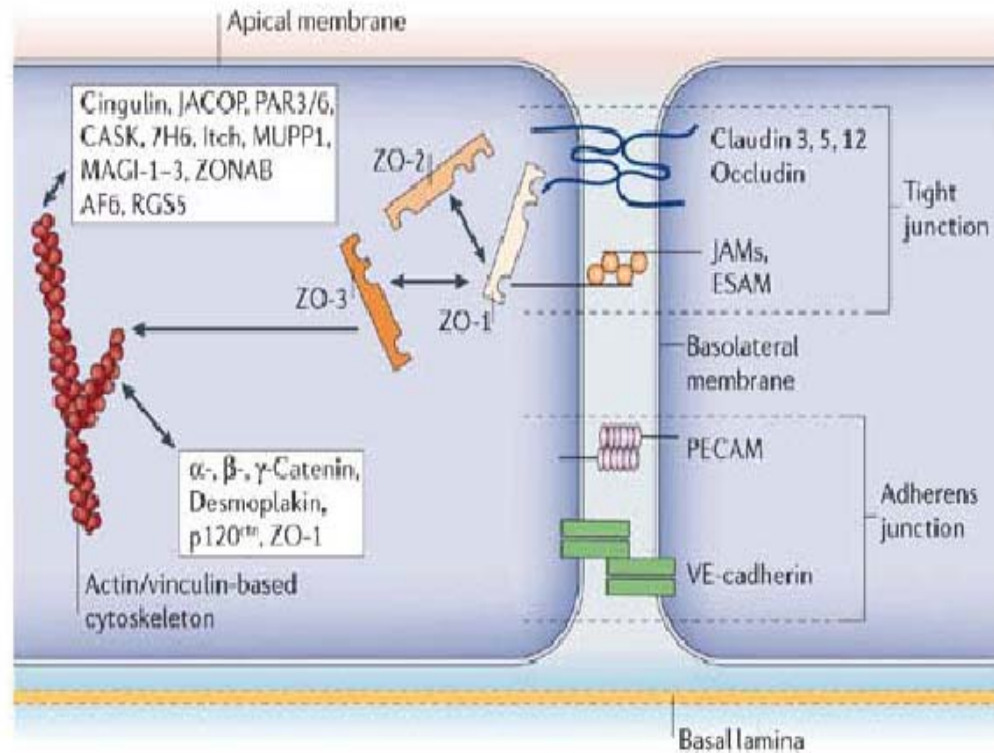
Figure 1.1 SIMPLIFIED AND INCOMPLETE SCHEME SHOWING THE MOLECULAR COMPOSITION OF ENDOTHELIAL TIGHT JUNCTIONS. Occludin and the claudins are the most important membranous components. The junctional adhesion molecules (JAMs) and the endothelial selective adhesion molecule (ESAM) are members of the immunoglobulin superfamily. Within the cytoplasm are many first-order adaptor proteins, including zonula occludens 1, 2 and 3 (ZO-1–3) and Ca2+-dependent serine protein kinase (CASK) that bind to the intramembrane proteins. Among the second-order adaptor molecules, cingulin is important, and junction-associated coiled-coil protein (JACOP) may also be present. Signalling and regulatory proteins include multi-PDZ-protein 1 (MUPP1), the partitioning defective proteins 3 and 6 (PAR3/6), MAGI-1–3 (membrane-associated guanylate kinase), ZO-1-associated nucleic acid-binding protein (ZONAB), afadin (AF6), and regulator of G-protein signalling 5 (RGS5). The most important molecule of endothelial adherens junctions is vascular endothelial cadherin (VE-cadherin). In addition, the platelet–endothelial cell adhesion molecule (PECAM) mediates homophilic adhesion. The chief linker molecules between adherens junctions and the cytoskeleton are the catenins, with desmoplakin and p120 catenin (p120ctn) also involved. Itch, E3 ubiquitin protein ligase (**29).**

Endothelial cells

The endothelial cells are a major component of the blood brain barrier. Their principal characteristic is to form tight connections with neighboring endothelial cells restricting paracellular flow. Four major characteristics distinguish the cerebral capillary endothelial cell from the peripheral endothelial cell: (i) increased mitochondrial content, which is a characteristic of secretory epithelium since ionic transport is sustained by ATP hydrolysis from ion pumps (**30**) and (ii) lack of fenestrations, (iii) minimal pinocytotic activity and (iv) presence of tight junctions, which are characteristic that decrease paracellular and transcellular transport (**31**, **32**, **33**) confers the endothelial cells all necessary tools for a selective water transport property. In the contest of ischemic stroke the understanding of endothelial cells properties and protective mechanisms able to inhibit paracellular pathway water transport are key in the development of future treatments for cerebral edema.

The basal lamina, a membrane 30 to 40-nm thick composed of collagen type IV, heparin sulfate, proteoglicans, laminin, fibronectin, and other extracellular matrix proteins ensheathes both pericytes and endothelial cells (**34**). The basal lamina interacts with the cerebral microvascular endothelium and the disruption of those interactions are strongly associated with increased blood-brain barrier permeability in pathological states (**35**, **36**). The extracellular matrix anchors the endothelium via interaction of laminin and other matrix proteins with endothelial integrin receptors (**37**); these interactions can stimulate a number of intracellular signaling pathways (**38**) that influence the expression of endothelial tight junction proteins (**39**, **40**) and therefore being important in the

maintenance of tight junctions. The disruption of any component of the blood brain barrier might affect blood brain barrier structure and therefore have an impact in cerebral edema formation. Other components, such as astrocytes, are well known to be responsible for blood brain barrier maintenance.

Astrocytes and pericytes

Astrocytes and pericytes are also important cellular components of the barrier. Astrocytes end-feet process surround the endothelial cells and pericytes making an extra layer around the blood brain barrier. Astrocytes are important in generating the full blood–brain barrier phenotype in brain capillaries (**41**, **42**) although underlying mechanisms are being elucidated at the molecular and genomic levels (**43**). Studies of cultured endothelial cells have shown that blood-brain barrier characteristics appear only when the cells are co-cultured with astrocytes (**44**). Pericytes are also present in between the endothelial cells and are divided into granular and filamentous subtypes (**45**). Pericytes are also suspected to be involved in the induction or maintenance of the blood-brain barrier (**46**, **47**). Pericytes express a contractile protein, actin isoform, and are credited to be involved in capillary blood flow regulation, although more research is needed (**48**). Pericytes may also be involved in increasing blood-brain barrier permeability since pericytes migrate away from the blood-brain barrier after hypoxia and trauma (**49**, **50**). It has also been speculated that astrocytes act together with neurons mediating the regulation of cerebral microvascular permeability (**48**).

Another important characteristic of the brain microcirculation is to adapt to regional metabolic need of brain activity by a dynamic and highly responsive change in flow to sustain neuronal metabolism (**51**). Although the cellular mechanisms of this process are not well established, an important role for astrocytes in neurovascular metabolic coupling is recognized. Neurons directly innervate the microvascular endothelium and astrocytic processes, through noradrenergic (**52**, **53**), serotonergic (**54**), cholinergic (**55**, **56**), and GABA-ergic (**57**) neurons, as well as others (**58**). Therefore, it appears that there is an interaction between neurons and the blood-brain barrier to mediated cerebral flow in normal and pathological conditions.

Brain Water Homeostasis

Water crosses cell membranes by several routes: across lipid bilayers, through specific water channels, and via transmembrane proteins usually associated with other functions such as uniports and cotransporters. The involvement of aquaporin channels in brain water transport at the endothelial cell level is still under debate. The presence of aquaporins in endothelial cells remains to be proven although recent research claims the presence of aquaporin-4 in the endothelium cells of the brain microcirculation (**59**).

The brain has unique characteristics for maintaining water homeostasis and those characteristics can be modeled using an equation called the Starling relationship. The Starling relationship can be used to describe water flow from the blood to the parenchyma. In the blood brain barrier, the hydraulic conductivity is affected by the

tightness of the endothelial cells and the expression pattern of the endothelial cellular proteins able to transport water. Water flux (J_{cap}) is determined by the hydrostatic pressure difference between plasma and tissue and the osmotic pressure difference between plasma and tissue multiplied by the hydraulic conductivity (L_{cap}) as described in the following equation (**60**, **61**, **62**).

$$J_{cap} = L_{cap} \left[\{P_{plasma} - P_{tissue}\} - \sigma_{protein} \{\pi_{protein,\ plasma} - \pi_{protein,\ tissue}\} \right] \qquad [1]$$

Where, $P_{plasma} - P_{tissue}$ is the hydrostatic pressure difference between plasma and tissue in mm (Hg), $\pi_{protein,\ plasma} - \pi_{protein,\ tissue}$ is the difference in protein osmotic pressure between plasma and tissue in mm (Hg). L_{cap} is capillary hydraulic conductivity in cm^3sec^{-1}. This will be per gram of tissue when L is expressed g^{-1} or can be for the whole tissue when the g constant is multiplied by the weight of the whole tissue, such as 1500 for a human 1500g brain. Osmotic reflection coefficient, which is a measurement of particles (e.g. salt, proteins) movement from the blood to the tissue, for salt (σ_{salt}) equals 0 at the peripheral capillaries indicating that plasma fluid entering tissue will contain its normal salt content. Osmotic reflection for protein ($\sigma_{protein}$) has a value of 0.93 at peripheral capillaries indicating that about 7% of the plasma protein will leek to the tissue from the vascular bed. Protein flux due to bulk fluid flow ($mg.sec^{-1}$) is directly proportional to J_{cap} (cm^3sec^{-1}) and the albumin concentration ($C_{protein,plasma}$) ($mg.cm^{-3}$)

$$(1 - \sigma_{protein}) = C_{protein,plasma}\ X\ J_{cap} \qquad [2]$$

In the low-pressure end of the capillary bed, the retained proteins are responsible for a net osmotic driving force of fluid from tissue towards the blood and this phenomenon is known as the Starling's relationship. The protein that extravasated to the peripheral tissues determines that a smaller amount of fluid will be retained in the parenchyma. The lymphatics remove this additional extravasated fluid and prevent edema. In the central nervous system, the blood brain barrier effectively prevents the movement of hydrophilic substances, including monovalent cations such as Na^+ and K^+, and proteins. Thus in the brain both σ_{salt} and $\sigma_{protein}$ have a potential contribution to fluid movement, as follows:

$$J_{cap} = L_{cap} \left[\{P_{plasma}-P_{tissue}\} - \sigma_{protein} \{\pi_{protein,\ plasma}-\pi_{protein,\ tissue}\} - \sigma_{salt} \{\pi_{salt,\ plasma}-\pi_{salt,\ tissue}\} \right] [3]$$

Because there is no movement of ions and proteins towards the brain tissue, σ_{salt} and $\sigma_{protein}$ are equal to 1. To allow adequate blood flow arterial blood pressure must be higher than intracranial pressure. So, any movement of water into the central nervous system driven by the blood pressure, is immediately opposed by the osmotic pressure gradient generated by the ions and proteins retained in the vascular lumen and the dilution of the extravascular ions, which are the major constituents of extracellular fluid (**figure 1.2**). When some water is forced into the brain due to the driving force of P_{plasma}-P_{tissue} it dilutes $\pi_{salt,tissue}$ and concentrate $\pi_{salt,plasma}$ that immediately set up an opposing salt

Figure 1.2. SCHEMATIC OVERVIEW OF WATER FLUX. Indicates tha the water flux (J_{cap}) in normal physiological conditions (**Table 1.1**) is very small (upper) and (lower) that water flow cannot be reached with small dilutions of brain extracellular fluid with an intact blood brain barrier. Once the blood brain barrier is dirupted the resulting net increase in brain volume leads to edema and a life threatning rise in intracranial pressure. Essentially σ_{salt} goes to zero and $\sigma_{protein}$ becomes <1. $\sigma_{protein}$ may decrease to the 0.93 value of the capillaries of peripheral tissue or less depending on the degree of the disruption of the blood-brain barrier (**22**). Cerebrospinal fluid (CSF), $\pi_{salt,tissue}$ (tissue salt osmotic pressure), $\pi_{salt, plasma}$ (plasma salt osmotic pressure), $\pi_{pt,plasma}$ (plasma protein osmotic pressure), P_{tissue} (tissue pressure = intracranial pressure), P_{plasma} (capillary pressure), J_{cap} (water flow).

Table1.1 Typical mammalian CSF and plasma concentrations of ions (meq/l) and glucose and proteins (mg/100ml) (22)			
	CSF	Plasma	CSF/Plasma
K⁺	2.8	4.5	0.6
Na⁺	138	138	1.0
Cl⁻	119	102	1.2
HCO₃⁻	22	24	0.9
Ca²⁺	2.1	4.8	0.4
Mg²⁺	2.3	1.7	1.4
PO₄³⁻	0.5	1.8	0.3
Albumin	20	7000	0.003

osmotic driving force to reduce J_{cap} and therefore reduce further movement of water into the central nervous system (**63**). The structure of the blood brain barrier results in a negligible passive water transport under normal physiological conditions from the blood to the brain parenchyma. Based on this evidence it appears that the presence of aquaporin-4 at the endothelial cells are not a contributing factor in water transport since any dilutions in the brain parenchyma would create an counterbalance force inhibiting water movement. It appears that water follows an active ionic transport in endothelial cells; this active transport might be generated by cotransporters.

Brain Endothelial Cell Cotransporters

Several cotransporters that are expressed in the brain (**Table 1.2**) have been found to transport water: the KCC (K^+-Cl^-), the NKCC (Na^+-K^+-Cl^-), the MCT (H^+-lactate), the GAT (Na^+-GABA), and the EAAT (Na^+-glutamate) (**64, 65**). The precise mechanism of water transport in cotransporters is not entirely understood and the mechanism is specific to each cotransporter. Cotransport of water has been demonstrated in a number of physiological phenomena, which cannot be explained by simple osmosis, such as the water transport in small intestine, glandular secretion (secretion of saliva), and the retinal pigment water transport. **Table 1.2** summarizes the principal transporters in the brain and summarizes their major physiological role and localization (**66**). Aquaporin-4 water channels are highly expressed at the end feet of astrocytic cells and might be an important in accommodating excess water that crossed the endothelial cells. Therefore an

aquaporin-4 channels blocker might have a beneficial effect in decreasing the formation

of cerebral edema.

Cotransporter name	Major physiological role	Isoforms	Tissue localization	Co-localization
KCC (K$^+$ and Cl$^-$)	Volume regulation	KCC1-4	• KCC1- brain (undefined) • KCC2- N • KCC3- CP (bl) • KCC4- CN, SC, CP (ap)	Na$^+$/K$^+$ ATPase
Na$^+$/K$^+$/Cl$^-$ symporter	Electroneutral cotransport	NKCC1-2	• NKCC1- most cells, EP bl, CP (ap), RP ap, AC • NKCC2- ascending loop of Henle	
MCT (H$^+$-coupled monocarboxylate)	Glucose substitutes transport	MCT1-4	• MCT1- EP, CP, AC, N, M • MCT2-N, G • MCT3-RP, CP • MCT4- AC	NKCC1
EAAT (Na$^+$-coupled glutamate)	Glutamate reuptake	EAAT1-5	• EAAT1- G • EAAT2- G • EAAT3- N • EAAT4- PK • EAAT5- retina	
GAT (Na$^+$-coupled GABA)	GABA reuptake	GAT1-3 BTG1	• GAT1- N, AC • GAT2- PC, AR • GAT3- N, AC • BGT1- most brain regions	

Table 1.2. BRAIN COTRANSPORTERS: PHYSIOLOGY, LOCALIZATION, NOMENCLATURE AND CO-LOCALIZATION. Table abbreviations: bl (basolateral membrane), ap (apical membrane), CP (choroid plexus), CN (cranial nerves), SC (spinal cord), EP (epithelium), RP (retinal pigment), AC (astrocytes), N (neurons), G (glial cells), M (Muller cells), PK (Purkinje cells), PC (Pia cells), AR (arachnoid membranes) (**11**).

Aquaporin Channels

The existence of a channel pore for water was realized prior to the identification of the protein, based on observations that red blood cells have higher water permeability than would be expected from an equivalent area of bilayer lipid membrane. This hypothesis was confirmed in 1992 by Peter Agre and colleagues with the identification the first member of the aquaporin family of water channels (**67**). Aquaporins are members of the membrane intrinsic protein family of channel-forming proteins. The mammalian aquaporin protein family has more than 11 members (**68**). Aquaporins are transmembrane proteins that assemble as homotetramers (**figure 1.3**). Each individual monomer is formed by six transmembrane domains with intracellular carboxyl (C) and amino (N) terminals.
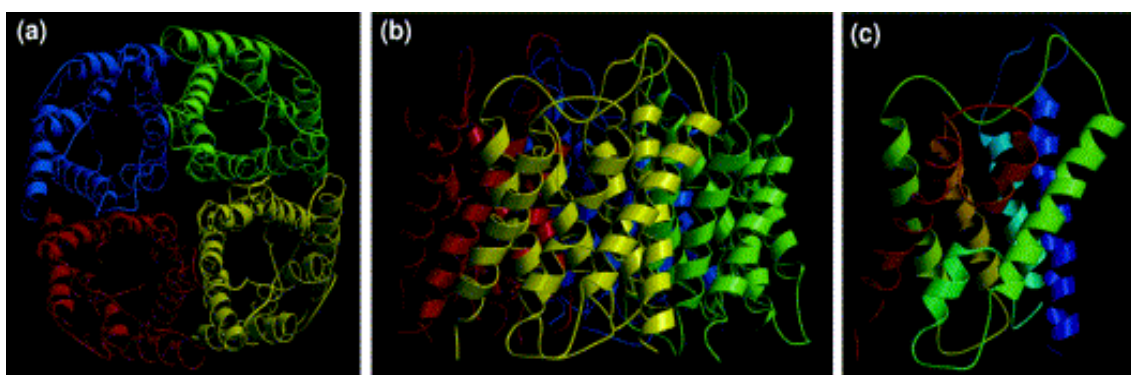
Figure 1.3. AQP1 STRUCTURE. Top-view (a) and side-view (b) of the tetrameric structure of hAQP1, (ref) and a close-up of the monomeric structure (c). The pictures were generated with a modified version of Molscript and Raster3D (**69**).

Aquaporins are divided in two groups based on the carboxy and amino terminal sequence homology (**70**) and function. Aquaporins (aquaporin-0, 1, 2, 4, 5, and 8) are proteins, which transport water; aquaglyceroporins (aquaporin-3, 6, 7, 9, and 10) are channels permeable to glycerol, urea, and other solutes. Aquaporin-4, first isolated in 1994 (**71**), has two methionine initiation sites (M1 and M23), which yield products at 32 and 30kDa respectively. Transport studies found that aquaporin-4 heterologously expressed in *Xenopus laevis* oocytes increased water permeability by 20-fold and was not blocked by $HgCl_2$ even after cysteine substitution to mimic the site that creates mercury-sensitivity in aquaporin-1 (cysteine 189 in loop E), thus aquaporin-4 also is known as the «mercury-insensitive water channel» (**72**). Aquaporin-4 has the highest water permeability followed by aquaporin-1 and 9, 2 and 5, 3 and 10.

Aquaporins have been found to facilitate transmembrane transport of water in a number of organs, such as the kidney, lungs and secretory glands (**73**). Aquaporin-4 channels are found in tissues such as kidneys, lungs, ears, sweat glands, and were one of the first subtypes described in the central nervous system. Aquaporin-4 is concentrated in the astrocyte end-feet membrane adjacent to blood vessels in neocortex and cerebellum by association with alpha-syntrophin protein (**74**). Studies (**71**, **75**, **76**, **77**) have demonstrated the presence of aquaporin-4 in glial limitan, ependymal lining system, cerebellum, hippocampal dentate gyrus, hypothalamus, neocortex, hippocampal areas CA1-CA3, in the nucleus of stria terminalis, medial habenular nucleus, and supraoptic nuclei.

There have been a number of studies showing that aquaporin-4 is member of a signaling protein complex (**78**). In the dystrophin- deficient mouse, dystrophin deficiency leads to severe injury of the endothelial and glial cells with disturbance in alpha-actin cytoskeleton, ZO-1, claudin-1, and aquaporin-4 assembly, as well as blood-brain barrier breakdown (**79**) (**figure 1.4**). Aquaporin-4 is anchored at these membranes by its carboxyl terminus to alpha-syntrophin, an adapter protein associated with dystrophin.
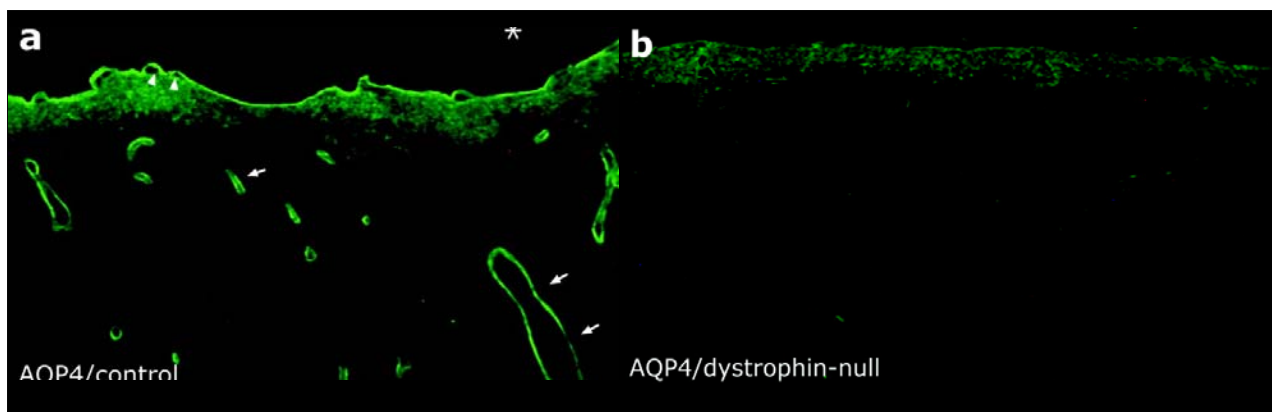
Figure 1.4. IMMUNOFLUORESCENCE LOCALIZATION OF AQP4 IN BRAIN. (a) In brain from control mice, AQP4 labeling is concentrated in glial processes forming the glia limitans (arrowheads) and surrounding intracerebral capillaries (arrows), but AQP4 labeling is not associated with neuronal elements or meninges (asterisk). (b) In brain from the dystrophin-null mice, AQP4 labeling is markedly decreased. Magnifications: ×250 (**2**).

The advantage of aquaporin-4 selective localization is presumably to rapidly facilitate water transport from the extracellular space into the cytoplasm of astroglial cells, to accommodate glucose transport from the blood and K^+ buffering after K^+ release from neurons during the falling phase of the action potential. (**80, 81, 82**). Under this circumstance, it seems reasonable that water movement from the capillaries to the brain

has to be facilitated by a active transport system with the consumption of energy, which might be important in maintaining brain homeostasis since water transport has to be connect to a active ionic transport and therefore subject to a more strict regulation.

Pharmacological Inhibition

Previous studies Andrea Yool and colleagues (**83**, **84**) were conducted to find novel agents that could be used to block water transport through aquaporin-1. The strategy to screen for ion channel blockers as novel inhibitors for aquaporin-1 permeability was based on structural similarities between membrane intrinsic protein family and ion channels (**85**). Tetraethylammonium was identified as a nonmercurial blocker of water transport through aquaporin-1 channels (**83**). The fact that tetraethylammonium sensitivity was removed by site-directed mutagenesis of aquaporin-1 confirms that inhibitory action. Using a standard swelling assay method tetraethylammonium was found to inhibit the water permeability of aquaporin-1-expressing oocytes in a dose-dependent and reversible manner. Mutagenesis of tyrosine 186 reduced the sensitivity of aquaporin-1 channels to block caused by external tetraethylammonium, demonstrating that the inhibitory effect of tetraethylammonium was mediated directly by aquaporin-1, not by native oocyte channels, and loop E region is involved directly or indirectly in forming the tetraethylammonium binding site.

Figure 1.5 demonstrates that aquaporin-1 function can be modified by pharmacological agents other than mercurial compounds. Tetraethylammonium, unlike mercury, is a reversible blocker that does not need treatment with reducing agents (**83**).

This observation is an exciting one because it may identify a potential lead compound for development of drugs for therapeutic intervention in clinical disorders that could be associated with disturbances in aquaporin-1 function, such as glaucoma, pulmonary edema, and autosomal dominant polycystic kidney disease. It was also found that tetraethylammonium blocks water permeability of aquaporin-1 channels in kidney and kidney-derived Madin-Darby Canine Kidney cells, demonstrating this effect is not limited to the oocyte expression system. Those studies support the idea that aquaporin-4 blockers can be identified and used as therapeutic tool (**84**).
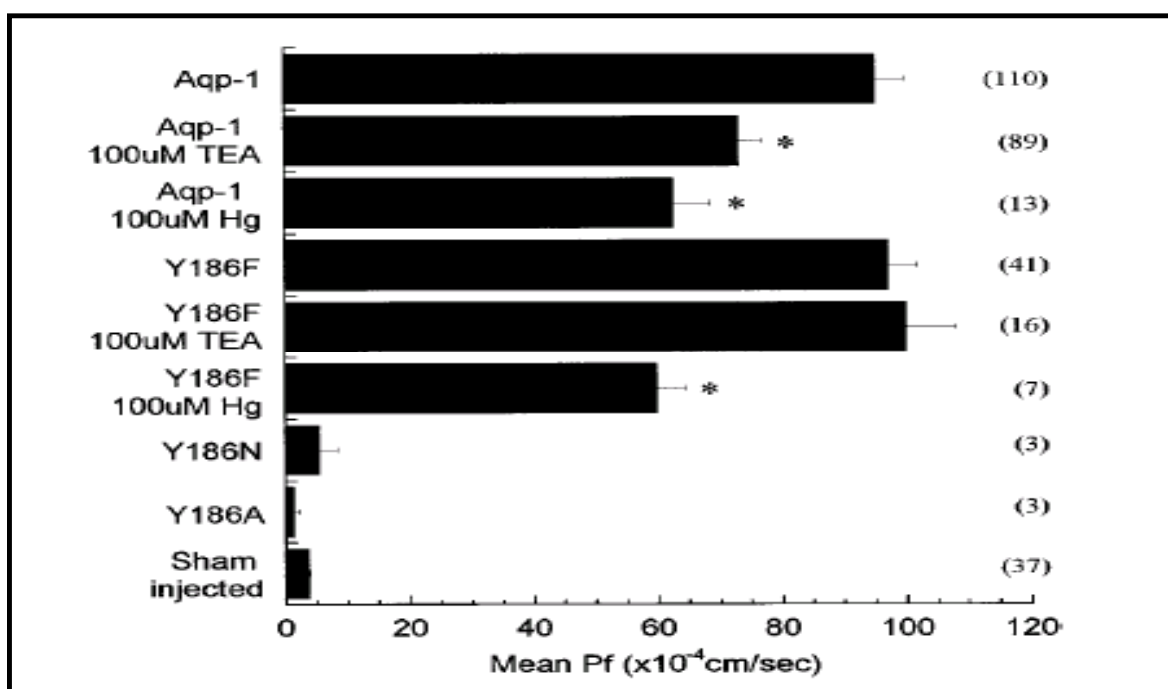
Figure 1.5 Summary of the blocking effects of tetraethylammonium on aquaporin-1 channels expressed in oocytes (**84**). Aquaporin-1 expressing oocytes have a decrease in water permeability when treated with 100μM tetraethylammonium and 100μM HgCl$_2$, but with the Y186F mutant the blocking effect is abolished.

Pathophysiology of Cerebral Ischemia and Reperfusion

Cerebral ischemia is a complex insult that involves loss of blood flow and consequently depletion of oxygen and essential nutrients like glucose (**86**); the pathology is also associated with increased microvascular permeability (**87**, **88**). The brain is dependent on blood flow for normal function as well as maintaining cellular ionic gradients. Two distinguished zones are identified in the ischemic brain: the core and the penumbra (**89**). The core of the ischemic event has a massive reduction of blood flow with shutdown of metabolic processes, decrease cellular energy supply, ion homeostasis, and consequently cellular integrity; cell death generally occurs by necrosis. The penumbra of the ischemic event still has the collateral circulation that provides a residual flow; cell death is a slow process that occurs through inflammation and apoptosis. Penumbra can account for up to 50% of the infarct volume. The mechanisms that are involved in the pathophysiology of stroke are energy failure and excitotoxicity, peri-infarct depolarization, inflammation, apoptosis and edema (**7**). **Figure 1.6** shows a schematic representation of the mechanisms involved in the ischemia-reperfusion pathophysiology.

Energy failure and excitotoxicity

The drastic reduction of cerebral blood flow restricts the delivery of substrates, particularly oxygen and glucose, and impairs the energetic required to maintain ionic gradients. Consequently, neurons and glia hyperpolarize and activate voltage-gated

calcium channels, which release excitatory amino acids, especially glutamate, in the extracellular space. Due to the lack of energy, presynaptic reuptake mechanisms are absent leading to NMDA and metabotropic glutamate receptor activation; the result is an increase in intracellular calcium concentration, and Na^+ and Cl^- influx. Water follows the ionic disturbance leading to cellular swelling, and eventually osmotic lysis and necrosis (**90**, **7**).

Figure 1.6. SIMPLIFIED OVERVIEW OF PATHOPHYSIOLOGICAL MECHANISMS OF FOCAL ISCHEMIC STROKE. Energy depletion and consequent neuron depolarization leads to activation of specific glutamate receptor. Glutamate receptors activation increase Ca^{2+}, Na^+, and Cl^- levels while K^+ is realesed in the extracellular space. Water follows the osmotic gradient causing cellular edema and lately cell death (excitotoxicity). Diffusion of glutamate and K^+ in the extracellular space can propagate a series of spreading waves of depolarization (peri-infarct depolarization). Intracellular calcium increase overactivates numerous enzyme systems (proteases, lipases, endonucleases, etc) generating oxygen free radicals, which damage membranes (lipolysis), mitochondria, DNA, and activates caspase-mediated cell death (apoptosis). Free radicals also induce the formation of inflammatory mediators, which activate microglia and lead to the invasion of blood-borne inflammatory cells (leukocyte infiltration) via upregulation of endothelial adhesion molecules (modified from **7**)

Periinfarct depolarization

Periinfarct depolarization refers to the depolarization of the surrounding areas, which might be originated by the release of glutamate and potassium in the core of the infarct. Glutamate and potassium diffusion to adjacent areas lead to an excitatory and

electrochemical depolarization of adjacent neurons and glia in the penumbra dispensing more glutamate and potassium which propagates from the core of the ischemic area to neighboring areas (**91**, **92**). Periinfarct depolarization has been shown experimentally to occur at a frequency of one to four events per hour (**92**, **93**). Periinfarct depolarization compromises cells in the penumbra and may contribute to the growth of the lesion from the core into the penumbra (**91**, **92**, **93**, **94**, **95**).

Inflammation

The key players of inflammation after cerebral ischemia are adhesion molecules in the vascular endothelium and circulating leukocytes. Leukocytes adhere to the endothelium and transmigrate from the blood into the brain parenchyma. This interaction of endothelium and circulating leukocytes is an important factor in stroke-induced brain inflammation. Antibodies against adhesion molecules (CD18, CD11b, or ICAM-1) not only reduce accumulation of leukocytes, but also the size of the infarct (**96**, **97**, **98**). Neurons, astrocytes, microglia, leukocytes (granulocytes, monocytes or macrophages and lymphocytes) produce cytokines and chemokines that play an important role as mediators of the inflammatory phase of cerebral ischemia (**99**, **100**, **101**). Inflammation is initiated by intracellular calcium increase that initiates several cascades of event that culminate with the release of inflammatory mediators and ultimately leukocyte migration and microglial cell activation. Calcium also activates another mechanism of cellular death called apoptosis.

Programmed cell death (apoptosis)

Apoptosis takes place in a similar time frame as inflammation. It starts hours after ischemia onset and lasts for days. It is also a more characteristic phenomenon of the penumbra region differently from the fast neuronal and glia cell death in the core. During apoptosis, a biochemical cascade leads to the activation of caspases, which catalyze the destruction of the cell, its compartments and molecules (**90**, **7**).

Figure 1.7 shows a general estimation of their relative impact over time. Excitotoxicity and peri-infarct depolarization are events that occur early in stroke and together with the fact that most patients take an average of 3 hours to receive medical support the treatment window might be lost explaining why some clinical trials targeting those components had failed.

Inflammation and apoptosis are events that occur simultaneously and most researchers have examined apoptosis and inflammation at hours and days after the ischemic injury. Ritter and colleagues found that the inflammatory response to ischemia reperfusion was significant within minutes of reperfusion, evidenced by significant leukocyte and platelet adherence in the microcirculation (**102**). The same experiments showed that fluid flux from the venules in the first minutes of reperfusion was increased (**103**). After 4 hours of ischemia and 24 hours of reperfusion, anti-selectin adhesion molecule treatment reduced both cerebral infarction and cerebral edema (**102**). While these results emphasized the contribution of the early inflammatory response to the formation of edema, little is known about the additional mechanisms of edema formation early in reperfusion and its early mechanisms are still under debate.

The integrity of the blood-brain barrier is sustained by the interaction of the cellular matrix, which is composed of endothelial cells and astrocytes. During ischemia, this cellular matrix and the intercellular signal exchange is damaged. Proteases, such as metalloproteases (MMP2 and MMP9) are induced and its expression correlates with the damage of the blood-brain barrier, the risk of hemorrhagic transformation, and the extent of neuronal damage (**104**, **105**, **106**). The destruction of the basal lamina by metalloproteases permits the immigration of leukocytes and the formation of vasogenic edema. Inhibition of metalloproteases not only reduces the damage to the blood-brain barrier, but also reduces infarct volume (**107**, **108**).

Figure 1.7. TIME COURSE AND RELATIVE IMPACT OF THE MECHANISMS OF INJURY AFTER ISCHEMIC STROKE (modified from **7**)
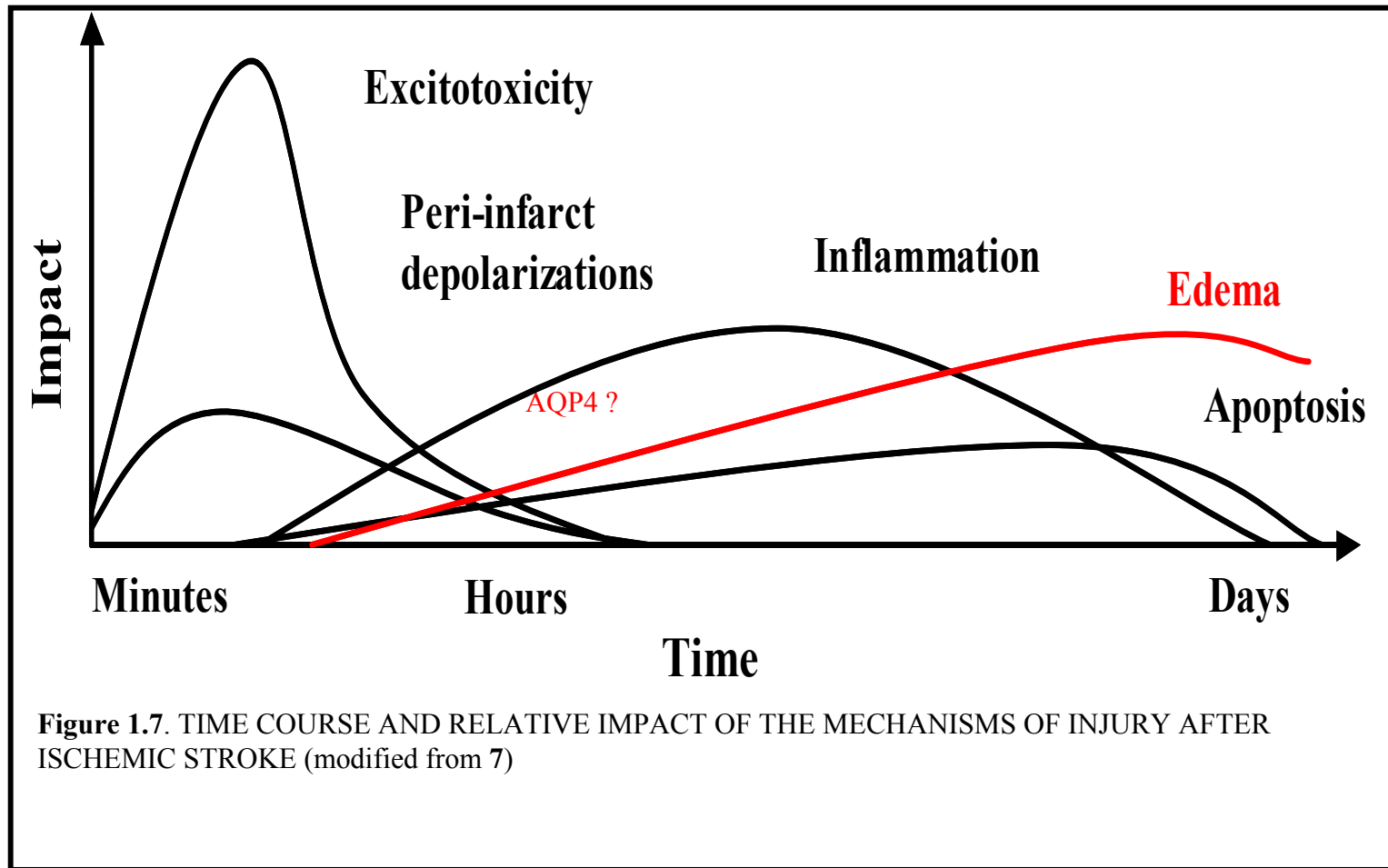
Cellular and Vasogenic Edema

Swelling of brain tissue is a common feature accompanying several pathological states such as brain trauma, brain ischemia and central nervous system tumors (**109**, **110**, **111**). In the the 60's, two forms of cerebral edema were defined and are currently accepted: one was "vasogenic edema:" characterized by the breakdown of the blood-brain barrier and accumulation of water into the surrounding brain tissue; the other was termed "cytotoxic edema," characterized by intracellular swelling, vascular permeability remaining relatively undisturbed (**112**).

Cytotoxic or Cellular Edema

Early stages of vasogenic edema after stroke or trauma involve initial astroglial swelling in both gray and white matter (**109**). Cellular edema consists principally of swelling of the astrocytic soma and processes, plus some swelling of the neuronal dendrites. Reduction of the extracellular space is observed (**113**, **114**) although neuronal cell (soma and axons) and oligodendroglia is generally not affected. In ischemic conditions, astrocytes appear swollen and neurons shrunken within 30 min or so of initiation of the ischemia (**109**, **115**, **114**) followed by a 50% decrease of the extracellular space (**115**).

Vasogenic Edema

Total brain volume is limited by its bone cage and is a net of blood, extracellular space, and cellular volumes. Brain swelling must always involve a gain of water to the extracellular space and after compensatory mechanisms reach its full capacity it can be measured as a rise in intracranial pressure (**115**) or by measuring total brain water using MRI (**116**). Hypoxia (permanent occlusion) and hypoxia followed by reoxygenation have been shown, using in *vitro* models of the blood-brain barrier, to increase permeability and sometimes is associated with the disruption of blood-brain barrier tight junctions (**117**, **118**, **119**). Hypoxic stress may increase water permeability via the transcellular route as well (**120**, **121**). With the breakdown of the blood-brain barrier, the ability to retain water is lost; the barrier is breached, and a filtrate of blood, including plasma proteins, is driven by the blood pressure into the brain. The blood cells are presumably retained in the vessels by the residual permeability of the blood-brain barrier, except in injury sufficient to lead to hemorrhage. Most of this ultrafiltrate fluid accumulates in the white matter due to the greater compliance of this region, i.e. white matter will more easily accept the increased volume at a given pressure. This is likely due to the greater ease of separation of the parallel oriented white matter tracts when compared with the gray matter (**112**, **61**). Astrocytic swelling also occurs concomitantly in vasogenic edema and can involve uptake of the extravasated plasma proteins (**122**).

The frequency of vasogenic edema in stroke and closed head injury and the degree to which it contributes to an impaired outcome is by no means clear. The existence of an increased intracranial pressure often is seen after head injury and is a clear life-threatening signal (**115**). As has been suggested, "cytotoxic edema" with its

potential for widespread metabolic dysfunction may be an equally serious problem since it will ultimately lead to cell lysis and necrosis (**109**). The two phenomena are both termed *edema* and involve unbalanced water movements, but in one case, it is cellular, primarily involving astrocytes, and in the other is due to increased permeability or breakdown of the blood-brain barrier. Thus, while water movement is the major characteristic underlying both phenomena, the mechanisms and effects are quite different. It seems that aquaporin-mediated edema could only be involved in cellular edema once vasogenic edema is related with the breakdown of the blood-brain barrier. But mice lacking aquaporin-4 expression show less brain glial cell (astrocyte) swelling, reduced edema, and a better neurological outcome after ischemia (**1**). Studies of the physiological roles of aquaporins in the brain are important and will lead to a better understanding of water movements accompanying solute movements involved in water homeostasis in the brain which, when the homeostasis breaks down in brain trauma and ischemia, is life-threatening.

Possible roles of AQP4 in blood-brain-barrier integrity and brain edema after ischemia.

Although cytotoxic edema might be closely related with infarct size, it does not contribute to an increase in brain volume. Vasogenic edema is the cerebral edema component that is clinically important. Astrocytes play a role in both vasogenic and cytotoxic processes. Astrocyte processes (end-feet) cover much of the abluminal capillary surface and thereby form part of the physical blood-brain barrier. Astrocytes also

contribute to the function of the blood-brain barrier by inducing formation of tight intercellular junctions between capillary endothelial cells and by regulating the expression and function of several endothelial transporters. Several lines of evidence suggest that astrocytes are in close apposition to the cerebral endothelial cell layer and play an important role in blood-brain barrier maintenance (**123**). After ischemia, vasogenic edema and blood-brain barrier disruption may occur by several mechanisms, including active solute transport, vesicular transport (**124**), opening of paracellular channels (**125**), and physical disruption of astrocyte-endothelial junctions (**126**). And as described by Leslie Ritter and colleagues in an in *vivo* microcirculation study during stroke, inflammation increases fluid movement from vascular bed to the brain early after reperfusion (**102**).

Aquaporin-4 localization in astrocytes and ultrastructural studies indicates that pericapillary astrocyte end-feet are the first cellular elements to swell during brain ischemia (**127**) would place aquaporin-4 channels as an important pharmacological candidate. Astrocyte swelling can result from uptake (cotransport) of extracellular K^+, Cl^- and Na^+ with subsequent osmotic movement of water (**128**), impaired extrusion of ions by failure of the membrane Na^+, K^+-ATPase, or from increased production of cytosolic solutes by breakdown of macromolecules. Recent studies suggest that aquaporins are the primary route by which water moves in and out of the astrocytes in response to these osmotic changes and that aquaporins play an important role in astrocyte swelling and cerebral edema formation (**129**). The concept is that initially a solute driven force for water movement is formed, followed by water movement through aquaporin-4 into

astrocyte end-feet processes. Subsequently, astrocyte swelling physically detaches astrocytes from the endothelial cell layers and is followed by a compromise in blood-brain barrier integrity. Early inhibition of aquaporin-4 water permeability would therefore prevent acute vasogenic edema and blood-brain barrier disruption.

Results of experiments using aquaporin-4-null mice have shown the involvement of aquaporin-4 in both cytotoxic and vasogenic edema. Mice lacking aquaporin-4 expression show less brain glial cell (astrocyte) swelling, reduced edema, and a better neurological outcome after ischemic stroke and water intoxication (**1**). α-syntrophin knockout mice (**74**) and dystrophin-null mice (**59**) indirectly affect aquaporin-4 expression. In both α-syntrophin and dystrophin-null mice, aquaporin-4 is not targeted correctly to the plasma membrane and therefore is not functional. *Dmd^{mdx}* mice (C57BL/10ScSnDMD<mdx>J) have a decreased expression of AQP4 protein (by 90% in adult mdx mice) without changes in the AQP4 mRNA levels; while the disruption of α-*syn* gene (α-Syntrophin is a member of the dystrophin-associated protein membrane complex and play an important role in connecting the cytoskeleton to the extracellular matrix) indicates that the protein is essential for localization of AQP4 protein in astrocyte end-feet membrane domains adjacent to brain capillaries (**59**, **130**). Studies by Ottersen and colleagues with α-syntrophin knockout mice after ischemic stroke (**74**) and dystrophin-null mice after water intoxication (**59**) also suggested that the decreased expression of aquaporin-4 is protective. Studies by Verkaman and colleagues with aquaporin-4-null mice also suggested that the aquaporin-4 deletion limits brain swelling in cytotoxic edema, but aggravates brain swelling in vasogenic edema (**131**). The

opposing actions of aquaporin-4 are probably related to the bi-directional water transport through aquaporin-4 channel (**131**). Aquaporin-4-null mice are surprisingly normal in terms of neurological status and gross neuroanatomical features (**1**). They had no general behavioral, motor, sensory, or coordination deficits. Comparison of brains from aquaporin-4$^{-/-}$ and aquaporin-4$^{+/+}$ mice indicated no gross differences in size or anatomy. There were no gross differences in the posterior, anterior, or middle cerebral artery anatomy. The distribution of the middle cerebral artery territory seemed to be identical for aquaporin-4$^{-/-}$ and aquaporin-4$^{+/+}$ mice. Microscopic examination of hematoxylin and eosin stained brain sections also indicated no histological differences. Blood-brain barrier permeability in aquaporin-4$^{-/-}$ and aquaporin-4$^{+/+}$ control mice was evaluated with Evans blue. The blood brain barrier was intact in both groups of mice except in choroid plexus where there is no barrier. Serum sodium and osmolality were not different in aquaporin-4$^{-/-}$ and aquaporin-4$^{+/+}$ mice, and expression of other aquaporins appeared to be unchanged as compared with wild type (**1**).

When stressed by transient cerebral ischemia, brain edema was attenuated in alpha-syntrophin (-/-) mice, indicative of reduced water influx. Surprisingly, aquaporin-4 was strongly reduced but alpha-syntrophin was retained in perivascular astroglial end-feet in wild-type mice examined 23 h after transient cerebral ischemia. Thus, alpha-syntrophin-dependent anchoring of aquaporin-4 is sensitive to ischemia, and loss of aquaporin-4 from this site may retard the dissipation of post-ischemic brain edema (**74**). Other studies also shown that aquaporin-4 is colocalized with potassium channels such as

$K_{ir}1.4$ and Ca^{+2}-activated rSlo, which infers its participation in potassium clearance (**132**, **133**).

To our knowledge, no compounds capable of inhibiting water permeability through aquaporin-4 channels have been described. Studies form animals models that disrupt the expression or the localization of aquaporin-4 channels indicate that a aquaporin-4 blocker will attenuate cerebral edema after stroke.

Significance of the Present Study

The unique feature of this study is the discovery and characterization of a novel pharmacological compound able to inhibit water movement through aquaporin-4 channels and the analysis of ischemic stroke after middle cerebral artery occlusion in dystrophin-deficient mice. The knowledge gained from this study may lend further insight in the treatment of cerebral edema after stroke.

Hypothesis

We hypothesized that an aquaporin-4 water channel blocker would decrease the formation of cerebral edema after ischemic stroke in mice. The purpose of this study was to determine if pharmacological blockers of aquaporin-4 water permeability can be identified, and if these agents will significantly decrease the formation of cerebral edema after ischemic stroke in mice. Particular emphasis was placed on comparing the

formation of cerebral edema after ischemic stroke in dystrophin-deficient mice. The specific aims of the project were as follows:

1- Identify novel aquaporin-4 blockers capable of inhibiting water permeability. (a) Use quantitative assays to characterize water flux through cloned aquaporin-4 channels expressed in *Xenopus* oocytes, and screen for pharmacological agents that significantly decrease water flux. Determine a dose-response curve. (b) Determine amino acids in the outer vestibule of the aquaporin-4 water pore that influence the inhibitory effect of the blocker using site-directed mutagenesis. (c) Measure the protective effects of aquaporin-4 blockers identified in Aim 1 on cerebral edema, infarct size, neurological outcome, and mortality rate, using the middle cerebral artery occlusion model in mice.

2- Evaluate the physiological response of dystrophin deficient (*mdx)* mice, C57Bl/10ScSnDMD<MDX>J, after ischemic stroke using a filament method. Using anatomical measurements of cerebral edema, infarct size and functional measurements of neurological outcome after 24h reperfusion.

CHAPTER 2. DISCOVERY AND CHARACTERIZATION OF A NOVEL AQUAPORIN-4 WATER CHANNEL BLOCKER.

Abstract

Aquaporins are members of the major intrinsic protein (MIP) family of channel-forming proteins. Aquaporin-4 is a member of the aquaporin channel family and it is widely distributed in the central nervous system. It is localized at the astrocytic end feet membrane facing the blood-brain barrier; prompting the hypothesis, that aquaporin-4 mediates water transport from the blood into the brain. Evidence of a protective effect in aquaporin-4 deficient mice in classic models of cerebral edema have also implicated it as a key player in the formation of cerebral edema after ischemic stroke. The objective of this work is: 1) to identify and characterize novel aquaporin-4 blockers capable of inhibiting water permeability in aquaporin-4 expressing oocytes; 2) to evaluate the effect of an aquaporin-4 blocker in the cerebral edema formation after ischemic stroke. We found that bumetanide inhibits water permeability through aquaporin-4 channels in a dose dependent and reversible manner. We also developed novel bumetanide derivatives that showed inhibitory properties in aquaporin-4 channels. Bumetanide was previously described as a protective agent against cerebral edema after ischemic stroke in rats; we confirmed this effect in mice and hypothesized that its protective mechanism in cerebral edema formation might involve a combination of inhibitory actions on the Na^+, K^+, Cl^- cotransporter and aquaporin-4.

Introduction

No compounds able to inhibit water permeability in aquaporin-4 channels have previously been described. The unique finding of this work is that bumetanide significantly inhibited the water permeability of AQP4-expressing oocytes. The inhibitory effect of bumetanide on AQP4 water permeability was dose dependent and reversible.

Aquaporin-4 (AQP4) is a member of the major intrinsic protein family of channel-forming proteins. The mammalian aquaporin protein family has 11 members. Aquaporins are transmembrane proteins that assemble as homotetramers. Each individual monomer is formed by six transmembrane domains with intracellular carboxyl (C) and amino (N) terminals. AQP4 was first cloned in 1994 (**71**) and has two methionine initiation sites (M1 and M23) which yield products at 32 and 30kDa respectively. Transport studies showed that AQP4 heterologously expressed in *Xenopus laevis* oocytes increased water permeability by 20-fold and was not blocked by $HgCl_2$ even after cysteine substitution to mimic the site that creates mercury-sensitivity in AQP1 (cysteine 189 in loop E), thus AQP4 also is known as the «mercury-insensitive water channel.»

Several groups have proposed the involvement of AQPs in the pathophysiology of brain edema (**127**, **134**, **135**, **72**). AQP4 is the predominant water channel in normal brain. It is strongly expressed in the astrocyte end-feet plasma membrane facing the blood brain barrier and at the CSF-brain interface. AQP1 and AQP9 are also expressed in normal brain, but the distribution appears to be limited to the choroid plexus, glia limitans

and tanycytes (**136**). At present, its possible expression in the endothelial cells is still under debate; in lieu of aquaporin-mediated fluxes, water transport from the blood to the CNS parenchyma (through the endothelial cells) might involve a route other than water channels, such as cotransporters (**66**). The presence of water channels in astrocytes suggests that AQP4 mediates the rapid fluid exchange in the extracellular space and allows accommodation for changes in volume in the cytoplasm of the astrocytes.

Results of experiments using AQP4-null mice reveal the involvement of AQP4 in both cytotoxic and vasogenic edema (**1**). Some other genetically modified mice also have a protective effect in edema thought to be due to decreased function of AQP4: α-syntrophin knockout mice (**72**) and dystrophin-null mice (**130**) presented alterations in the pattern of AQP4 expression or the protein is not targeted correctly to the plasma membrane.

Our study was initiated to find agents capable of blocking water transport through AQP4. We hypothesized that an AQP4 blocker would decrease the formation of cerebral edema after ischemic stroke in mice. Various compounds (**Table 2.1 and Table 2.2**) that are known to affect channels, transporters, or receptors were chosen with the singular goal of identifying a lead compound for further development. One of those compounds, bumetanide, had a significant effect on osmotic swelling rate. Our studies indicated that bumetanide reversibly blocked the water permeability of AQP4 in a dose-dependent manner. Our studies also indicates that bumetanide has a protective effect in the cerebral edema formation after ischemic stroke in mice as its was previously demonstrated in rats (**4**). The uniqueness of our study is that bumetanide was administered after ischemic,

more relevant from the clinical perspective. A novel compound derived from bumetanide was generated and showed inhibitory properties in AQP4 channels.

Material and Methods

Preparation of Oocytes

Oocytes at stage V and VI were harvested from female *Xenopus laevis* and prepared as described previously (**137**). Oocyte placed in 30ml of OR-2 saline solution (82mM NaCl, 2.5mM KCl, 1mM CaCl, 5mM HEPES, 30mg Penicillin, 50mg Streptomycin) containing 0.015g Trypsin inhibitor (Sigma-Aldrich Co.) plus 0.045g Collagenase (Sigma-Aldrich Co.) at 18°C for 1.5 to 2h to achieve 50% loss of follicular coats. After oocyte digestion, oocytes were washed 3 times with OR-2 saline solution for 15min and 3 times in ND96P (96mM NaCl, 2mM KCl, 1.8mM $CaCl_2$, 5mM HEPES, pH 7.6) plus 2.5mM sodium pyruvate. Oocytes were stored in ND96P saline solution at 18°C overnight. Cloned rat AQP4 DNA was provided by Peter Agre. Oocytes were injected on the following day harvest with either 50nl of DEPC water or 50nl of DEPC water containing AQP4 RNA. Oocytes were incubated for 48hrs at 18°C in ND96P.

Bursting Time

Bursting time during swelling was recorded at 22°C, using a Cohu CCD video camera (Cohu, San Diego, CA). After 5-minute incubation with 200mOsM NaCl saline or 200mOsM NaCl saline plus a drug candidate (**Table 2.2**) oocytes were transferred

(time 0) from 200mOsM NaCl saline to 0mOsM NaCl saline (control group) or 0mOsM NaCl saline with drug candidates and time of bursting was measured visually through continuous recording of aquaporin water channel expressing oocytes.

Measurements of Osmotic Permeability (P$_f$).

Oocytes were transferred from the culture medium (ND96P) to 200mOsM NaCl saline (control group) or 200mOsM NaCl saline with a selected drug candidate, and incubated for 5min at room temperature. At time 0 in the swelling assay, oocytes were transferred into 100mOsM NaCl saline with or without drug, to match the pre-incubation condition. Osmotic swelling was performed at 22°C, recorded with a Cohu CCD video camera (Cohu, San Diego, CA), and analyzed by computer using Scion Image software (Scion Corporation). Images were captured every 2s for a period of 1.5min. The area of the oocyte was recorded, and used to calculate the relative volume change and the water permeability value (P$_f$), as previously described (**67**). The measured increase in relative volume as a function of time was fit optimally with a second order polynomial, and the initial rates of swelling were calculated between 4 and 120s, as $d(V/V_o)/dt$, from the linear component of the fits. This measurement is used in the formula $P_f = [V_o \times d(V/V_o)/dt] / [S \times V_w \times (osm_{in} - osm_{out})]$, where initial oocyte volume is $V_o = 9 \times 10^{-4}$, molar ratio of water is $V_w = 18 cm^3/mol$, initial oocyte surface area is $S = 0.045 cm^2$, osmolarity inside the oocyte is estimated as $osm_{in} = 200mOsM$, and osmolarity outside the oocyte in hypotonic saline is $osm_{out} = 100mOsM$. P$_f$ values are calculated individually for each oocyte and the groups are analyzed as P$_f$ mean ± SD.

Site-Directed Mutagenesis.

Aquaporin-4 mutants were generated by using site-directed mutagenesis strategy. The purpose of this experiment is to evaluate if the blocking effect observed is directly related to aquaporin-4 channels and not in native channels expressed in Xenopus oocytes. Site-directed mutagenesis takes advantage of the QuikChange Site-directed mutagenesis method available from Stratagene (La Jolla, CA), (**83**). Synthetic oligonucleotide primers (**Table 2.3**), complementary to opposite strands of the vector carrying the AQP4 gene that contain the desired mutation are designed. The product is then treated with DpnI endonuclease that is specific for methylated and hemimethylated DNA; this digests the parental DNA template to select for mutation-containing synthesized DNA. The vector DNA incorporating the desired mutation is then transformed into Epicurian coli XL1-Blue supercompetent cells. Successful incorporation of the mutations is confirmed by sequence analysis, using forward and reverse sequencing primers to double check the correct sequence. RNA synthesized in vitro for each mutant was injected, and the expression of channels in oocyte was verified by swelling assay.

Middle Cerebral Artery Occlusion in Mice.

Animal Preparation

The purpose of this experiment is to test the effect of an aquaporin-4 channel blocker in the cerebral edema formation after ischemic stroke. C57Bl/J mice (male, 8-

10weeks, 20-25g) were obtained from Jackson Laboratories and housed with free access to food and water at the University Animal Care Facility at the University of Arizona. All mouse procedures were approved by the University Animal Care and Use Committee in accordance with IACUC guidelines. Mice were housed in a quiet room before surgery. All mice were subjected to temporary occlusion (60 min) of the right middle cerebral artery with the silicone-coated filament technique and 24hrs reperfusion (**figure 2.1**), as previously described (**138**).

Briefly, the animals were anesthetized via inhalation mask with 3.0V% isofluorane and maintained with 1.5% to 1.75% isofluorane in a mixture of 30% oxygen and 70% nitrox. Rectal temperature was monitored and held constant during surgery using a thermostatically regulated heating lamp. A skin incision in the right temporoparietal area was made, the temporalis muscle was retracted, and a microtip of the laser-Doppler probe (Periflux system 5000, Perimed, Stockholm, Sweden) was placed on the skull surface (bregma 0 and 6 mm, probe tip 0.5 mm in diameter) to monitor blood flow from the beginning of the time of anesthesia until 15 min after removal of the occluding filament (**Figure 2.1**). The common carotid was occluded with a slip knot immediately before filament placement, and remained occluded during the total ischemic period. A 7-0 monofilament silicone-coated nylon surgical suture with a diameter varying between 150-250μm was prepared the day before the experiment. The occluding filament was threaded through the external carotid and into the internal carotid, up to the bifurcation to the middle cerebral artery. MCAO was considered successful if there was greater than 85% reduction in blood flow, compared to baseline values, throughout the

entire ischemic period. For the following 60 minutes, the animal remained untouched under constant conditions. At the end of the ischemic period, the filament was withdrawn, the external carotid artery stump was tied, the common carotid artery was untied, and reperfusion was confirmed by laser Doppler (>50% of baseline). The animals were then permitted to recover from anesthesia at room temperature and sheltered from drafts. In all experimental animals, blood flow returned to near pre-MCAO levels within 15 min of the removal of the suture.

Mice undergoing surgery were divided into 2 groups, a control and a treated group. Animals in the treated group were given 60mg/kg of bumetanide to achieve a plasma concentration of 100uM bumetanide 10 minutes before reperfusion and animals in the control non-treated group were administered placebo-saline. Placebo-saline or saline plus bumetanide were administered intravenously in the jugular vein.

Neurological Function

At 24 hours after reperfusion, the animals were scored for neurological deficit by a 28-point focal scoring system. The neurological exam was combined from studies by Clark and colleagues (**138**) and Hurn and colleagues (**139**), who used the exams to describe postischemic neurologic deficits in mice.

Cerebral Edema and Infarct Size Determination

After neurological scoring, the mice were deeply anesthetized with isoflurane inhalant and euthanized by cervical dislocation. Brains were isolated rapidly, the

olfactory bulb and cerebellum were removed, and the brain was sectioned into four 2-mm slices. These slices were placed in a well plate containing 2% tetrazolium chloride (TTC) solution (Sigma-Aldrich, Inc.) and allowed to develop for 30 minutes. TTC stains the live mitochondria and therefore isolates the live tissue (red) from the dead tissue (white). The tissue was then placed in 10% formalin and all slices were scanned in a table top light scanner, and images were captured with Adobe Photoshop (7.0). The National Institutes of Health Image Analysis program (ImageJ software-\; Scion Image Co.) was then used to measure the area of ischemia and total hemisphere area. Cerebral edema was measured by subtracting the total contralateral volume from the total ipsilateral volume divided by the total contralateral volume and expressed and percentage (**140**).

$$\text{Edema (\%)} = \frac{\text{(Total ipsil. volume-total contralat. volume)}}{\text{Total contralat. volume} *100}$$

Total infarct volume was calculated by adding the product of the measured infarct area in each slice by 2 (since each slice is 2 mm thick). To partially correct for effects of edema on the ipsilateral side, infarct volumes were corrected by (**140**):

$$\text{Infarcted volume (mm}^3) = \Sigma \text{ (Infarcted area *(total Ipsil. area / total contralat. area) * 2)}$$

All results are expressed as mean ± Standard Deviation. ANOVA and post hoc (Holm-Sidak method) were used to assess the significant differences in cerebral edema and infarct volumes ($P<0.05$).

Results

Oocyte bursting times were used to identify potential inhibitors of AQP4 water permeability. **Figure 2.2** indicates the mean and standard deviation bursting time for each treatment group. To account for variability in the level of protein expression between oocytes from different frogs, each treatment group was standardized to the mean value of the non-treated AQP4 group (control) measured on the same day. AQP4-expressing oocytes were pre-incubated for 5 minutes with and without the drug candidate (**Table 2.1** and **Table 2.2**). Non-treated AQP4-expressing oocytes pre-incubated with isotonic saline had a rapid osmotically driven increase in cellular volume leading to an average bursting time of 305.79 ± 97.27 sec. In contrast, AQP4-expressing oocytes that were pre-incubated in 25mM CsCl, 100μM bumetanide, 100μM kynurenic acid or 1μM charybdotoxin significantly increased in the bursting time suggesting that those compounds inhibited the osmotically induced swelling (**Table 2.4**). Sham injected control oocytes did not show any appreciable increase in relative volume. One-way analysis of variance (ANOVA) followed by Holm-Sidak method was used for statistical analysis.

Quantitative oocytes swelling assays were used to further characterize potential inhibitors of AQP4 water permeability. Osmotically induced swelling was measured by transferring oocytes to 50% hypotonic saline (at time 0) and recording the relative volume increase over 90s. **Figure 2.3** indicates the mean relative area change (RAC) and standard deviation in each treatment group, for AQP4-expressing oocytes that were pre-

incubated for 5min in control isotonic saline (non-treated) or in isotonic saline containing either 25mM CsCl, 100μM bumetanide, 100μM furosemide, 100μM kynurenic acid or 0.1μM charybdotoxin (treated). Non-treated AQP4-expressing oocytes had a rapid osmotically driven increase in relative volume. In contrast AQP4-expressing oocytes that were pre-incubated in 100μM bumetanide showed a marked reduction in the rate of relative area change after their transfer into 50% hypotonic solution also containing 100 μM bumetanide (**Table 2.5**), suggesting that bumetanide inhibited the osmotically induced swelling. AQP1-expressing oocytes treated with bumetanide and furosemide did not have similar swelling rates with non-treated AQP1-expressing oocytes.

Increased concentrations of bumetanide indicated a dose-dependent inhibitory effect on the osmotic water permeability of AQP4-expressing oocytes (**Figure 2.4**). To avoid the variability of the protein expression between oocytes collected from different frogs each treatment group was corrected to the mean value of the non-treated AQP4 group measured on the same day. Data in **figure 2.4** are compiled from a total of 195 oocytes (from 11 different frogs); each oocyte was previously tested with control saline without any treatment and used as its on control for the treatment analysis; also the same oocyte was used a third time to assess its recovery to bumetanide treatment. There was a non-significant increase of the inhibitory effect of the bumetanide treatment between 1μM to 500μM (**Table 2.6**), but for the highest dose tested, there was a decrease of the inhibitory effect. Blocking effect was calculated by correcting the RCA for the treated swelling by the control swelling in regular saline.

The inhibitory effect of bumetanide on osmotic water permeability was reversible (**Figure 2.5**). After testing the rate of volume increase after pre-incubation in several different treatment concentrations of bumetanide, the oocyte was allowed to recover to normal volume over a period of an hour. The oocyte was then tested again in a swelling assay in hypotonic saline. The rapid osmotic swelling response seen in the recovered oocyte demonstrated that the inhibitory effect of bumetanide was reversible.

Structural studies suggested that the interaction sites for bumetanide in AQP4 channels are located on the cytoplasmic side of the protein. Intracellular administration of bumetanide indicated a dose-dependent inhibitory effect on the osmotic water permeability of AQP4-expressing oocytes (**Figure 2.6**). Data in **figure 2.6** are compiled from a total of 175 oocytes (from 8 different frogs); each oocyte was tested with 50% hypotonic saline. Non-treated oocytes were injected with 3ng of AQP4 RNA in 50nl of DEPC water (control group) and treated oocytes were injected with 3ng AQP4 RNA with DMSO or 3ng AQP4 RNA with DMSO plus 5, 15, or 45μM bumetanide. The inhibitory effect of the bumetanide treatment was tested at calculated final intracellular concentrations from 5μM to 45μM (**Table 2.7**). At the intracellular concentration of 45μM bumetanide significantly reduced osmotically induced swelling in oocytes.

To increase the membrane permeability of bumetanide our collaborator, Dr. Gary Flynn (an organic chemist in the Univ. Ariz. BIO5 Institute) developed a set of methylated bumetanide derivatives. The prediction is that once the compound crosses the membrane, endogenous esterases clip the modified portion, simultaneously restoring the original bumetanide structure and trapping the compound in the cytoplasmic

compartment. Synthetic bumetanide derivatives are predicted to increase intracellular availability of bumetanide and consequently increasing the potency of the blocking effect.

Two of the new compounds showed an inhibitory effect on the osmotic water permeability of AQP4-expressing oocytes (**Figure 2.7**). Data in **figure 2.7** are compiled from a total of 29 oocytes (from a single frog); each oocyte was tested with 50% hypotonic saline (**table 2.8**). There is a greater inhibitory effect of the bumetanide derivative #3 than unmodified parent compound.

Computational analyses have identified specific amino acids of AQP4 and the structural features of bumetanide likely to be involved in binding. While this diagram is not necessarily correct, it generates testable predictions for sites in the AQP4. The character of the putative binding sites can be used to identify specific amino-acid residues that are predicted to play a role in ligand binding. The rationale for designing mutants was based on ligand protein binding studies that identified possible interactions sites for bumetanide in AQP4. As well, the model of the binding sites predicted the nature of the interaction (*e.g.*, hydrogen bonding, electrostatic, pi-electron, and hydrophobic interactions). These predictions were tested experimentally by site-directed mutagenesis of AQP4. A series of amino acid substitutions tested the contributions of candidate sites (**Table 2.3**). Certainly there are more possibilities than are listed here. The effect of bumetanide on the water permeability of mutant AQP4-expressing oocytes was evaluated by osmotic swelling assays in 50% hypotonic saline. **Figure 2.8** shows the relative area change for oocytes that were pre-incubated in either control saline or in saline containing

100μM bumetanide for 15 minutes. Sham injected (control) oocytes were resistant to osmotically induced swelling and were unaffected by the presence of bumetanide. Substitutions of phenylalanine (F) with alanine (A) in the position 175 generated a mutant resistant to bumetanide blocking effect. Osmotic water permeability (P_f) values were calculated for oocytes expressing wild type or mutant AQP4 and for sham oocytes. The results shown in **Figure 2.8** are compiled from oocytes taken a single frog. The lack of effect of bumetanide in the Phe175Ala mutant suggests that bumetanide inhibitory effect involves AQP4 channels and is not related to native volume regulatory channels present in oocytes.

In order to assess the effect of bumetanide in the formation of cerebral edema and infarct size, we compared two groups subjected to 1h ischemia and 24h reperfusion. Data in **Figure 2.9** are compiled from a total of 8 mice, four in the control and four in the bumetanide group. While not statistically significant, bumetanide-treated animals showed reduced (37.3% reduction) cerebral edema and smaller (75.83% decrease) infarct volume when compared with placebo treated animals. Neurological evaluation showed no statistical difference between placebo-treated and bumetanide-treated animals.

Discussion

No compounds able to inhibit water permeability in aquaporin-4 channels have previously been described. The unique finding of this work is that extracellularly applied bumetanide and a novel bumetanide derivative significantly inhibited the water permeability of AQP4-expressing oocytes at 100μM; intracellular delivery of bumetanide

confirmed our initial prediction of an intracellular binding site. The inhibitory effect of bumetanide on AQP4 water permeability was dose dependent and reversible.

Bumetanide is a potent diuretic agent. Bumetanide, furosemide, and ethacrynic acid belong to the class of diuretics referred to as the "high-ceiling" or "loop" diuretics, which exert their effects in the ascending limb of the loop of Henle. Bumetanide is known to block Na^+, K^+, Cl- cotransporter. The active secretion of bumetanide into the renal tubule filtrate occurs in cells of the proximal tubule through a process involving transporters of the renal organic anion (OA) secretory pathway. It is interesting that the concentrations of bumetanide that block the Na,K,Cl cotransporter (<1μM; **141**) and that can saturate renal OA transporters (<10μM, **142**) are much lower than the concentration reported to have a beneficial effect in post-stroke edema (100μM, **143**); this higher concentration of bumetanide is curiously similar to the amount needed *externally* for block in our studies of AQP4. This difference, though not proof, is consistent with the idea that AQP4 is one of the targets in the observed beneficial effect in cerebral edema formation of bumetanide in *vivo*.

The crystal structure of AQP1, obtained by x-ray crystallography, showed that each subunit narrows at the central NPA region (a conserved asparagine-proline-alanine signature motif) to a diameter near that of a single water molecule. All aquaporins with solved structures thus far share the same organization (**144**). Superimposed polypeptide backbones for the known structure of bovine AQP1, and a proposed structure for rat AQP4 derived from a comparative model building showed a similar structure of AQP4 and AQP1. Using a pilot homology structure of AQP4 based on the crystal structure of

AQP1, Dr. Yool and our colleagues in BIO5 (The University of Arizona Institute for Collaborative Research) identified two possible binding domains for bumetanide, both at the intracellular face. Site I is near the water pore, and site II is in a pocket formed by different domains including the carboxyl terminus and an intracellular loop. The finding of internal sites for bumetanide suggested that this poorly membrane-permeant compound and should be more effective when applied intracellularly.

Intracellular administration of bumetanide proved to be effective. Since bumetanide slowly crosses biological membranes, we developed several compounds derived from bumetanide. We found that one derivative (bumetanide #3) significantly reduces water permeability of AQP4 expressing oocytes. This agent might have promise in the treatment of cerebral edema after stroke.

As described above, bumetanide was shown by others to decrease the formation of cerebral edema associated with ischemic stroke at 100μM plasma concentration administered in advance of the ischemia event (**140**). My work extended the possible therapeutic significance of this finding by testing the effects of administering bumetanide after the stroke at the time of reperfusion, a scenario more likely to occur in practice since at best, patients arrive at the emergency room 1 to 3 hrs after the onset of the ischemic event. Treatment of the vascular clot with tissue plasminogen activator is clearly effective and used in reducing the infarct core. This initiates reperfusion and consequently increases the formation of cerebral edema. We propose that an additional agent that mitigates cerebral edema would be beneficial at the reperfusion period as well as in patients with persistent stroke at the time of arrival at the hospital. Although the data do

not show statistically significant levels, we note that despite the small n values, the trend towards a protective effect clearly supports what has been described previously by others.

Bumetanide has been described as a potential treatment for cerebral edema after stroke; our work is the first to describe a potential molecular target for this compound as an aquaporin-4 blocker. An encouraging finding of this work is the demonstration that bumetanide is effective after the ischemic event, and thus holds promise as a therapeutic agent in the realistic setting of emergency clinical medicine.

| Compound name	Synonym	Molecular Formula	Molecular Weight	Action
Bumetanide	3-(Aminosulfonyl)-5-(butylamino)-4-phenoxybenzoic acid	$C_{17}H_{20}N_2O_5S$	364.42	Inhibitor of Na^+,K^+,Cl^- cotransporter (283)
Cesium chloride		CsCl	168.36	Ion channel blocker (284)
TRIS hydrochloride	Tris(hydroxymethyl)aminomethane hydrochloride	$NH_2C(CH_2OH)_3 \cdot HCl$	157.60	Inhibitor of NMDA receptors (285)
.Tetramethylammonium chloride	TMA	$(CH_3)_4N(Cl)$	109.60	
4-Amino-3-(trifluoromethyl)pyridine		$C_6H_5F_3N_2$	162.11	
Mercury Chloride	Calomel Mercurous chloride	Hg_2Cl_2	472.09	AQP1 blocker (286)
Disopyramide	α-Diisopropylaminoethyl-α-phenylpyridine-2-acetamide	$C_{21}H_{29}N_3O$	339.47	Class IA antiarrhythmic; sodium channel blocker (296)
Clofilium tosylate	4-Chloro-N,N-diethyl-N-heptylbenzenebutanaminium tosylate	$C_{21}H_{37}ClN \cdot C_7H_7O_3S$	510.17	K^+ channel blocker; cardiac depressant; anti-arrhythmic (295)
(±)-3-Aminobutanoic acid	(±)-3-Aminobutyric acid DL-3-Aminobutyric acid	$CH_3CH(NH_2)CH_2COOH$	103.12	GABA receptor inhibitor (294)
Kynurenic acid	4-Hydroxyquinoline-2-carboxylic acid	$C_{10}H_7NO_3$	189.17	Non-selective antagonist at NMDA and AMPA/kainate receptors; blocks kainic acid neurotoxicity (293)
N-methyl-D-aspartate				NMDA receptor inhibitor (292)
Phosphopentanoic				Chloride channel blocker (291)
Colchicine		$C_{22}H_{25}NO_6$	399.44	
Forskolin	7β-Acetoxy-8,13-epoxy-1α,6β,9α-trihydroxylabd-14-en-11-one Coleonol	$C_{22}H_{34}O_7$	410.50	Cell-permeable diterpenoid that possesses anti-hypertensive, positive inotropic, and adenylyl cyclase activating properties. Many of its biological effects are due to its activation of adenylyl cyclase and the resulting increase in intracellular cAMP concentration.[1] Forskolin effects calcium currents and inhibits MAP kinase (290)
Tetrodotoxin	Fugu poison Maculotoxin Tarichatoxin TTX	$C_{11}H_{17}N_3O_8$	319.27	Reversible, selective blocker of Na^+ channels; blocks propagation of impulses in excitable membranes. Used to characterize sodium channels in excitable membranes and to study the role of sodium channels in normal physiology and disease (289)
Tetraethylammonium chloride	TEA chloride	$(C_2H_5)_4N(Cl)$	165.70	Blocks K^+ channels; blocks nicotinic acetylcholine neurotransmission by blocking the receptor-mediated K^+ currents. AQP1 blocker (286)
Charybdotoxin		$C_{176}H_{277}N_{57}O_{55}S_7$	4295.89	Potent and selective inhibitor of the Ca^{2+}-activated K^+ channel present in GH_3 anterior pituitary cells and primary bovine aortic smooth muscle cells (288)
Anthracine				Chloride channel blocker (287)

Table 2.1. SHOWS CANDIDATE COMPOUNDS. Compounds were selected for AQP4 blocking screening and display its molecular formula, molecular weight, action and names. Compounds where selected based on previous reports of blocking effect in channels or transporters.

Table 2.1 continued
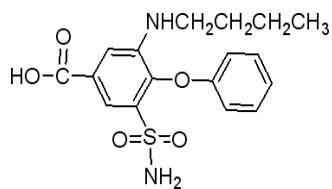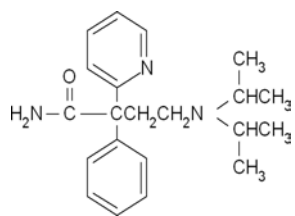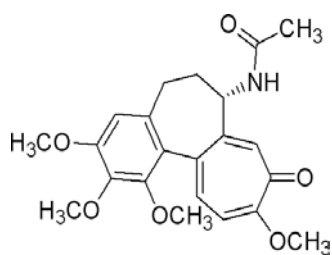
Bumetanide
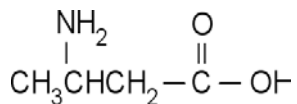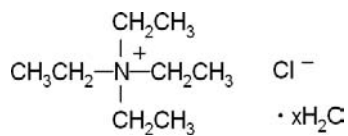
Aminobutanoic acid

Tris Cl

Disopyramide

Tetraethylammonium chl oride

Kynurenic acid

Colchicine
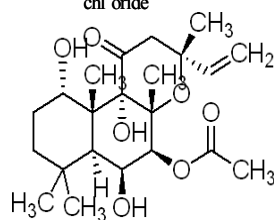
Forskolin
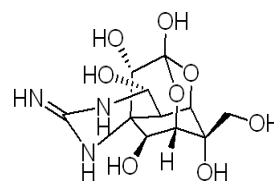
4-amino pyridine

Tetrodoxin
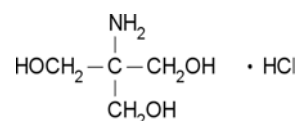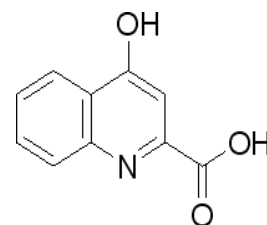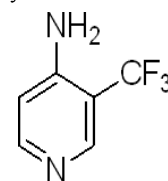
Compound name	Dose	Compound name	Dose
Bumetanide	100μM	Kynurenic acid	100μM
Cesium Chloride	25mM	N-methyl-D-aspartate	100μM
Tris hydrochloride	25mM	Phosphopentanoic	100μM
Tetramethylammonium chloride	25mM	Tetraethylammonium chloride	100μM
4-Amino-pyridine	5mM	Forskolin	100μM
Mercury chloride	300μM	Tetrodoxin	100μM
Disopyramide	100μM	Charabdotoxin	1μM
Clofilium tosylate	100μM	Colchicine	100μM
3-Aminobutanoic acid	100μM	Anthracine	100μM

Table2.2. LIST OF CANDIDATE COMPOUNDS AND PRELIMINARY DOSE TESTED.

A)

	predicted interaction	*substitutions*
SITE I		
ser 177	polar	gly, ala, thr, phe
gly 93	main chain C-O	ala, val (alter bulk)
his 95	H-bond	gly, lys, asp, val,
val 189	hydrophobic	leu, trp, phe, ala
SITE II		
cys 253	main chain C-O	ala, val (alter bulk)
asp 255	electrostatic	asn, lys, ala, glu
arg 108	electrostatic	asn, lys, ala, glu
arg 261	electrostatic	asn, lys, ala, glu
lys 181	electrostatic π electron	ala, arg, glu, ser
lys 109	electrostatic π electron	ala, arg, glu, ser
phe 175	hydrophobic	ala, tyr, trp, val

B)

Mutant	Primers (Sense)	Primers (Antisense)
H95A	5'-c atc agc ggt gcc atc aac cca gcg –3'	3'-g tag tcg cca ccg cgg tag ttg ggt cgc-5'
F175A	5'-cag ctg gta ttc acc acc att gct gcc agc tgt gat tcc-3'	3'-gtc gac cat aag tgg taa cga cgg tcg aca cta agg-5'
R261D	5'-ct gac gtg ctc aaa cgt gac cta aag gaa gcc-3'	3'-ga ctg cac ctc gag ttt gca ctg gat ttc ctt cgg-5'
S180R	5'-gcc agc tgt gat cgc aaa cgg act gat gtt act gg-3'	3'-cgg tcg aca cta gcg ttt gcc tga cta caa tga cc-5'
V189A	5'-gat gtt act ggt tcc gct gct tta gca att ggg-3'	3'-cta caa tga cca agg cga cga aat cgt taa ccc-5'

Table 2.3 SITE DIRECTED MUTAGENESIS A) Partial listing of mutagenesis studies of bumetanide candidate biding sites. B) Lists the primer design used to generate the mutants.
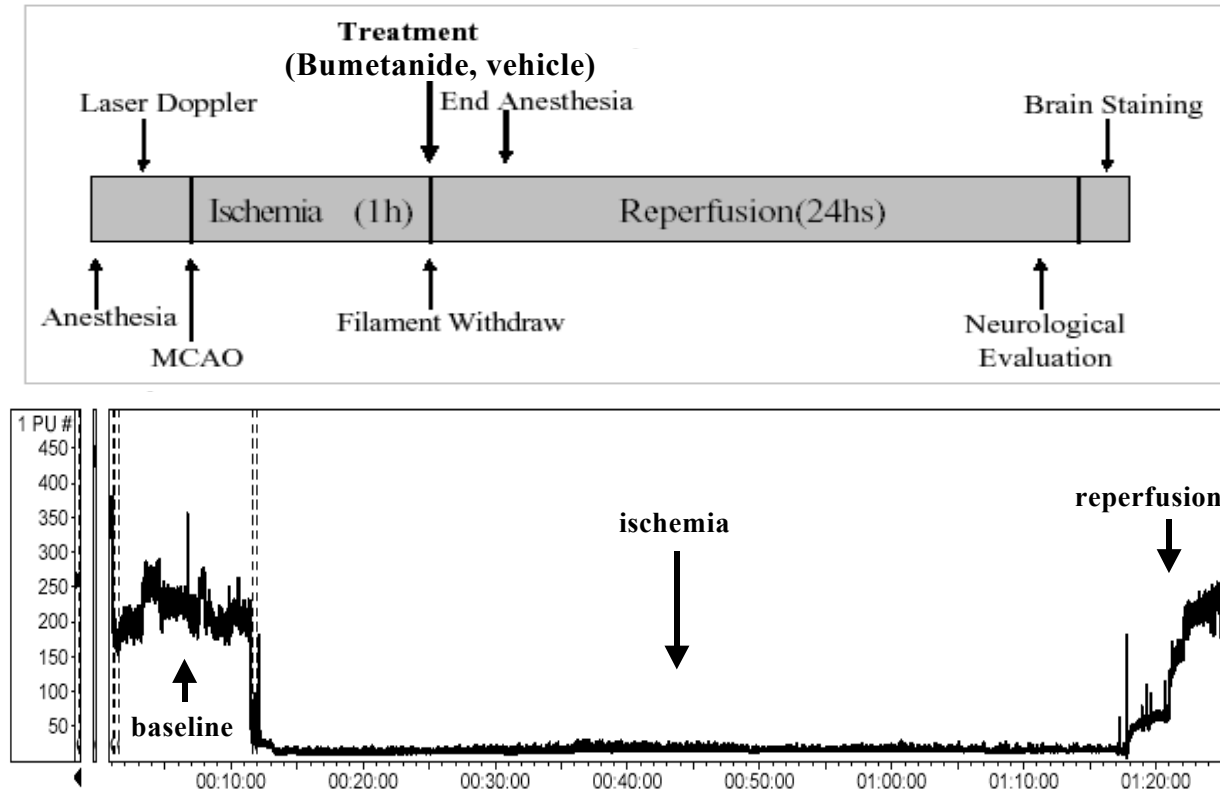
Figure 2.1. EXPERIMENTAL DESIGN TIME LINE. It also reveals a representative Doppler flow recording from a C57BL/6J male mouse subjected to one hour of ischemia and 24 hrs of reperfusion. It also indicates absolute values and the percent reduction during ischemia. This animal had a 91.51% decrease in blood flow over the ischemic period which, after 15min, had recovered to 66.52% of baseline flow.
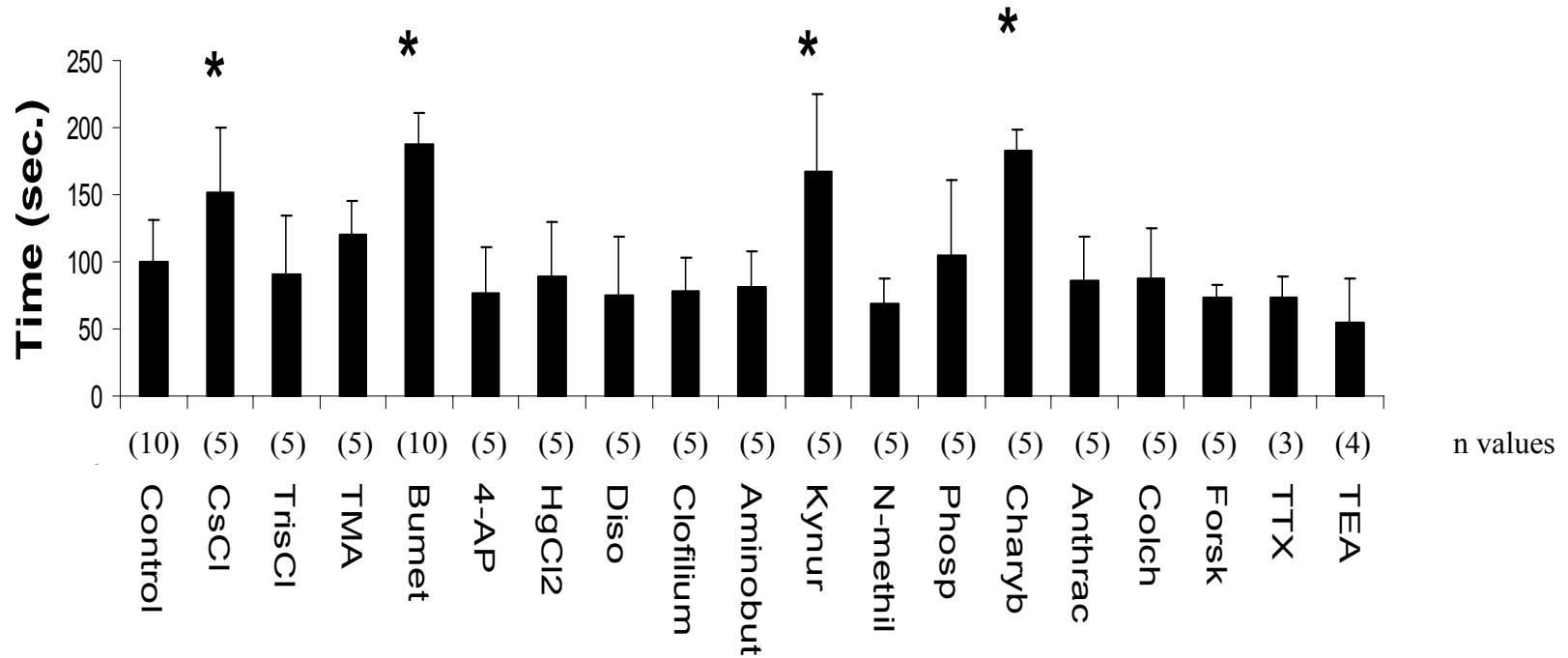
Figure 2.2. AQP4 BLOCKER DRUG SCREENING. The bursting time of Xenopus oocytes expressing aquaporin-4 water channels from several different groups were compared with a control group from the same preparation. The groups with asterisks were selected for a more quantitative swelling assay experiment. non-treated group (Control), cesium chloride (CsCl), tris hydrochloride (TrisCl), tetramethylammonium chloride (TMA), bumetanide (Bumet), 4-amino-pyridine (4-AP), mercury chloride ($HgCl_2$), disopyramide (Diso), clofilium tosylate (Clofilium), 3-aminobutanoic acid (Aminobut), kynurenic acid (Kynur), N-methyl-D-aspartate (N-Methyl), phosphopentanoic acid (Phosp), charybdotoxin (Charyb), anthracine (Anthrac), colchicines (Colch), forskolin (Forsk), tetrodoxin (TTX), tetraethyammonium chloride (TEA).

Treatment	AQP4 wild type	CsCl	Tris Cl	TMA	bumet	4AP	$HgCl_2$	diso	clofilium
AV	336.56	434.20	258.60	346.40	537.50	221.60	257.20	217.20	224.60
STDEV	74.40	140.10	129.74	70.36	69.62	97.18	115.77	124.32	72.87
AV (#)	100	151.11	90.00	120.56	187.07	77.12	89.51	75.59	78.17
STDEV (#)	31.80	48.76	45.15	24.49	24.23	33.82	40.29	43.27	25.36
n values	24	5	5	5	10	5	5	5	5

aminobut	kynur	N-Methyl	Phosp	charyb	anthrac	colchicine	forsk	TTX	TEA
233.00	480.00	232.80	349.80	614.40	290.00	292.6	244.60	244.67	181.75
74.84	164.34	60.84	190.83	52.41	107.88	127.60	35.10	56.44	112.25
81.09	167.05	69.17	103.94	182.56	86.17	86.94	72.68	72.70	54.00
26.05	57.20	18.08	56.70	15.57	32.05	37.91	10.43	16.77	33.35
n values	5	5	5	5	5	5	5	3	4

Table 2.4. AQP4 BLOCKER DRUG SCREENING. Shows the average (AV) and standard deviation (STDEV) of bursting time in seconds of aquaporin-4 expressing oocytes (oocytes were injected with 3ng RNA) incubated with normal saline and saline with drug candidates (see **Figure 2.2**) for 5 minutes. It also shows AV and STDEV of the bursting time corrected (#) for the aquaporin-4 wild type.
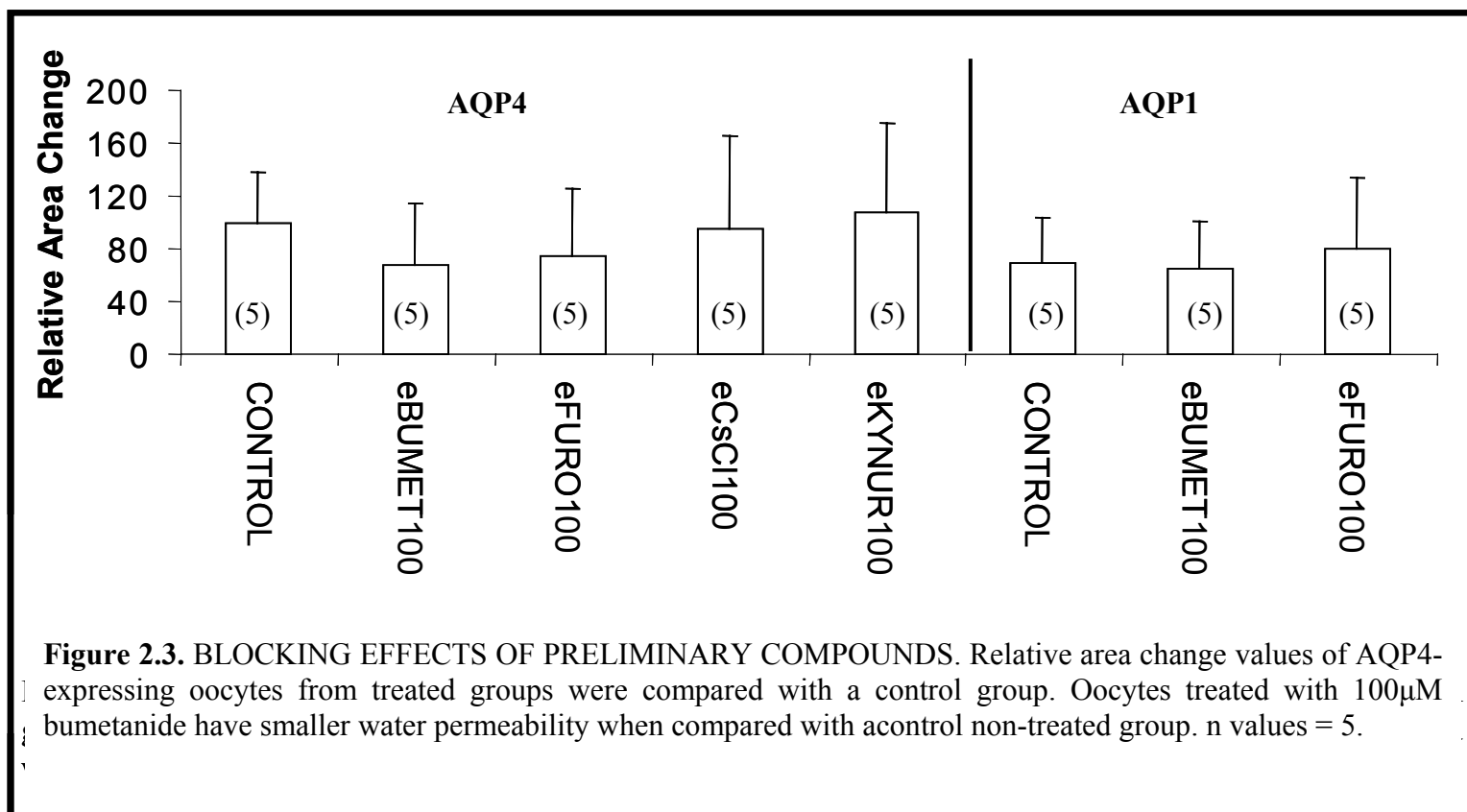
Figure 2.3. BLOCKING EFFECTS OF PRELIMINARY COMPOUNDS. Relative area change values of AQP4-expressing oocytes from treated groups were compared with a control group. Oocytes treated with 100μM bumetanide have smaller water permeability when compared with acontrol non-treated group. n values = 5.

Groups	100µM bumet	100µM furo	0.1µM charab	25mM CsCl	100µM kynur	AQP1 wt	100 µM bumet	100 µM furo
Mean	35.60	38.81	31.49	42.74	48.52	38.95	37.02	42.50
stdev	25.25	25.34	23.38	30.55	28.33	19.92	20.21	24.73
n values	5	5	5	5	5	5	5	5

Table 2.5. BLOCKING EFFECTS OF PRELIMINARY COMPOUNDS. Shows the average (AV) and standard deviation (STDEV) of relative area change in seconds of AQP4 expressing oocytes and AQP1 (oocytes were injected with 3ng AQP4 and AQP1 RNA) incubated with normal saline and saline with drug candidates (100µM bumetanide(bumet), 100µM furosemide (furo), 0.1µM charybdotoxin (charyb), 25mM CsCl, 100µM kynurenic acid (kynur), AQP1 wild type (wt), 100µM bumetanide (bumet), 100µM furosemide (furo)) for 5 minutes. The values are corrected for the mean value of the AQP4 non-treated group.

Figure 2.4. DOSE-RESPONSE OF AQP4- EXPRESSING OOCYTES TREATED WITH BUMETANIDE. Relative area change values of oocytes treated groups were compared with a control group (bigger graph). Blocking effect (smaller graph) was calculated by correcting the treated value to the previous control RCA for every oocyte. Increased bumetanide concentrations showed a proportional increased blocking effect in water permeability of oocytes when compared with a non-treated group.
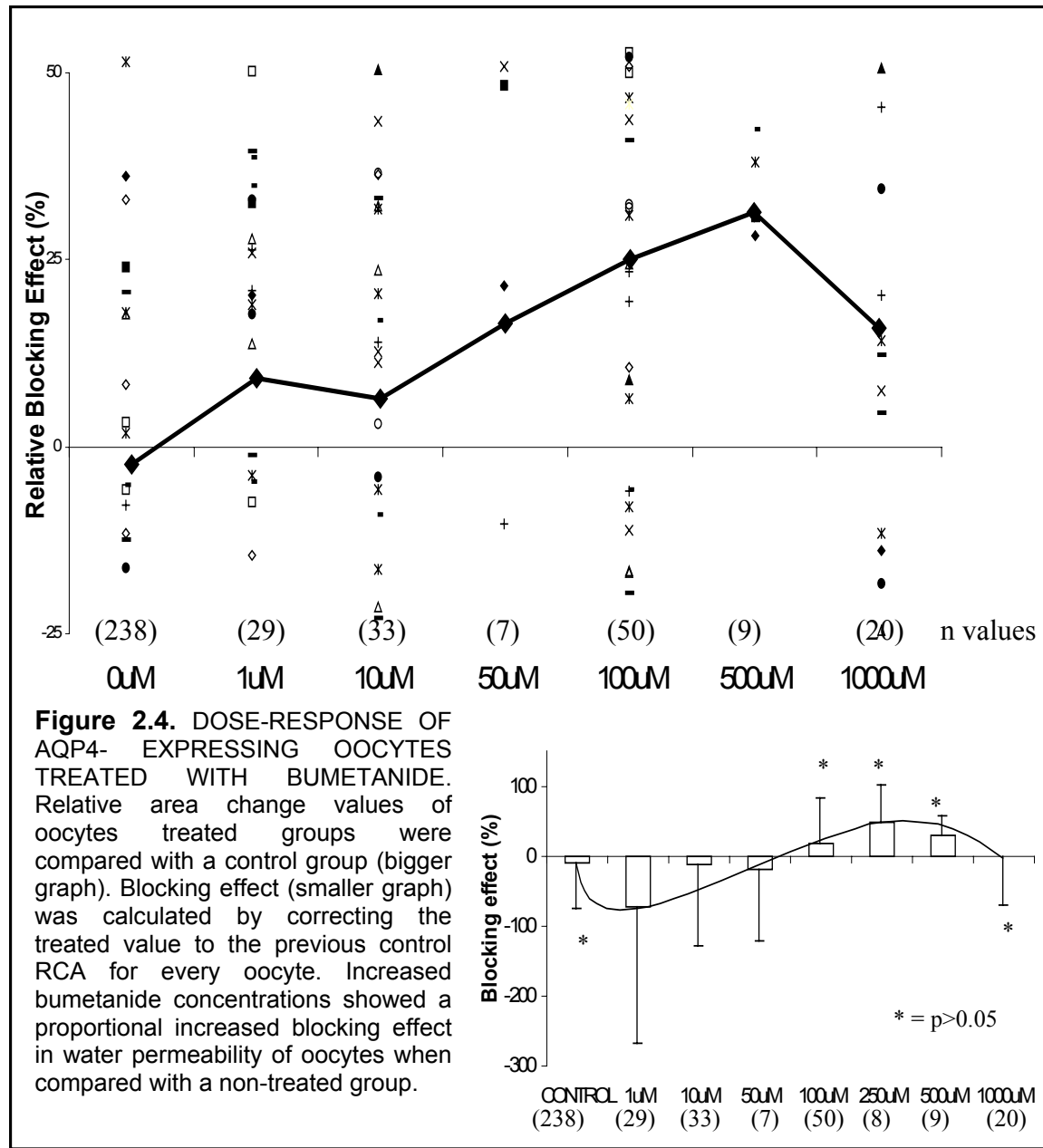
Groups	1μM bumet	10μM bumet	50μM bumet	100μM bumet	500μM bumet	1000μM bumet
Mean	90.87	93.60	83.56	75.01	68.68	84.05
stdev	56.38	52.61	65.75	52.66	39.97	36.57
n values	29	33	7	50	9	20

Table 2.6. DOSE RESPONSE OF BUMETANIDE TREATED OOCYTES. Shows the average (AV) and standard deviation (STDEV) of relative area change in seconds of AQP4 expressing oocytes (oocytes were injected with 3ng AQP4 RNA) incubated with normal saline and saline with increased bumetanide (bumet) concentration (1, 10, 50, 100, 500, 1000μM) for 5 minutes. The values are corrected for the mean value of the AQP4 non-treated group.

Figure 2.5. RECOVERY EFFECT OF AQP4-EXPRESSING OOCYTES AFTER BUMETANIDE TREATMENT. Relative area change values of oocytes from treated groups were compared with a control group. Recovery effect was calculated by correcting the recovery value to the previous control RCA for every oocyte. No residual effect in water permeability of oocytes when compared with a
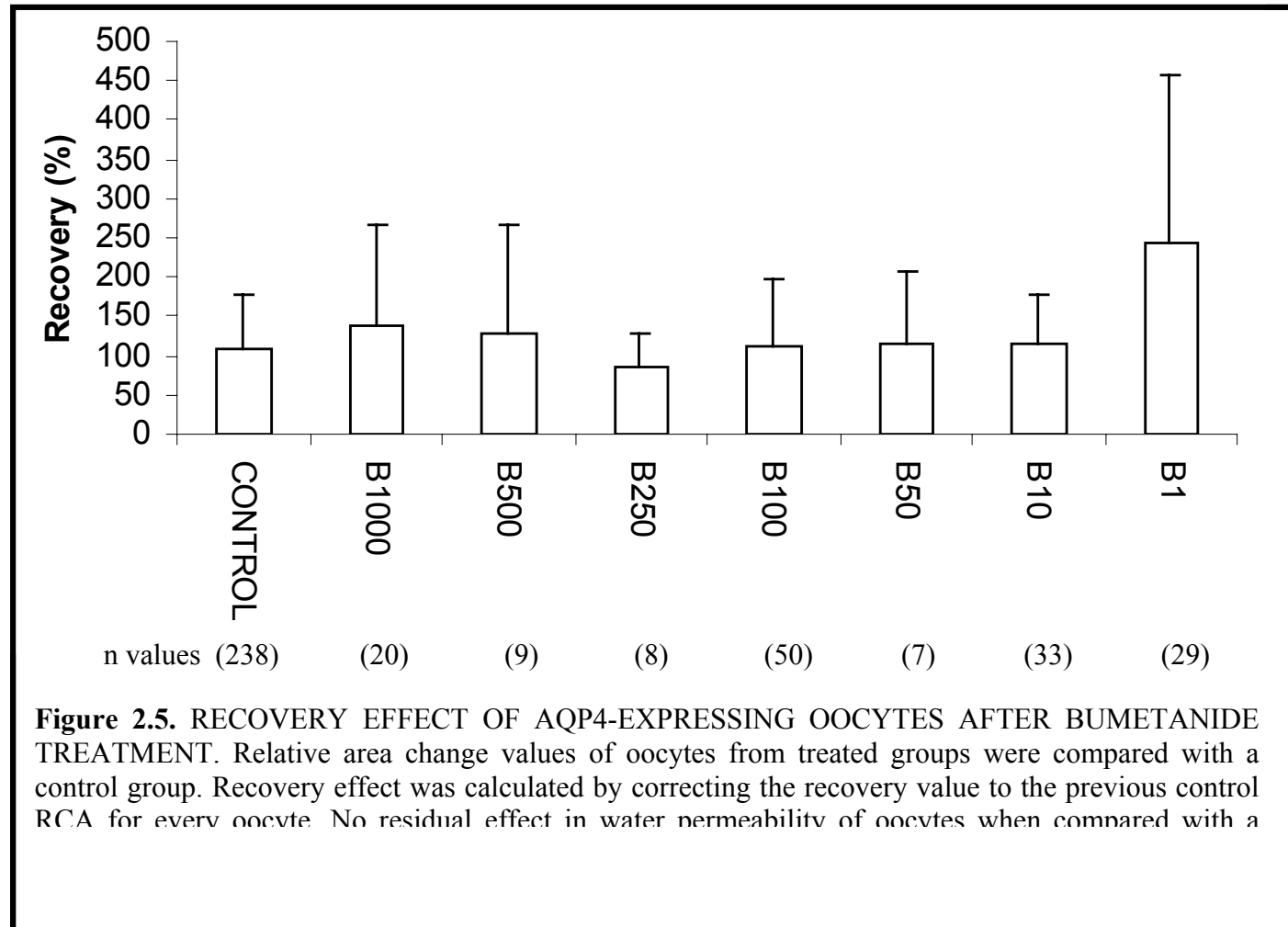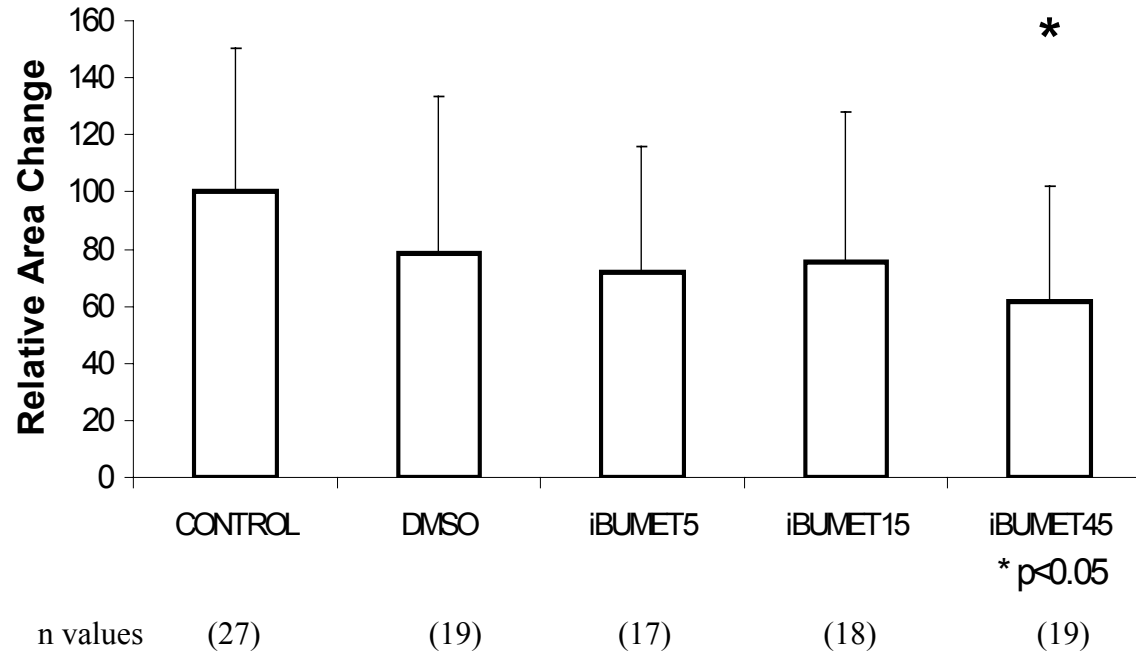
Figure 2.6. INTRACELLULAR ADMINISTRATION OF BUMETANIDE. Relative area change values of oocytes from treated groups were compared with a control group. Oocytes treated with 45μM intracellular bumetanide have smaller water permeability when compared with a control non-treated group

Groups	DMSO	5µM bumet	15µM bumet	45µM bumet
Mean		72.13	75.39	61.39
stdev		44.01	52.79	40.90
n values	19	17	18	19

Table 2.7. INTRACELLULAR ADMINISTRATION OF BUMETANIDE. Shows the average (AV) and standard deviation (STDEV) of relative area change in seconds of AQP4 expressing oocytes. Oocytes were injected with 3ng AQP4 RNA plus DMSO and increased concentration of bumetanide (bumet) (5, 15, 45µM). The values are corrected for the mean value of the AQP4 non-treated group.

Figure 2.7. BUMETANIDE DERIVATIVES AQP4-EXPRESSING OOCYTE TREATMENT. Relative area change values of oocytes from treated groups were compared with a control group. Oocytes treated with 100μM extracellular bumetanide #3 have smaller water permeability when compared with a non-treated group.
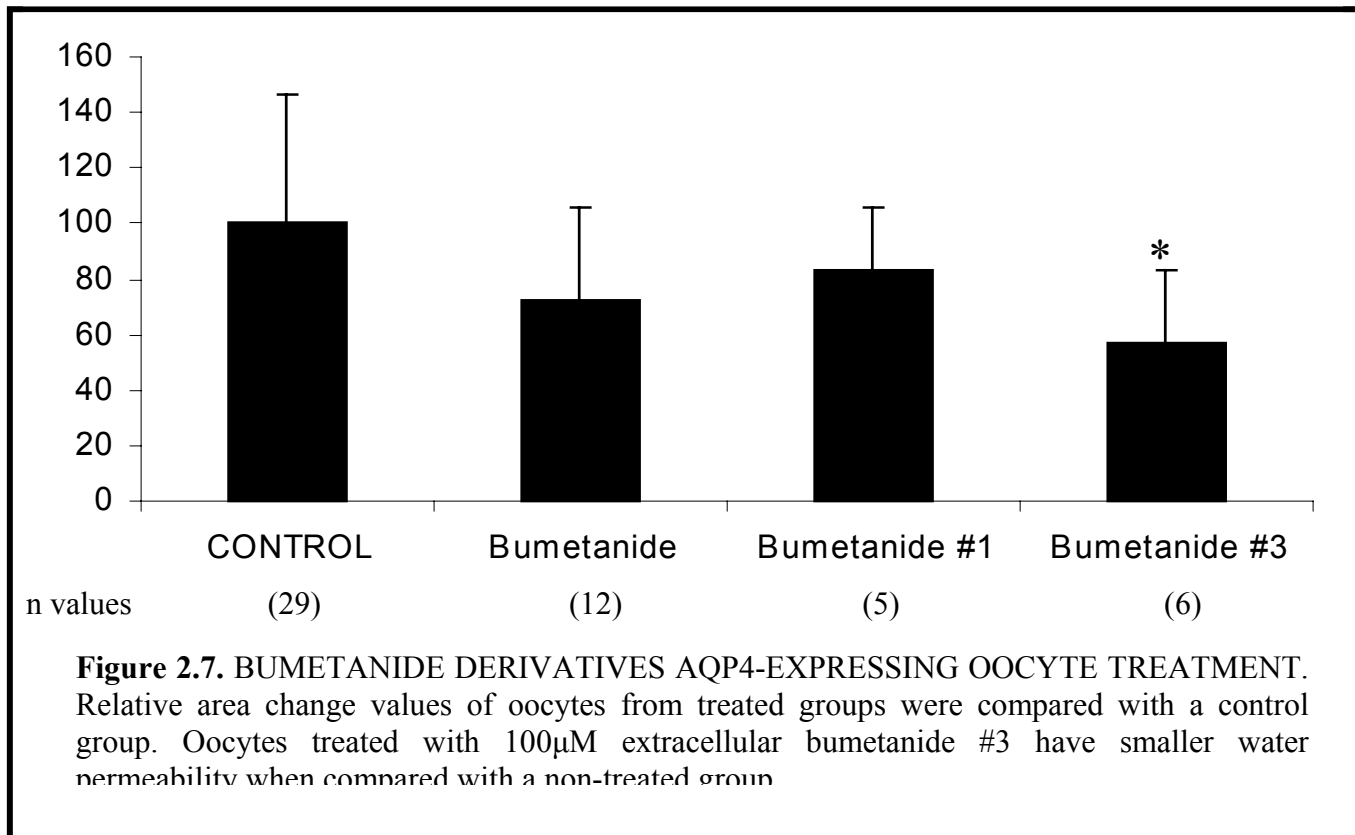
Groups	100μM bumet	100μM bumet #1	100μM bumet #3
Mean		83.03	56.61
stdev		22.53	26.38
n values	12	5	6

Table 2.8. BUMETANIDE DERIVATIVES AQP4-EXPRESSING OOCYTE TREATMENT. Shows the average (AV) and standard deviation (STDEV) of relative area change in seconds of AQP4 expressing oocytes (oocytes were injected with 3ng AQP4 RNA) incubated with normal saline and saline with 100μM bumetanide (bumet), 100μM bumetanide derivative #1 (bumet #1), and 100μM bumetanide derivative #3 (bumet #3) for 5 minutes. The values are corrected for the mean value of the AQP4 non-treated group.

Figure 2.8. BUMETANIDE BIDING-SITE DETERMINATION ON AQP4-EXPRESSING OOCYTES. Relative area change values of oocytes from treated groups were compared with a control group. Wild type oocytes treated with 100μM extracellular bumetanide have smaller water permeability when compared with a control non-treated group
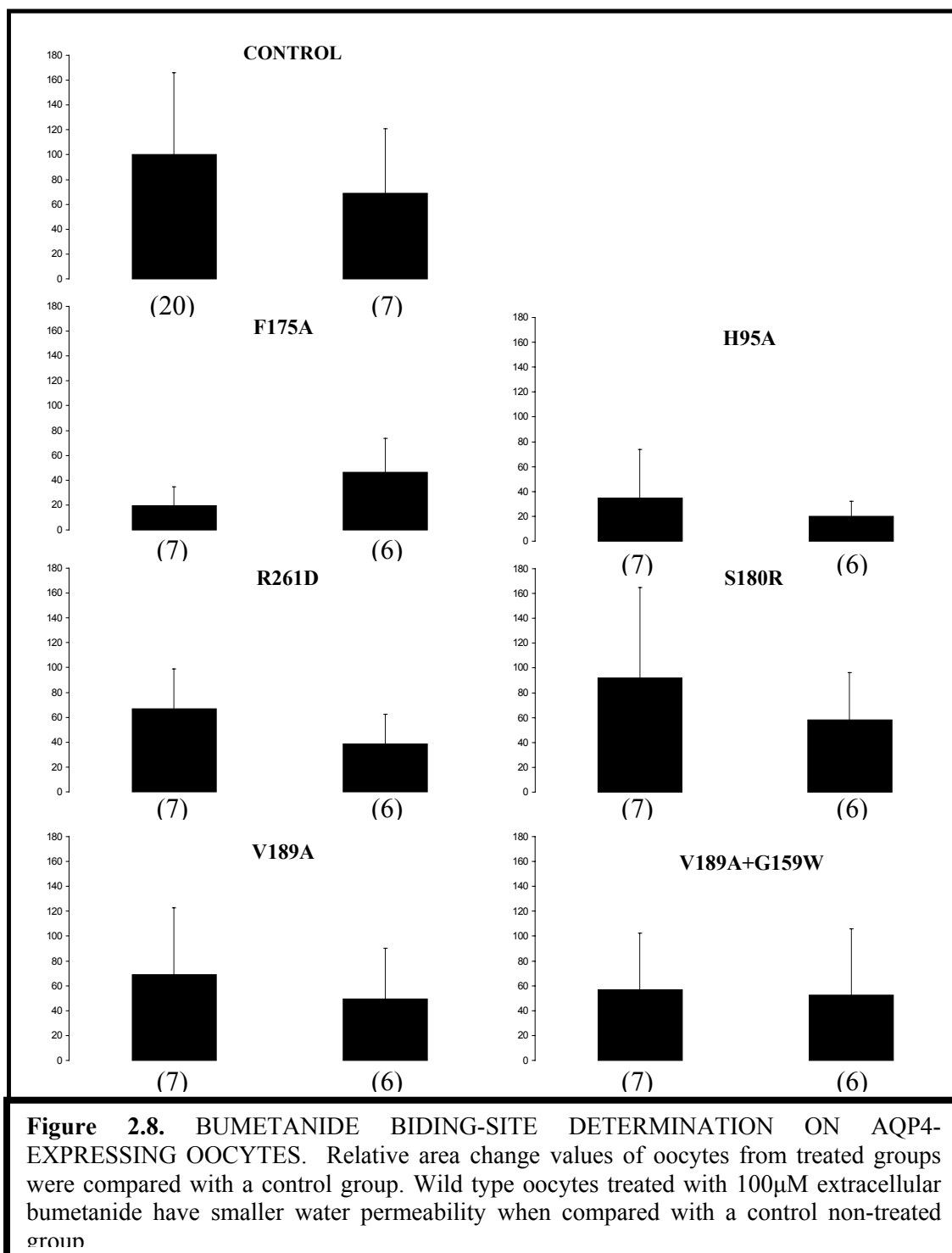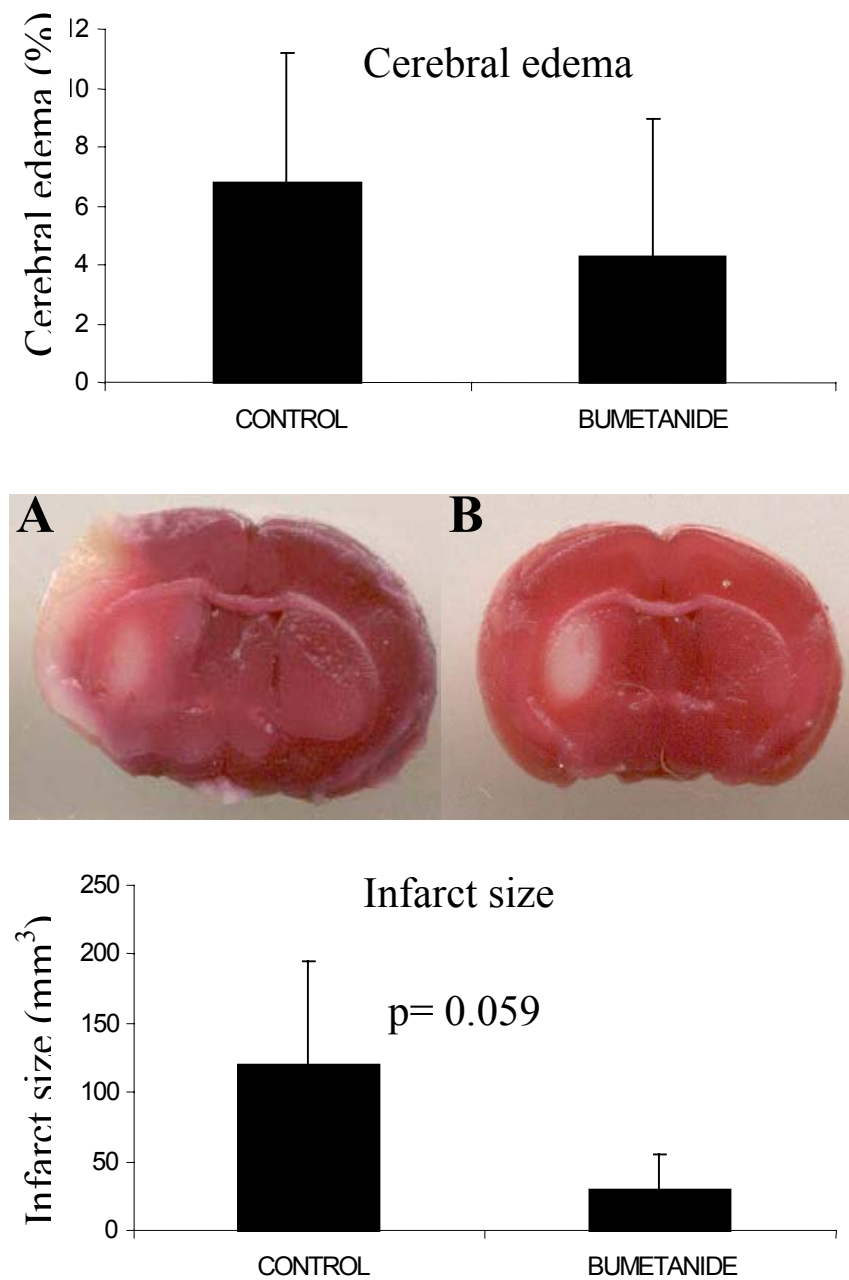
Figure 2.9. CEREBRAL EDEMA AND INFARCT SIZE DETERMINATION. Cerebral edema and infarct size of C57Bl/6J male mice subjected to 1hr ischemia and 24hrs reperfusion. A- shows a representative brain slice stained with TTC from a placebo-treated animal and B- shows a representative brain slice from bumetanide-treated animal.

Groups	Control IS	Bumetanide IS	Control CE	Bumetanide CE
Mean	120.55	29.14	6.81	4.28
stdev	74.38	25.27	4.39	4.64

Table 2.9. CEREBRAL EDEMA AND INFARCT SIZE DETERMINATION. Shows the average (AV) and standard deviation (STDEV) of infarct size (IS) and cerebral edema (CE) in control non-treated and bumetanide treated C57Bl/6J mice. All animals were subjected to 1hr ischemia and 24hrs reperfusion. Bumetanide was administered to achieve an estimated 100μM plasma concentration.

CHAPTER 3. EVALUATION AND CHARACTERIZATION OF *MDX* KNOCK OUT MICE SUBJECTED TO ISCHEMIC STROKE.

Abstract

Several groups have proposed the involvement of aquaporin channels (AQP) in the pathophysiology of brain edema. AQP4 deficient mice had a protective effect after permanent ischemia and water intoxication. Another knockout mouse, α-syntrophin, that mistarget the AQP4 protein to the cellular membrane also showed less cerebral edema after transient ischemia and reperfusion. Dystrophin deficient mice, that had a decreased expression of AQP4 by 90%, also reveal protective effects after water intoxication. To our knowledge, no studies have been performed to characterize the effects of transient ischemia and reperfusion in dystrophin deficient mice. The purpose of this study was to evaluate the physiological response of dystrophin deficient (*mdx)* mice, C57Bl/10ScSnDMD<MDX>J, after ischemic stroke using a filament method. We hypothesized that the absence of aquaporin-4 water channels at the blood-brain barrier would decrease the formation of cerebral edema after ischemic stroke in mice. We found significant differences in ipsilateral brain water content formation after ischemic stroke in *mdx* (dystrophin deficient) mice when compared with all other strain controls. We also found that *mdx* mice showed increased mortality and increased epileptic-like activities that might be related with a higher plasma K^+ concentration when compared with other strains.

Introduction

Stroke is a devastating disease; with a mortality rate near 30% it is the third leading cause of death in the United States when considered separately from heart disease (**6**, **7**). Brain edema, characterized by water accumulation in the brain tissue, is an acute, serious complication in stroke, often determining the clinical outcome. The mortality of progressive cerebral edema after middle cerebral artery strokes approaches 80% (**10**). The propensity of ischemic brain tissue to develop edema and swelling remains the major cause of death in patients with large infarctions, particularly for those occurring within the middle cerebral artery territory and cerebellum (**9**). Therefore, the understanding of brain edema mechanisms is a major area of research.

Several groups have proposed the involvement of aquaporin channels in the pathophysiology of brain edema (**127**, **134**, **135**, **72**). The mammalian aquaporin family has 11 members and are transmembrane proteins that assemble as homotetramers. AQP4 is abundantly expressed in ependymal cells and astrocytes (**71**, **145**), with a highly polarized distribution in glial membranes to face the capillaries and pia mater (**75**). AQP4 is abundant in Müller glial cells with a polarized distribution at the end feet process. It colocalizes with the inward rectifying K^+ channel Kir4.1 (**146**, **147**, **148**). This supports the view that AQP4 may serve a role in activity dependent water and K^+ redistribution; clearance of K^+ by astrocytes serves to maintain the extracellular space homeostasis after neuronal activity. By short-circuiting osmotic gradients and by directing water flux to specific extracellular compartments, AQP channels facilitate K^+ clearance. AQP1 and AQP9 are also expressed in normal brain, but the distribution appears to be limited to the

choroid plexus, glia limitans and tanycytes (**77**) reinforcing the importance of AQP4 in water transport through the blood-brain barrier (BBB).

A knockout mouse is a genetically engineered mouse in which one or more genes have been made inoperable. Knockout is a route to learning about a gene that has been sequenced but has an unknown or incompletely known function. AQP4-deficient mice are surprisingly normal in terms of neurological function and macroscopic neuro-anatomy. Two other knockout models also interfere with the normal expression of AQP4 at the astrocytic end feet plasma membrane. Dmd^{mdx} mice (C57BL/10ScSnDMD<mdx>J) have a decreased expression of AQP4 protein (by 90% in adult mdx mice) without changes in the AQP4 mRNA levels; while the disruption of α-*syn* gene (α-Syntrophin is a member of the dystrophin-associated protein membrane complex and play an important role in connecting the cytoskeleton to the extracellular matrix) indicates that the protein is essential for localization of AQP4 protein in astrocyte end-feet membrane domains adjacent to brain capillaries (**149**). In contrast to findings in the Dmd^{mdx} mice (**150**), immunoblots of brain and cerebellar samples from the *α*-syntrophin knockout mice revealed that AQP4 protein expression was quantitatively unchanged (**149**).

AQP4 deletion or mislocalization in mice reveal several improved outcomes compared to strain matched control when subjected to four classic models of cerebral edema: permanent or transient middle cerebral artery occlusion (MCAO), water intoxication, freeze-injury model and continuous intracerebral fluid infusion. The absence of AQP4 channels were linked with smaller mortality rate, improved clinical outcome or smaller neurological deficit, decreased pericapillary astrocytic foot process swelling,

smaller intra cranial pressure (ICP) and brain water content, decreased cerebral edema and infarct volume in those experiments. Experimental data by Verkman and colleagues reveal worse clinical outcome and ICP in AQP4 null mice after brain tumor implantation also supports the conclusion that AQP4 facilitates removal of excess brain water in vasogenic edema (**151**). AQP4-null mice and dystrophin null (*mdx*) mice had differences in survival after water intoxication and that might be in part related to baseline morphological alterations found in the dystrophin null mice such as increased BBB permeability (**77**), which may enhance the transport of water from the intravascular space to the brain thereby increasing cerebral edema and worsening outcome. To our knowledge, no studies have been done to evaluate cerebral edema in *mdx* mice after ischemic stroke.

The purpose of this study was to evaluate the physiological response of dystrophin deficient (*mdx)* mice, C57Bl/10ScSnDMD<MDX>J, after ischemic stroke using a filament method. We hypothesized that the absence of aquaporin-4 water channels at the blood-brain barrier would decrease the formation of cerebral edema after ischemic stroke in mice.

Material and Methods

Middle Cerebral Artery Occlusion in Mice.

C57Bl/6J, C57Bl/10SnJ and C57Bl/10ScSnDMD<mdx>J mice (male and female, 8-10 weeks, 20-25g) were obtained from Jackson Laboratories and housed at the

approved University Animal Care facility at the University of Arizona, with free access to food and water. All mouse procedures were approved by University Animal Care & Use Committee in accordance with IACUC guidelines. Mice were housed in a quiet room before surgery. Mice undergoing surgery were divided into 4 groups: C57Bl/6J male (6JM), C57Bl/6J female (6JF), C57BL/10SnJ female (SnJF) and C57Bl/10ScSnDMD<mdx>J female group (*mdx*).

Animal Preparation

The purpose of this experiment is to test the effect of an aquaporin-4 channel blocker in the cerebral edema formation after ischemic stroke. C57Bl/J mice (male, 8-10weeks, 20-25g) were obtained from Jackson Laboratories and housed with free access to food and water at the University Animal Care Facility at the University of Arizona. All mouse procedures were approved by the University Animal Care and Use Committee in accordance with IACUC guidelines. Mice were housed in a quiet room before surgery. All mice were subjected to temporary occlusion (60 min) of the right middle cerebral artery with the silicone-coated filament technique and 24hrs reperfusion (**figure 2.1**), as previously described (**138**).

Briefly, the animals were anesthetized via inhalation mask with 3.0V% isofluorane and maintained with 1.5% to 1.75% isofluorane in a mixture of 30% oxygen and 70% nitrox. Rectal temperature was monitored and held constant during surgery using a thermostatically regulated heating lamp. A skin incision in the right temporoparietal area was made, the temporalis muscle was retracted, and a microtip of

the laser-Doppler probe (Periflux system 5000, Perimed, Stockholm, Sweden) was placed on the skull surface (bregma 0 and 6 mm, probe tip 0.5 mm in diameter) to monitor blood flow from the beginning of the time of anesthesia until 15 min after removal of the occluding filament (**Figure 2.1**). The common carotid was occluded with a slip knot immediately before filament placement, and remained occluded during the total ischemic period. A 7-0 monofilament silicone-coated nylon surgical suture with a diameter varing between 150-250μm was prepared the day before the experiment. The occluding filament was threaded through the external carotid and into the internal carotid, up to the bifurcation to the middle cerebral artery. MCAO was considered successful if there was greater than 85% reduction in blood flow, compared to baseline values, throughout the entire ischemic period. For the following 60 minutes, the animal remained untouched under constant conditions. At the end of the ischemic period, the filament was withdrawn, the external carotid artery stump was tied, the common carotid artery was untied, and reperfusion was confirmed by laser Doppler (>50% of baseline). The animals were then permitted to recover from anesthesia at room temperature and sheltered from drafts. In all experimental animals, blood flow returned to near pre-MCAO levels within 15 min of the removal of the suture.

Mice undergoing surgery were divided into 2 groups, a control and a treated group. Animals in the treated group were given 60mg/kg of bumetanide to achieve a plasma concentration of 100uM bumetanide 10 minutes before reperfusion and animals in the control non-treated group were administered placebo-saline. Placebo-saline or saline plus bumetanide were administered intravenously in the jugular vein.

Neurological Function

At 24 hours after reperfusion, the animals were scored for neurological deficit by a 28-point focal scoring system. The neurological exam was combined from studies by Clark and colleagues (**138**) and Hurn and colleagues (**139**), who used the exams to describe postischemic neurologic deficits in mice.

Cerebral Edema and Infarct Size Determination

After neurological scoring, the mice were deeply anesthetized with isoflurane inhalant and euthanized by cervical dislocation. Brains were isolated rapidly, the olfactory bulb and cerebellum were removed, and the brain was sectioned into four 2-mm slices. These slices were placed in a well plate containing 2% tetrazolium chloride (TTC) solution (Sigma-Aldrich, Inc.) and allowed to develop for 30 minutes. TTC stains the live mitochondria and therefore isolates the live tissue (red) from the dead tissue (white). The tissue was then placed in 10% formalin and all slices were scanned in a table top light scanner, and images were captured with Adobe Photoshop (7.0). The National Institutes of Health Image Analysis program (ImageJ software-\; Scion Image Co.) was then used to measure the area of ischemia and total hemisphere area. Cerebral edema was measured by subtracting the total contralateral volume from the total ipsilateral volume divided by the total contralateral volume and expressed and percentage (**140**).

$$\text{Edema (\%)} = \frac{\text{(Total ipsil. volume-total contralat. volume)}}{\text{Total contralat. volume}} *100$$

Total infarct volume was calculated by adding the product of the measured infarct area in each slice by 2 (since each slice is 2 mm thick). To partially correct for effects of edema on the ipsilateral side, infarct volumes were corrected by (**140**):

Infarcted volume (mm^3) = Σ (Infarcted area *(total Ipsil. area / total contralat. area) * 2)

Dehydration

Previous experiments done in our laboratories showed that mice subjected to 1h ischemia and 24h reperfusion lost approximately 10% of the body weight (data not shown). We concluded that water intake deprivation after surgical procedure leads to body weight loss and possibly dehydration. To avoid dehydration, animals were injected immediately after ischemia with 150μl/per gram of sterile PBS saline in the subcutaneous space for slow absorption. To address this additional experimental variable, mice were evaluated for dehydration by monitoring urine osmolarity before surgery and after reperfusion monitoring urine osmolarity, plasma Na$^+$, K$^+$, and Cl$^-$ concentrations and plasma osmolarity. All samples were stored at -20°C overnight and submitted to University Animal Care laboratory for testing.

All results are expressed as mean ± Standard Deviation. ANOVA and post hoc (Holm-Sidak method) were used to assess the significant differences in cerebral edema

Results

Dehydration

Table 3.2 illustrates that, although there were no significant difference between the strains in any variable, plasma K^+ concentrations were elevated in *mdx* mice. Previous studies (**152**) were done to evaluate the normal plasma electrolyte concentration in *mdx* mice and found that plasma K^+ increases over time after first week of life. **Table 3.2** also indicates that plasma electrolyte concentration in *mdx* mice returns to normal values after the surgical procedure.

Cerebral edema in mdx mice

Figure 3.2 is a TTC stained brain slice illustrating the extent of edema in a C57Bl male animal. **Figure 3.3** indicates the results of cerebral edema analyses in 6JM, 6JF, 10SnJ, and *mdx* mice. The results indicate that both 10SnJ and *mdx* mice have a reduced edema formation when compared with the male and female C57Bl/6J (**table 3.3**).

Wet-to-dry measurements

Using this method (**figure 3.4**), we found that there was significant difference in cerebral edema between *mdx* mice and all other strains. 6JM, 6JF, and 10SnJ also have a significant increase in brain water content in the ipsilateral side compared to the contralateral side. The *mdx* mice did not have a significant increase in brain water content demonstrating a protective effect in the *mdx* knockout animals. (**Table 3.4**).

Infarct size

Figure 3.5 indicates the results of infarct size analyses conducted in 6JM, 6JF, 10SnJ, and *mdx* mice. There was no significant difference in infarct size between groups. There was a non-significant decrease in infarct size (cubic mm) in 10SnJ and *mdx* mice when compared with both male and female C57Bl/6J (**Table 3.5**).

Mortality rate

Mdx mice had a higher mortality rate (**figure 3.6**) (35.29%) when compared with all other strains (23.08, 15.38, 16.67%). Mortality was measured at any period after the end of the surgery and was not significant (**table 3.6**).

Seizures

We also found that 40% of the *mdx* mice presented with epileptic behavior after 1 h ischemia and 24 h reperfusion (**figure 3.6**). No other animal in any group (male and female C57Bl/6J and C57Bl/10SnJ female) displayed any epileptic behavior.

Neurological outcome

Figure 3.7, indicates the results of the assessments of neurological outcomes in 6JM, 6JF, 10SnJ, and *mdx* mice. We found that there was no difference in neurological outcomes between *mdx* and all other strains.

Discussion

We found that ipsilateral brain water content (BWC) was significantly decreased in C57Bl/10ScSnDMD<mdx>J mice when compared with all other strains. Those findings suggest that *mdx* mouse has a decrease cerebral edema formation when compared with all other strains.

Most studies using mice for understanding the mechanisms of cerebral edema after ischemic stroke have not examined daily water intake, and consequently, the effects of dehydration of water deprivation after cerebral ischemia and reperfusion have not been considered. Average water intake in mice varies between strains. The average 24-h water intake for a 30g mouse is 3-10 ml (**153**), although the majority of studies showed an average of 4ml/per day per animal (**154**). This represents a daily water intake between 150-250μl per gram per day. Another study indicates that activity started shortly after lights off and consumption rose to a peak of 0.9 ml/h during the first half of the dark phase, which, in our experimental setting, represents 6-10 h after the induction of ischemic stroke. During the dark phase, water uptake was significantly higher than during the light phase (**155**). Studies showed that average urine output is 2-3ml (**156**, **157**, **158**). Another study showed that 24hr deprivation was showed to increase plasma concentration and cause weight loss in mice (**159**). These values can increase remarkably in genetically modified animals as showed in **Table 3.1.**

AQP4-deficient mice urine concentrating ability was also evaluated from urine osmolalities after a 36-h water deprivation (**159**) No significant differences in urine osmolalities were found in hydrated mice (just before the water deprivation period). Serum sodium concentrations (ranging 151-161 mM) and osmolalities (ranging 304-335)

also did not differ significantly among hydrated mice of (+/+, +/-, and -/-) genotypes (n =2). However, there was a significant reduction in maximum urine osmolality in the (-/-) mice after a 36-h water deprivation. Urine osmolalities in mice dehydrated for 36 h did not increase further after desmopressin, a vasopressin analog, administration. These results demonstrate a mild urinary concentrating defect in the AQP4 null mice (**159**). To our knowledge no studies were done in *mdx* mice measuring water intake and urine concentrating abilities after water deprivation. Therefore, in prelimnary studies, we tested body weight loss in mice subjected to 1h ischemia and 24h reperfusion. Our preliminary results demonstrated that mice subjected to 1h ischemia and 24h reperfusion have a weight loss of about 10% of body weight. Therefore, to avoid dehydration effects after the water deprivation that follows the surgical procedure, we injected 150μl of PBS saline subcutaneously. Importantly, we found no differences in urine and plasma osmolarities between strains after stroke and reperfusion, and no animals presented with signs of dehydration.

Previous research showed that *mdx* mice have an increase in plasma K^+ starting after the first week of life and those values were sustained chronically. In our study plasma K^+ was significantly increased in *mdx* animals although the mean value was not above the normal values (7.5 mEq/L). Interestingly, after reperfusion, we found that K^+ values were not different from all other strains. A decrease in plasma K^+ is more likely to be related to the s.c. fluid administration.

Our results indicated a significant decrease in cerebral edema formation of *mdx*-deficient mice when compared with C57Bl/6J female (6J Female) control mice.

C57Bl/10SnJ (10SnJ Female) mice also had a significant decrease in cerebral edema formation when compared with C57Bl/6J female control mice. The fact the 10SnJ Female had a significant decrease in cerebral edema formation when compared with another control strain (6J Female) suggests that different mouse strains might be genetically different to the point that they might not be an appropriate control for ischemic stroke, and that could be the case of the 6J Female and the 10SnJ Female. Therefore, the fact that *mdx* mouse did not have a significant decrease in the cerebral edema formation when compared with 10SnJ Female could be related that the method is not sensitive enough to detect the differences of cerebral edema formation between *mdx* and 10SnJ animals.

The *mdx* deficient mice also did not reveal any protection after ischemic stroke as observed by the infarct size. Those results indicated that although *mdx* deficient mice had the same ischemic insult as the strain matched control, *mdx* had smaller edema formation when compared with all other strains. Another main difference between previous studies using aqp4 expression defective mouse and the experiments conduct in our laboratory is that there was an administration of saline solution in order to correct the dehydration effect. Since mice are sensitive to 24h water deprivation and AQP4 null mice had a decreased ability to concentrate urine we conclude that dehydration might be adding to the apparent beneficial protective effect of the deletion of AQP4 channels in cerebral edema. That might be adding to the decreased protection observed in *mdx* mouse when compared with strain matched controls.

In separate studies, *in vivo* EEG characterization of seizures induced by electrical stimulation in the hippocampus indicated greater electrographic seizure threshold and remarkably longer seizure duration in AQP4-null mice compared with wild-type mice (**31**). An important finding in our studies is that *mdx* mice presented with 29.41% of epileptic behavior after 1 h ischemia and 24 h reperfusion, while no other animal presented any epileptic behavior. This finding supports previous experiments (**74**), which indicated that AQP4 null mice and α-syntrophin deficient mice showed an increase in seizures activity. Our findings that *mdx* mouse have an increase in seizure activity after ischemic stroke supports the hypothesis that AQP4 and potassium channels $K_{ir}4.1$ mediates the buffering of K^+ in the extracellular space. We also were unable to find any improvements in neurological outcome of *mdx* deficient mice when compared with all other strains. All animals behaved equally on total neurological outcome after the ischemic event.

In summary, we hypothesized that acute water movement in cerebral edema is mediated by AQP4 and later water transport is occurring through the disruption of BBB. Our findings do support the role of AQP4 in cerebral edema in *mdx* mice. AQP4 channels are important in the formation and maintenance of the BBB. The formation of cerebral edema after ischemic stroke is demonstrated to start before the disruption of the BBB (**140**) and AQP4 channels might have a fundamental role in edema formation during this early time frame. If so, AQP4 channels may be novel target for neuroprotection after ischemic stroke. Our experiments did not test the mechanisms of early and late edema formation—we only tested edema after 24 h. Since cerebral edema is a dynamic

phenomenon, perhaps measuring the early and late phases of edema could be an important addition in the understanding of aquaporin-4 and cerebral edema involvement.
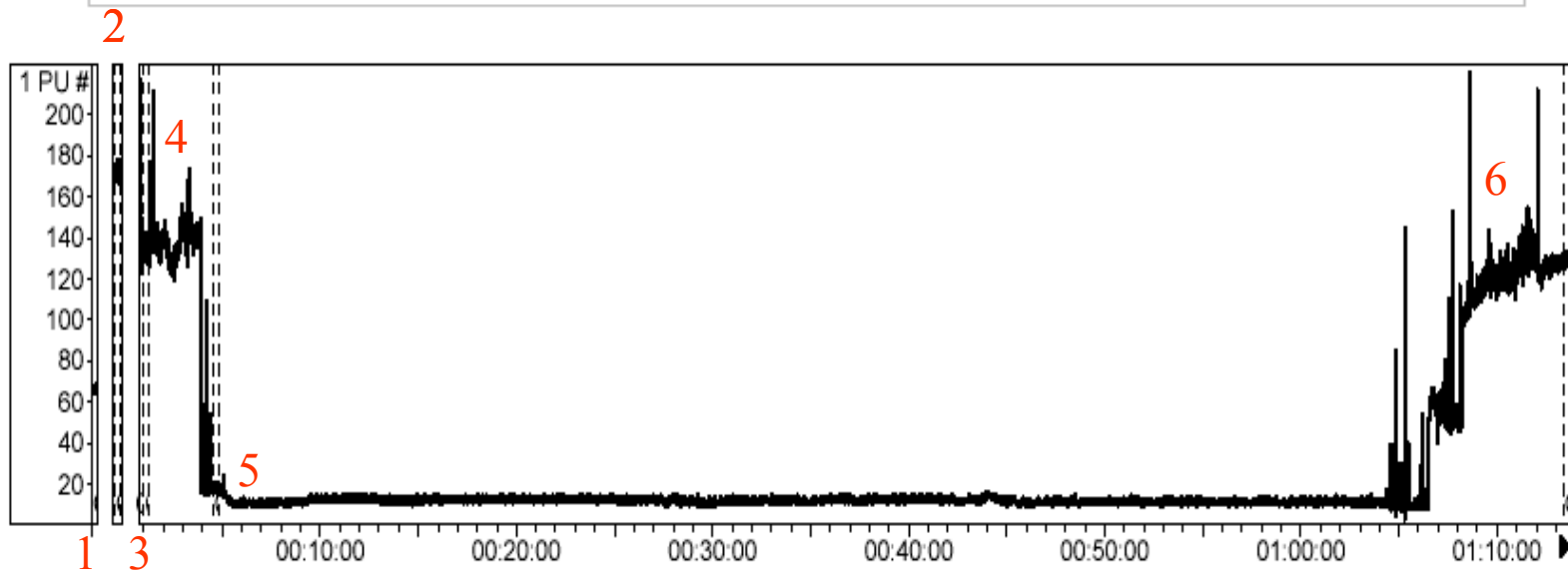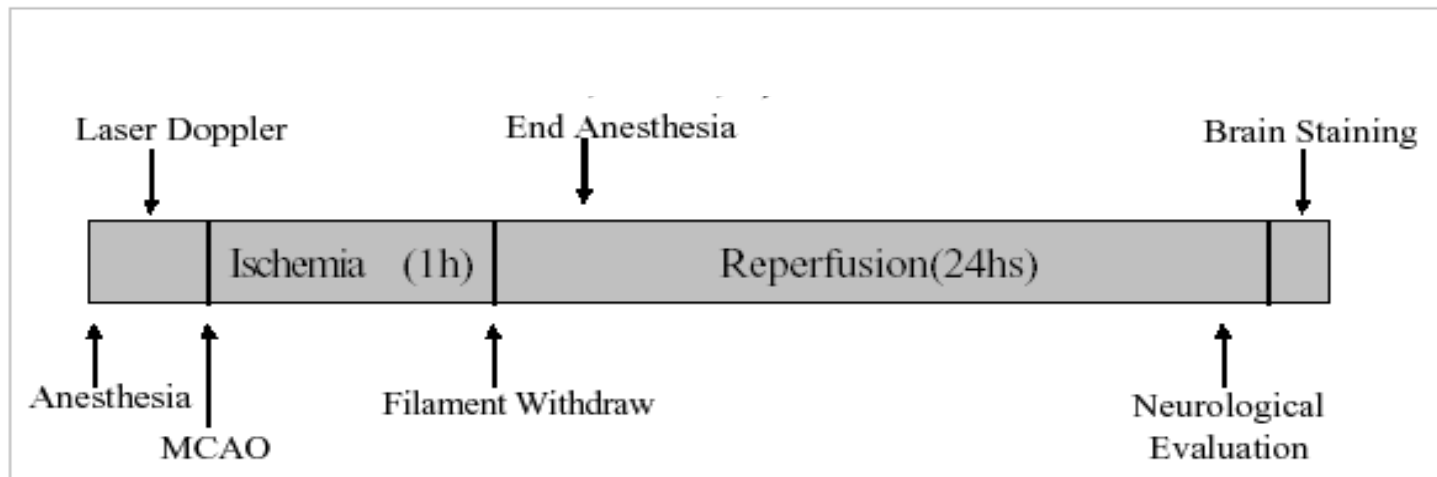
Figure 3.1. EXPERIMENTAL DESIGN TIME-LINE. It also reveal a representative Doppler flow recording from a C57BL/10ScSnDMD<mdx>J female mouse subjected to one hour of ischemia and 24 hrs of reperfusion. It also indicates absolute values and its percent reduction during ischemia. Numbers in red are placed to identify areas selected for calculation of blood flow changes. 1 baseline ventral position, 2 baseline dorsal position, 3 baseline immediately before ischemia, 4 after common carotid occlusion, 5 after filament placement, 6 after filament withdraw and common carotid release.

DWI	UO	AIUO	Strain	Reference
Increased fivefold			Os/+ (Diabetes insipidus)	**299**
Increased fourfold	Decreased		Angiotensin-deficient mice	**300**
Increased threefold	Decreased	Decreased	AQP1-deficient mice	**303, 304**
Increased eightfold	Decreased		AQP3-deficient mice	**305**
Increased three-fivefold	Decreased		Cl channel-deficient mice (CLC-k1)	**306**

Table 3.1. EFFECTS OF GENE DELETION ON RENAL PHYSIOLOGY. Demonstrates the effects of five different genetic knock out in daily water intake (DWI), urine osmolarity (UO) and ability to increase urine osmolarity(AIUO)

Groups	C57Bl/6J male	C57Bl/6J female	C57Bl/10SnJ female	C57Bl/10ScSnDMD<mdx>J
Baseline urine osmolarity	1435.67+ 363.93	841.67+ 400.11	1233.67+ 709.99	1209.33+ 350.61
Post reperfusion urine osmolarity	912+ 85.85	1444+ 447.23	1036+ 290.91	1241+ 506.48
Post reperfusion plasma osmolarity	294.67+ 4.16	275.33+ 18.78	269.33+ 11.59	282+ 11.14
Plasma electrolytes				
Na^+ baseline	172+5.66	177+21.21	147.33+26.10	221+100.41
Na^+ post reperfusion	193.33+20.53	138.4+16.83	128.33+7.37	140+5.66
K^+ baseline	4.7+0.14	4.8+1.13	4.77+1.00	7.1+1.56 *
K^+ post reperfusion	2.6+0.57	2.96+0.36	3.5+0.79	3.8+0.28
Cl^- baseline	134+12.00	136+11.31	111+16.82	166+70.71
Cl^- post reperfusion	100+56.57	100.6+14.48	103.33+8.08	96+5.66

Table 3.2. RENAL FUNCTION. Demonstrates mean and standard deviation values of urine osmolarity (before ischemia), urine osmolarity, plasma ions concentration, plasma osmolarity (after 24 h reperfusion) of animals subjected to 1 h middle cerebral artery occlusion and 24 h reperfusion. Osmolarity (mol/kg), ion concentration (mEq/l).(* $p > 0.05$)

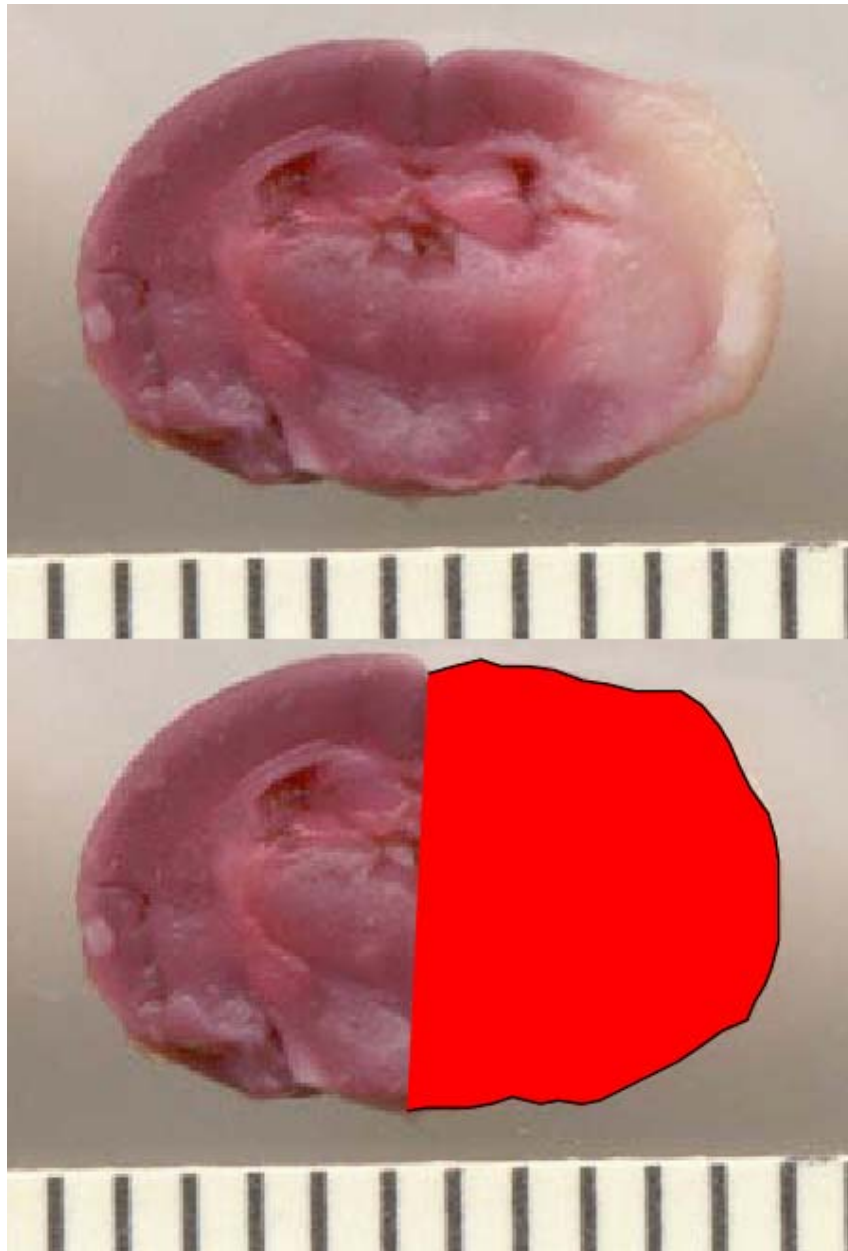**Figure 3.2**. ILLUSTRATIVE DRAWING OF CEREBRAL EDEMA MEASUREMENT.

Indicates cerebral edema (%) after 1 h ischemia and 24 h reperfusion in C57Bl/6J male

and a representative highlighted area used for edema measurement.
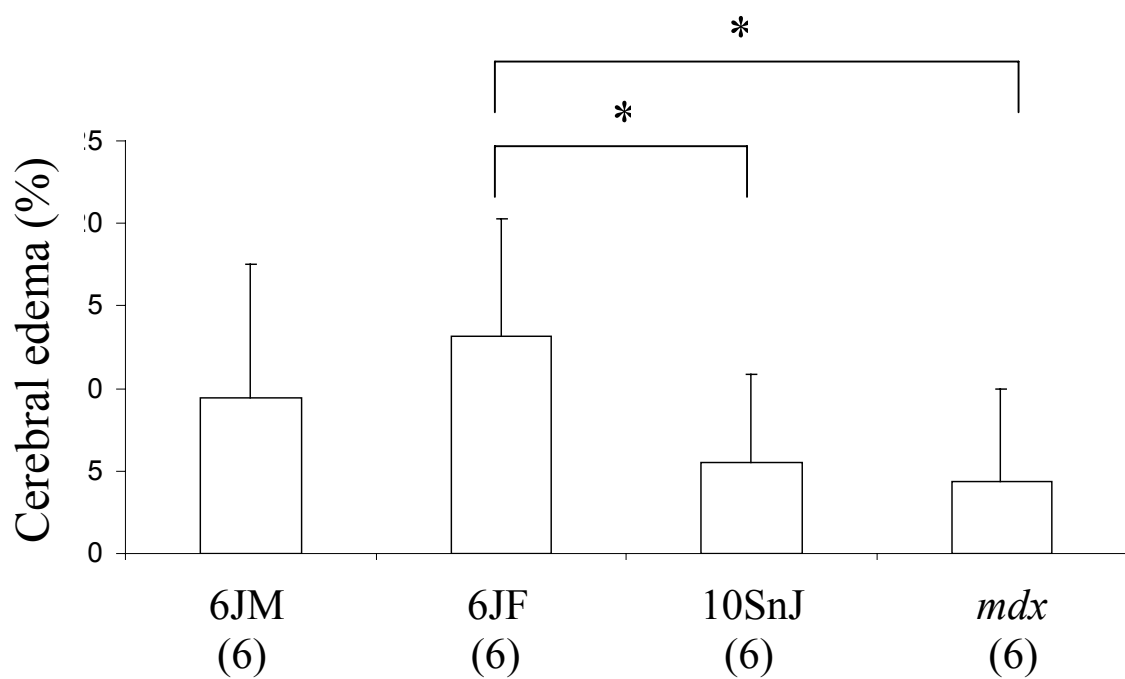
Figure 3.3. CEREBRAL EDEMA MEASUREMENT. Shows cerebral edema (%) after 1 h ischemia and 24 h reperfusion in C57Bl/6J male and female, C57Bl/10SnJ female and C57Bl/10ScSnDMD<mdx>J female mice. (* p>0.05)

Cerebral edema (%)	C57Bl/6J male	C57Bl/6J female	C57Bl/10SnJ female	C57Bl/10ScSnDMD<mdx>J female
Average	9.39	13.13	5.51	4.38
Standard Deviation	8.15	7.17	5.30	5.60

Table 3.3. CEREBRAL EDEMA MEASUREMENT. Shows average and standard deviation of cerebral edema (%) after 1 h ischemia and 24 h reperfusion in C57Bl/6J male and female, C57Bl/10SnJ female and C57Bl/10ScSnDMD<mdx>J female mice.

Figure 3.4. BRAIN WATER CONTENT. Shows cerebral edema (Brain Water Content) after 1 h ischemia and 24 h reperfusion in C57Bl/6J male and female, C57Bl/10SnJ female and C57Bl/10ScSnDMD<mdx>J female mice. (* = p> 0.05). Abbreviations: C- contralateral, I- Ipislateral.

BWC (%)	6JM Ipsil	6JM Contr	6J F Ipsil	6J F Contr	10SnJ Ipsil	10SnJ Contr	Mdx Ipsil	Mdx Contr
Average	81.03	78.83	80.04	78.31	81.44	78.49	77.75	76.85
Standard Deviation	0.97	0.64	0.09	0.23	1.15	0.37	1.53	2.25

Table 3.4. BRAIN WATER CONTENT. Shows average and standard deviation of cerebral edema (brain water content) after 1 h ischemia and 24 h reperfusion in C57Bl/6J male and female, C57Bl/10SnJ female and C57Bl/10ScSnDMD<mdx>J female mice."

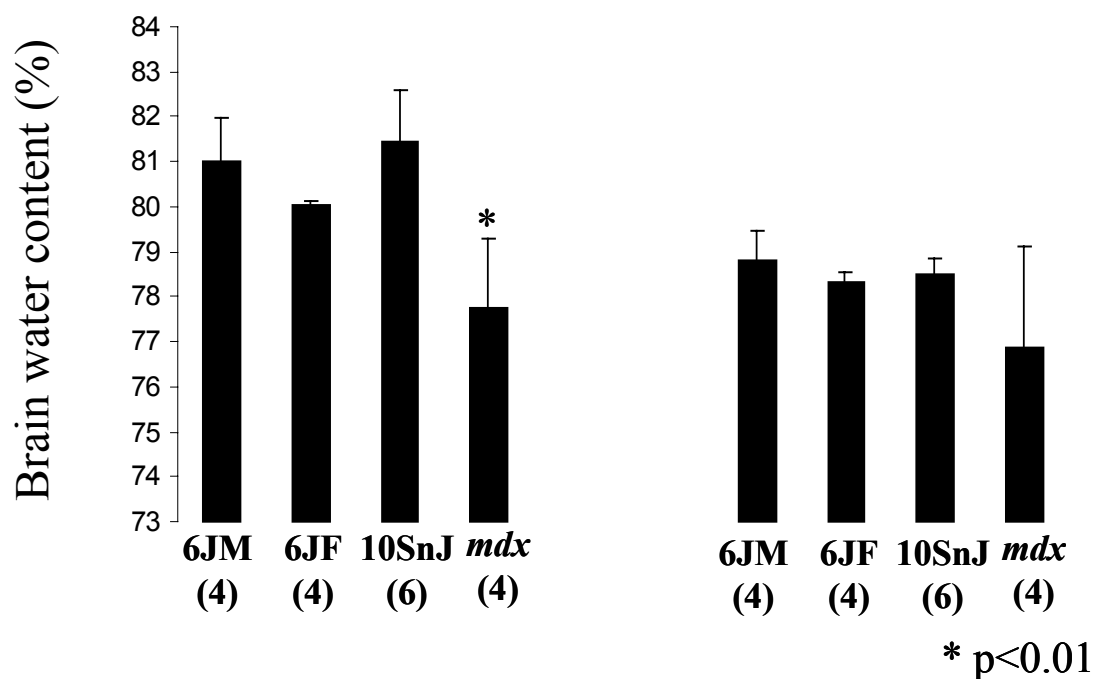**Figure 3.5** INFARCT SIZE DETERMINATION. Shows infarct size (cubic mm) after 1h ischemia and 24h reperfusion in C57Bl/6J male and female, C57Bl/10SnJ female and C57BlScSnDMD<mdx>J female mice.

Infarct size (mm^3)	C57Bl/6J male	C57Bl/6J female	C57Bl/10SnJ female	C57Bl/10ScSnDMD<mdx>J female
Average	94.98	82.90	38.20	28.53
Standard Deviation	70.10	53.23	23.64	34.28

Table 3.5. INFARCT SIZE DETERMINATION. Shows average and standard deviation of infarct size (cubic mm) after 1 h ischemia and 24 h reperfusion in C57Bl/6J male and female, C57Bl/10SnJ female and C57Bl/10ScSnDMD<mdx>J female mice.
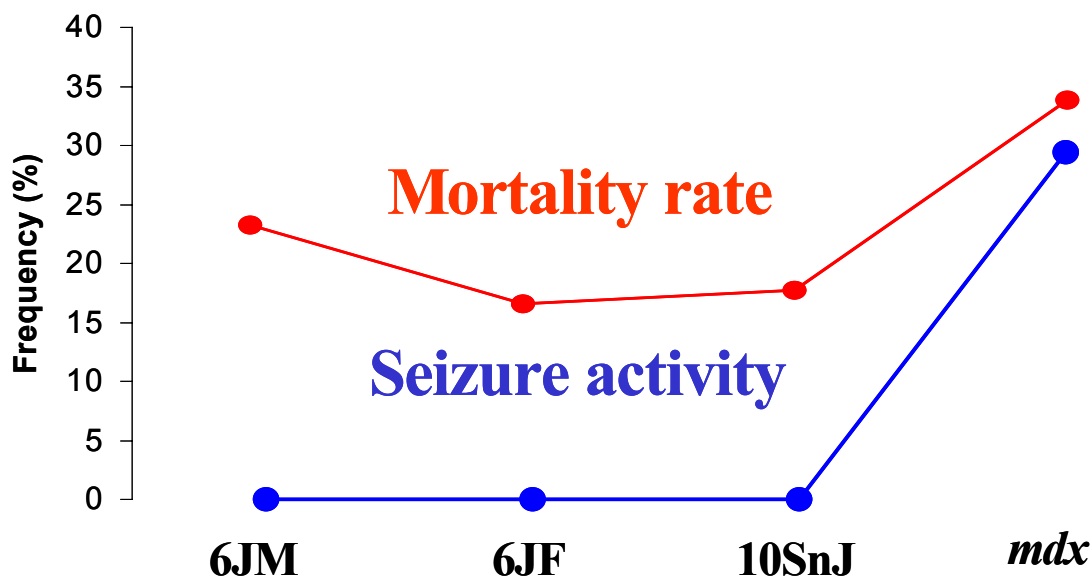
Figure 3.6. MORTALITY RATE AND SEIZURE ACTIVITY. Shows mortality rate (%) and seizure activity after 1 h ischemia and 24 h reperfusion in C57Bl/6J male and female, C57Bl/10SnJ female and C57Bl/10ScSnDMD<mdx>J female mice.

Mortality rate (%)	C57Bl/6J male	C57Bl/6J female	C57Bl/10SnJ female	C57Bl/10ScSnDMD<mdx>J female
	23.08	15.38	16.67	35.29

Table 3.6. MORTALITY RATE AND SEIZURE ACTIVITY. Shows mortality rate (%) after 1 h ischemia and 24 h reperfusion in C57Bl/6J male and female, C57Bl/10SnJ female and C57Bl/10ScSnDMD<mdx>J female mice.
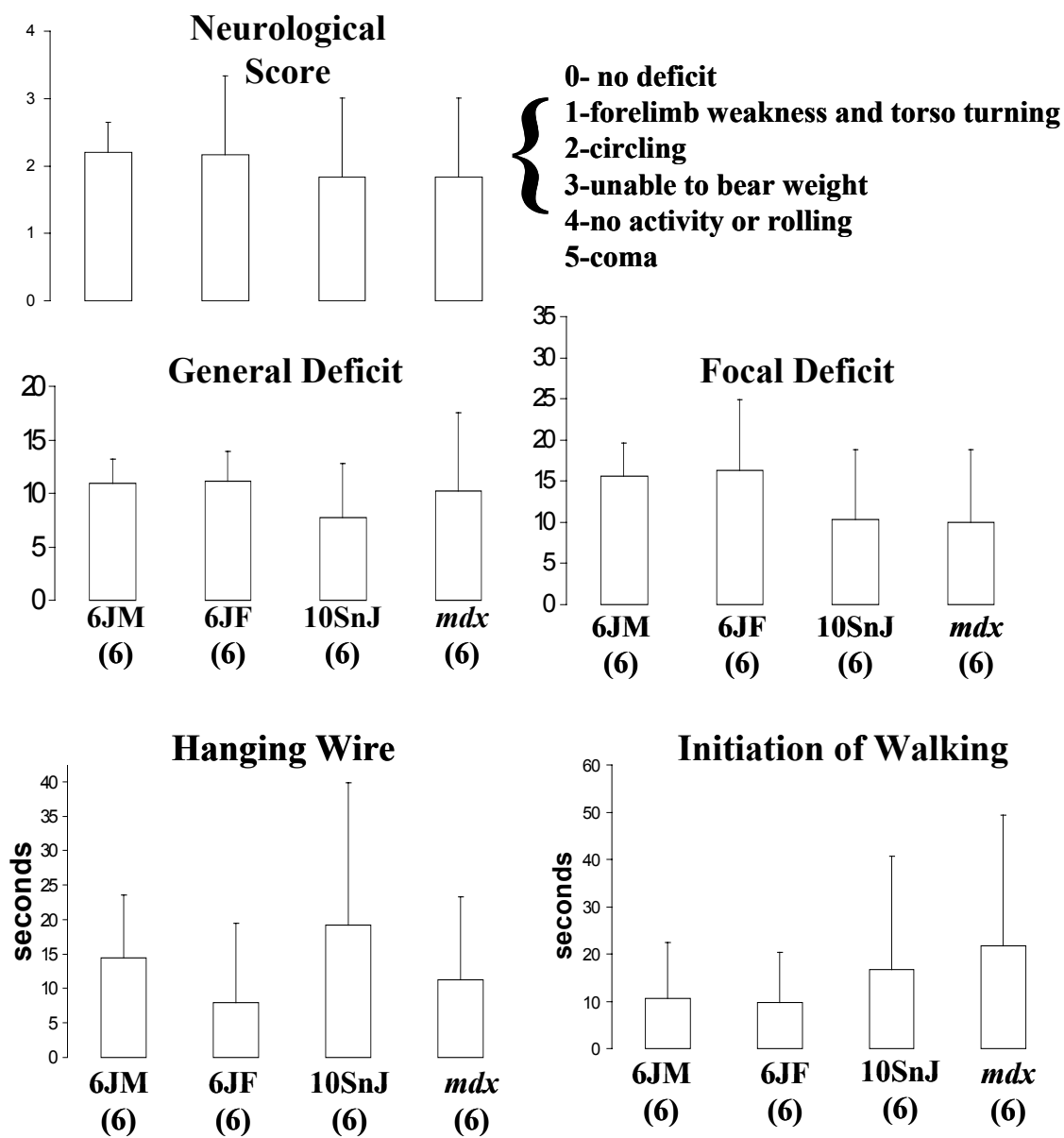
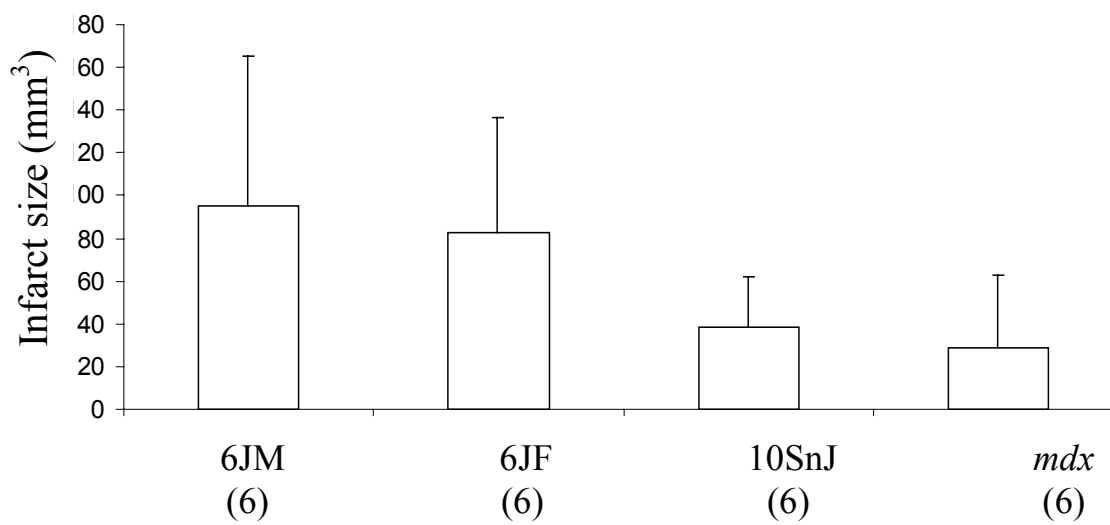**Figure 3.7.** NEUROLOGICAL OUTCOME. Shows neurological outcome (0-5 scale) of cortical area after 1 h ischemia and 24 h reperfusion in C57Bl/6J male and female, C57Bl/10SnJ female and C57Bl/10ScSnDMD<mdx>J female mice.

0-5 Neurological Scale	C57Bl/6J male	C57Bl/6J female	C57Bl/10SnJ female	C57Bl/10ScSnDMD<mdx>J female
Average	2.11	2.14	1.78	2.25
Standard Deviation	0.60	0.90	0.83	1.28

Table 3.7. NEUROLOGICAL OUTCOME (0-5 SCORE). Shows average and standard deviation of neurological outcome (0-5 scale) after 1 h ischemia and 24 h reperfusion in C57Bl/6J male and female, C57Bl/10SnJ female and C57Bl/10ScSnDMD<mdx>J female mice.

| General Deficit	C57Bl/6J male	C57Bl/6J female	C57Bl/10SnJ female	C57Bl/10ScSnDMD<mdx>J female
Average	13.39	17.64	7.96	16.90
Standard Deviation	9.54	14.95	4.86	19.08

Table 3.8. NEUROLOGICAL OUTCOME (GENERAL). Shows average and standard deviation of neurological outcome (General deficit) after 1 h ischemia and 24 h reperfusion in C57Bl/6J male and female, C57Bl/10SnJ female and C57Bl/10ScSnDMD<mdx>J female mice.

Focal Deficit	C57Bl/6J male	C57Bl/6J female	C57Bl/10SnJ female	C57Bl/10ScSnDMD<mdx>J female
Average	15.67	16.14	10.22	13.37
Standard Deviation	3.67	7.20	8.06	8.75

Table 3.9. NEUROLOGICAL OUTCOME (FOCAL). Shows average and standard deviation of neurological outcome (Focal deficit) after 1 h ischemia and 24 h reperfusion in C57Bl/6J male and female, C57Bl/10SnJ female and C57Bl/10ScSnDMD<mdx>J female mice.

Hanging Wire	C57Bl/6J male	C57Bl/6J female	C57Bl/10SnJ female	C57Bl/10ScSnDMD<mdx>J female
Average	14.41	7.94	19.15	11.28
Standard Deviation	9.14	11.46	20.64	12.04

Table 3.10. NEUROLOGICAL OUTCOME (HANGING WIRE). Shows average and standard deviation of neurological outcome (Hanging wire) after 1 h ischemia and 24 h reperfusion in C57Bl/6J male and female, C57Bl/10SnJ female and C57Bl/10ScSnDMD<mdx>J female mice.

Initiation of Walking	C57Bl/6J male	C57Bl/6J female	C57Bl/10SnJ female	C57Bl/10ScSnDMD<mdx>J female
Average	10.67	9.71	16.78	21.67
Standard Deviation	11.75	10.59	23.89	27.64

Table 3.11. NEUROLOGICAL OUTCOME (INITIATION OF WALKING). Shows average and standard deviation of neurological outcome (Initiation of Walking) after 1 h ischemia and 24 h reperfusion in C57Bl/6J male and female, C57Bl/10SnJ female and C57Bl/10ScSnDMD<mdx>J female mice.

CHAPTER 4. DISCUSSION AND CONCLUSIONS

The major finding of this work is a novel class of pharmacological agents that could significant decrease the formation of cerebral edema after ischemic stroke. Stroke is the third leading cause of death and disability in the United States; it affects over 700,000 people every year. With over 4 million survivors in US, stroke direct cost is estimated to be more than 57 billion dollars in 2006. Therefore, stroke is an important disease from the social perspective and from the economical perspective as well. Cerebral edema is a life-threatening consequence of stroke. Cerebral edema is the major cause of death after large infarcts of the middle cerebral artery territory. The mortality of progressive edema after middle cerebral artery infarcts approaches 80%. Cerebral edema occurs in 15-20% of all middle cerebral artery infarcts and in small infarcts of the cerebellum. An effective treatment for cerebral edema would have a significant positive impact in reducing the frequency of fatal cases of stroke.

Very few effective treatments are available in clinical practice. Great effort has been invested in finding new treatments for brain ischemia and reperfusion but most of the clinical trials have shown disappointing results. The only available treatment that showed convincing results in clinical trials culminated with the identification of tissue plasminogen activator (TPA) as an agent to restore blood flow to the affected area, although the window of opportunity is limited to the first three hours after stroke. Therefore, if the patient's condition matches all the relevant requirements, the first choice for action is to restore proper blood flow. Besides hypothermia, most treatments for

cerebral edema have proven to be of limited value. The reason for the disappointing results in clinical trials can be explained by the delayed arriving time at the hospital.

Stroke can be considered a "silent" disease since it is not accompanied with severe pain. Stroke is usually accompanied by disorientation and disruption of cognitive capabilities that can lead to a delay in the recognition of the problem, and in the arrival time at the emergency room. The average time of patient arrival at the emergency room is more than three hours after the stroke event. By this time, excitotoxicity and periinfarct depolarization mechanisms are already established and it seems clear that preventative treatments targeting those mechanisms would not be effective. Disappointing results in clinical trials with candidate blockers for excitotoxicity and depolarization can be explained because these mechanisms occur within minutes to few hours after ischemia. On another hand inflammation, apoptosis and cerebral edema mechanisms extend over days, and thus therapeutic intervention should have a better chance of being beneficial.

In addition to complexities caused by the various time frames of post-stroke pathologies, it also relevant that human stroke patients typically are older, and more likely to be affected by other diseases such as diabetes, hypertension, high cholesterol, or a combination of factors. These are difficult conditions to mimic in a laboratory setting. How can we translate a response from a neurological evaluation of a mouse to predict the comparable outcome in a highly developed human brain? This complexity is another important factor in explaining the history of disappointing results related to the use of animal models in the development of new pharmacological compounds for stroke treatment. Mice subjected to cerebral ischemia and reperfusion are not identical to

humans suffering from stroke. Most research necessarily is done in an artificial situation, isolating a discrete topic to study, such as the effect of nitric oxide (NO) in cerebral edema. In a clinical setting, we have a multifactorial set of phenomena occurring.

What do we know about cerebral edema? Water has to move from the blood to the brain parenchyma. With an intact blood-brain barrier, water transport is more likely to be mediated by cotransporters across the endothelial cells following a gradient of salt. The role of water channels in the brain endothelial cells is still unclear. Alternatively, once the blood-brain barrier is disrupted, water can move paracellularly because of the loss of the tight junctions. Viability of astrocytes is also an important aspect in maintaining the blood-brain barrier; astrocyte swelling during ischemia might precipitate early blood-brain barrier disruption. Landmark results published by Verkman and colleagues using aquaporin-4 knockout mice highlighted the idea that aquaporin-4 channels might be an important player in the development of cerebral edema after ischemic stroke (**1**). The few experiments done in this area have been followed by an enormous number of review papers reiterating that an aquaporin-4 blocker would be beneficial in cerebral edema management. Similar conclusions were reached in studies using other genetic knockout mice that showed changes in the normal localization and expression of aquaporin-4 channels such as the alpha syntrophin knockout mice.

The task of finding an aquaporin-4 blocker has been a difficult one. No compound able to inhibit water permeability through aquaporin-4 has been described prior to my work. We hypothesized that an aquaporin-4 water channel blocker would decrease the formation of cerebral edema after ischemic stroke in mice. The purpose of this study was

to determine if pharmacological blockers of aquaporin-4 water permeability can be identified, and if these agents will significantly decrease the formation of cerebral edema after ischemic stroke in mice.

We used a successful strategy previously used in our laboratory by Brooks et al (**83**) where tetraethylammonium was identified as an aquaporin-1 blocker. The strategy consisted of testing compounds known to block ion channels, receptors and compounds thought to have a beneficial effect in cerebral edema after stroke. Using this strategy, we determined that bumetanide inhibits water permeability through aquaporin-4 in a reversible and dose-dependent manner. Bumetanide is a potent diuretic that acts in the loop of Henle as a Na^+, K^+, Cl^- cotransporter inhibitor. It also has been shown to decrease the formation of cerebral edema after ischemic stroke in rats. Bumetanide decreases the formation of cerebral edema after 1h of ischemia and 23h of reperfusion in mice. I discovered that it also blocks AQP4 water channels. This is the first aquaporin-4 blocker to be characterized. The high dose necessary for reducing cerebral edema effects contrasts with the low dose needed for blocking Na^+, K^+, Cl^- cotransporter, and suggested that another target such as aquaporin-4 participates in the cerebral edema formation and is affected by the drug.

Bumetanide is poorly soluble in aqueous solutions and doesn't cross the lipophilic cellular membranes easily. Since computational studies pointed that interactions sites for bumetanide might be intracellular, we develop a novel derivative compound, predicting that this compound would cross the blood-brain barrier more easily. This novel compound effectively inhibited the water permeability in aquaporin-4 channels expressed

in *Xenopus* oocytes. Further studies are necessary to test the effect of this new compound in cerebral edema after ischemic stroke. It is also necessary to evaluate if this new compound inhibits the function of other transporters and channels, and if there is an improvement in availability (transmembrane transport) as result of the selected substitution of chemical groups on the parent compound template.

The fact that bumetanide reversibly blocks aquaporin-4 might be important for determining a strategic time frame for edema treatment. Previous research showed that aquaporin-4 knockout animals showed an increased formation in cerebral edema after brain tumors, from which it can be inferred that aquaporin-4 might be beneficial in draining the accumulated water in the brain. Bumetanide might be a effective treatment because it inhibits salt movement at the endothelial cells through block of Na^+, K^+, Cl^- cotransporters, and water flux at the astrocytes by inhibiting aquaporin-4 channels.

Besides the challenge to come up with new therapeutic tools to inhibit cerebral edema formation it is important to understand how edema is formed and how water moves to brain parenchyma after ischemia. Knockout mice are important tools used to isolate molecular candidates. We decided to characterize edema formation in a strain of mice lacking expression of dystrophin protein. Dystrophin deficient mice have a reduction in the expression of aquaporin-4 by 90% as compared with strain-matched wild type animals; aquaporin-4 is absent at the astrocytic end feet membrane in the dystrophin-deficient animals. Our initial hypothesis was that those animals would show a protective effect in stroke-induced edema similar to that described for aquaporin-4 and alpha-synthrophin-deficient animals. In agreement with our hypothesis, we found that

dystrophin-deficient *(mdx)* animals have a phenotype that includes a protective effect against edema after ischemic stroke. Ours results indicated that dystrophin deficient animals and the strain-matched controls had thea similar insult since both strains had a similar infarct size but the *mdx* animals showed protection for cerebral edema formation, in that the affected hemispheres were not significantly different from contralateral control hemispheres in volume. An unexpected observation was that *mdx* animals showed an increased mortality and seizure activity. An interesting point is that *mdx* animals have been found previously to show an increased plasma potassium concentration that might be caused by muscle necrosis (**152**). I propose that the depolarizing effects of elevated K^+ compounded with the further compromise of the blood-brain-barrier after stroke might explain the increased mortality and "seizure-like" activity observed in *mdx* animals when compared with other strains, although this idea remains to be tested. Impairment of renal compensatory mechanisms in the *mdx* animals might also be implicated in the increase of potassium concentration in the plasma since potassium channels might co-localize with dystrophin proteins this hypothesis needs to be further investigated.

Also unexpected were the differences in cerebral edema formation and infarct sizeobserved between the control strains in our experiments, which suggested that more research is necessary to understand the broader extent of mechanisms that are involved in edema and cell death after brain ischemia. Do differences in gene expression between mice strains confer a resistance in cerebral edema formation or do they create a more general resistance to a variety of causes of stress? More research is needed to elucidate the answers to those questions.

Stroke management involves multiple efforts to reduce incidence, including a massive campaign to decrease risk factors such as obesity, lack of exercise, high cholesterol, smoking, and others; and to instill a better public understanding of the disease and the importance of rapid recognition and access to medical help. In parallel, a better understanding of stroke mechanisms and the identification of drug agents and strategies for treatment would provide benefits in offsetting neurological damage and overall mortality that usually are associated with severe stroke.

In conclusion, we are the first group to describe a aquaporin-4 blocker and to show that this novel pharmacological compound decreases the formation of cerebral edema after stroke. We also show that a knockout mouse that doesn't have a normal expression and localization of aquaporin-4 in the astrocytes membrane surprisingly showed a worse outcome after cerebral edema when compared with strain-matched controls.

The future directions of this work are to test and identify novel bumetanide derivatives able to block aquaporin-4 channels that have increased water solubility and membrane permeant characteristics. Once this novel compound is identified, it would be necessary to test its protective effect in the formation of cerebral edema after ischemic stroke in mice. If we identify a water soluble and membrane permeant compound that has protective effects in cerebral edema formation, it would be important to evaluate its effects in other transporters (e.g., the Na^+, K^+, Cl^- cotransporter and organic anion transporters) in order to evaluate if its beneficial protection is directly associated with the aquaporin-4 channels. In addition, lately, it would be interesting to evaluate its

pharmacological proprieties such as half maximum dose and toxicological effects in animals and humans.

REFERENCES

1)   **Manley** GT, Fujimura M, Ma T, Noshita N, Filiz F, Bollen AW, Chan P, Verkman AS. Aquaporin-4 deletion in mice reduces brain edema after acute water intoxication and ischemic stroke. Nat Med. 2000 Feb;6(2):159-63. PMID: 10655103.

2)   **Vajda** Z, Pedersen M, Fuchtbauer EM, Wertz K, Stodkilde-Jorgensen H, Sulyok E, Doczi T, Neely JD, Agre P, Frokiaer J, Nielsen S. Delayed onset of brain edema and mislocalization of aquaporin-4 in dystrophin-null transgenic mice. Proc Natl Acad Sci U S A. 2002 Oct 1;99(20):13131-6. Epub 2002 Sep 13. PMID: 12232046

3)   **Amiry-Moghaddam** M, Williamson A, Palomba M, Eid T, de Lanerolle NC, Nagelhus EA, Adams ME, Froehner SC, Agre P, Ottersen OP. Delayed K+ clearance associated with aquaporin-4 mislocalization: phenotypic defects in brains of alpha-syntrophin-null mice. Proc Natl Acad Sci U S A. 2003 Nov 11;100(23):13615-20. Epub 2003 Nov 3. PMID: 14597704

4)   **O'Donnell** ME, Tran L, Lam TI, Liu XB, Anderson SE. Bumetanide inhibition of the blood-brain barrier Na-K-Cl cotransporter reduces edema formation in the rat middle cerebral artery occlusion model of stroke. J Cereb Blood Flow Metab. 2004 Sep;24(9):1046-56. PMID: 15356425

5)   **Paulson** OB. Blood-brain barrier, brain metabolism and cerebral blood flow. Eur Neuropsychopharmacol. 2002 Dec;12(6):495-501. Review. PMID: 12468012.

6) **Taylor** TN, Davis PH, Torner JC, Holmes J, Meyer JW, Jacobson MF. Lifetime cost of stroke in the United States. Stroke. 1996 Sep;27(9):1459-66. Review. PMID: 8784113.

7) **Dirnagl** U, Iadecola C, Moskowitz MA. Pathobiology of ischaemic stroke: an integrated view. Trends Neurosci. 1999 Sep;22(9):391-7. Review. PMID: 10441299.

8) **Thom** T, Haase N, RosamondW, Howard VJ, Rumsfeld J, Manolio T, Zheng ZJ, Flegal K, O'Donnell C, Kittner S, Lloyd-Jones D, Goff DC, Hong Y, Members of the Statistics Committee and Stroke Statistics Subcommittee: Adams R, Friday G, Furie K, Gorelick P, Kissela B, Marler J, Meigs J, Roger V, Sidney S, Sorlie P, Steinberger J, Wasserthiel-Smoller S, Wilson M, Wolf P. Heart Disease and Stroke Statistics—2006 Update. A Report From the American Heart Association Statistics Committee and Stroke Statistics Subcommittee Writing Group. http://circ.ahajournals.org/cgi/reprint/CIRCULATIONAHA.105.171600v1.

9) **Hacke** W, Schwab S, Horn M, Spranger M, De Georgia M, von Kummer R. 'Malignant' middle cerebral artery territory infarction: clinical course and prognostic signs. Arch Neurol. 1996 Apr;53(4):309-15. PMID: 8929152.

10) **Ayata** C, Ropper AH. Ischaemic brain oedema. J Clin Neurosci. 2002 Mar;9(2):113-24. Review. PMID: 11922696.

11) **MacAulay** N, Hamann S, Zeuthen T. Water transport in the brain: role of cotransporters. Neuroscience. 2004;129(4):1031-44. Review. PMID: 15561418.

12) **Bradbury**, MWB. *The Concept of a Blood–Brain Barrier,* Wiley (Ed.), Chichester, UK, 1979.

13) **Joo** F, Karnushina I. A procedure for the isolation of capillaries from rat brain. Cytobios. 1973 Sep-Oct;8(29):41-8. PMID: 4774116

14) **Abbott** NJ. Dynamics of CNS barriers: evolution, differentiation, and modulation. Cell Mol Neurobiol. 2005 Feb;25(1):5-23. Review. PMID: 15962506

15) **Firth** JA. Endothelial barriers: from hypothetical pores to membrane proteins. J Anat. 2002 Jun;200(6):541-8. Review. PMID: 12162722.

16) **Shafrir** E. Paul Ehrlich--pioneer in chemotherapy, histology and immunology. Isr J Med Sci. 1993 May;29(5):327. PMID: 8314701

17) **Reese** TS, Karnovsky MJ. Fine structural localization of a blood-brain barrier to exogenous peroxidase. J Cell Biol. 1967 Jul;34(1):207-17. PMID: 6033532

18) **Brightman** MW. The intracerebral movement of proteins injected into blood and cerebrospinal fluid of mice. Prog Brain Res. 1968;29:19-40. Review. PMID: 4898331

19) **Schulze** C, Firth JA. Immunohistochemical localization of adherens junction components in blood-brain barrier microvessels of the rat. J Cell Sci. 1993 Mar;104 (Pt 3):773-82. PMID: 8314872

20) **Kniesel** U, Wolburg H. Tight junctions of the blood-brain barrier. Cell Mol Neurobiol. 2000 Feb;20(1):57-76. Review. PMID: 10690502

21) **Wolburg** H, Lippoldt A. Tight junctions of the blood-brain barrier: development, composition and regulation. Vascul Pharmacol. 2002 Jun;38(6):323-37. Review. PMID: 12529927

22)   **Vorbrodt** AW, Dobrogowska DH. Molecular anatomy of intercellular junctions in brain endothelial and epithelial barriers: electron microscopist's view. Brain Res Brain Res Rev. 2003 Jun;42(3):221-42. Review. PMID: 12791441

23)   **Tao-Cheng** JH, Nagy Z, Brightman MW. Tight junctions of brain endothelium in vitro are enhanced by astroglia. J Neurosci. 1987 Oct;7(10):3293-9. PMID: 3668629

24)   **Braet** K, Paemeleire K, D'Herde K, Sanderson MJ, Leybaert L. Astrocyte-endothelial cell calcium signals conveyed by two signalling pathways. Eur J Neurosci. 2001 Jan;13(1):79-91. PMID: 11135006

25)   **Kojima** T, Yamamoto T, Murata M, Chiba H, Kokai Y, Sawada N. Regulation of the blood-biliary barrier: interaction between gap and tight junctions in hepatocytes. Med Electron Microsc. 2003 Sep;36(3):157-64. Review. PMID: 14505059

26)   **Simard** M, Arcuino G, Takano T, Liu QS, Nedergaard M. Signaling at the gliovascular interface. J Neurosci. 2003 Oct 8;23(27):9254-62. PMID: 14534260

27)   **Paulson** OB, Hertz MM, Bolwig TG, Lassen NA. Filtration and diffusion of water across the blood-brain barrier in man. Microvasc Res. 1977 Jan;13(1):113-24. PMID: 859448

28)   **Brightman** MW, Tao-Cheng JH. Tight junctions of brain endothelium and epithelium, in: W. M. Pardridge (Ed.), The Blood-Brain Barrier, Raven, New York, 1993, pp. 107-125.

29)   **Abbott** NJ, Ronnback L, Hansson E. Astrocyte-endothelial interactions at the blood-brain barrier. Nat Rev Neurosci. 2006 Jan;7(1):41-53. Review. PMID: 16371949

30)   **Oldendorf** WH, Cornford ME, Brown WJ. The large apparent work capability of the blood-brain barrier: a study of the mitochondrial content of capillary endothelial cells in brain and other tissues of the rat. Ann Neurol. 1977 May;1(5):409-17. PMID: 617259

31)   **Fenstermacher** J, Gross P, Sposito N, Acuff V, Pettersen S, Gruber K. Structural and functional variations in capillary systems within the brain. Ann N Y Acad Sci. 1988;529:21-30. PMID: 3395069

32)   **Sedlakova** R, Shivers RR, Del Maestro RF. Ultrastructure of the blood-brain barrier in the rabbit. J Submicrosc Cytol Pathol. 1999 Jan;31(1):149-61. PMID: 10363362

33)   **Kniesel** U, Wolburg H. Tight junctions of the blood-brain barrier. Cell Mol Neurobiol. 2000 Feb;20(1):57-76. Review. PMID: 10690502

34)   **Farkas** E, Luiten PG. Cerebral microvascular pathology in aging and Alzheimer's disease. Prog Neurobiol. 2001 Aug;64(6):575-611. Review. PMID: 11311463

35)   **Rosenberg** GA, Estrada E, Kelley RO, Kornfeld M. Bacterial collagenase disrupts extracellular matrix and opens blood-brain barrier in rat. Neurosci Lett. 1993 Sep 17;160(1):117-9. PMID: 8247322

36)   **Rascher** G, Fischmann A, Kroger S, Duffner F, Grote EH, Wolburg H. Extracellular matrix and the blood-brain barrier in glioblastoma multiforme: spatial segregation of tenascin and agrin. Acta Neuropathol (Berl). 2002 Jul;104(1):85-91. Epub 2002 Mar 28. PMID: 12070669

37) **Hynes** RO. Integrins: versatility, modulation, and signaling in cell adhesion. Cell. 1992 Apr 3;69(1):11-25. Review. PMID: 1555235

38) **Tilling** T, Engelbertz C, Decker S, Korte D, Huwel S, Galla HJ. Expression and adhesive properties of basement membrane proteins in cerebral capillary endothelial cell cultures. Cell Tissue Res. 2002 Oct;310(1):19-29. Epub 2002 Aug 24. PMID: 12242480

39) **Tilling** T, Korte D, Hoheisel D, Galla HJ. Basement membrane proteins influence brain capillary endothelial barrier function in vitro. J Neurochem. 1998 Sep;71(3):1151-7. PMID: 9721740

40) **Savettieri** G, Di Liegro I, Catania C, Licata L, Pitarresi GL, D'Agostino S, Schiera G, De Caro V, Giandalia G, Giannola LI, Cestelli A. Neurons and ECM regulate occludin localization in brain endothelial cells. Neuroreport. 2000 Apr 7;11(5):1081-4. PMID: 10790886

41) **Davson** H, Oldendorf WH. Symposium on membrane transport. Transport in the central nervous system. Proc R Soc Med. 1967 Apr;60(4):326-9. PMID: 6021942

42) **Willis** CL, Nolan CC, Reith SN, Lister T, Prior MJ, Guerin CJ, Mavroudis G, Ray DE. Focal astrocyte loss is followed by microvascular damage, with subsequent repair of the blood-brain barrier in the apparent absence of direct Astrocytic contact. Glia. 2004 Mar;45(4):325-37. PMID: 14966864

43) **Abbott** NJ. Dynamics of CNS barriers: evolution, differentiation, and modulation. Cell Mol Neurobiol. 2005 Feb;25(1):5-23. Review. PMID: 15962506

44) **Stewart** PA, Wiley MJ. Developing nervous tissue induces formation of blood-brain barrier characteristics in invading endothelial cells: a study using quail—chick transplantation chimeras. Dev Biol. 1981 May;84(1):183-92. PMID: 7250491

45) **Tagami** M, Nara Y, Kubota A, Fujino H, Yamori Y. Ultrastructural changes in cerebral pericytes and astrocytes of stroke-prone spontaneously hypertensive rats. Stroke. 1990 Jul;21(7):1064-71. PMID: 2368108

46) **Ramsauer** M, Krause D, Dermietzel R. Angiogenesis of the blood-brain barrier in vitro and the function of cerebral pericytes. FASEB J. 2002 Aug;16(10):1274-6. Epub 2002 Jun 21. PMID: 12153997

47) **Hori** S, Ohtsuki S, Hosoya K, Nakashima E, Terasaki T. A pericyte-derived angiopoietin-1 multimeric complex induces occludin gene expression in brain capillary endothelial cells through Tie-2 activation in vitro. J Neurochem. 2004 Apr;89(2):503-13. PMID: 15056293

48) **Ballabh** P, Braun A, Nedergaard M. The blood-brain barrier: an overview: structure, regulation, and clinical implications. Neurobiol Dis. 2004 Jun;16(1):1-13. Review. PMID: 15207256

49) **Gonul** E, Duz B, Kahraman S, Kayali H, Kubar A, Timurkaynak E. Early pericyte response to brain hypoxia in cats: an ultrastructural study. Microvasc Res. 2002 Jul;64(1):116-9. PMID: 12074637

50) **Dore-Duffy** P, Owen C, Balabanov R, Murphy S, Beaumont T, Rafols JA. Pericyte migration from the vascular wall in response to traumatic brain injury. Microvasc Res. 2000 Jul;60(1):55-69. PMID: 10873515

51) **Buxton** RB, Frank LR. A model for the coupling between cerebral blood flow and oxygen metabolism during neural stimulation. J Cereb Blood Flow Metab. 1997 Jan;17(1):64-72. Review. PMID: 8978388

52) **Ben-Menachem** E, Johansson BB, Svensson TH. Increased vulnerability of the blood-brain barrier to acute hypertension following depletion of brain noradrenaline. J Neural Transm. 1982;53(2-3):159-67. PMID: 6804601

53) **Cohen** Z, Molinatti G, Hamel E. Astroglial and vascular interactions of noradrenaline terminals in the rat cerebral cortex. J Cereb Blood Flow Metab. 1997 Aug;17(8):894-904. PMID: 9290587

54) **Cohen** Z, Bonvento G, Lacombe P, Hamel E. Serotonin in the regulation of brain microcirculation. Prog Neurobiol. 1996 Nov;50(4):335-62. Review. PMID: 9004349

55) **Vaucher** E, Hamel E. Cholinergic basal forebrain neurons project to cortical microvessels in the rat: electron microscopic study with anterogradely transported Phaseolus vulgaris leucoagglutinin and choline acetyltransferase immunocytochemistry. J Neurosci. 1995 Nov;15(11):7427-41. PMID: 7472495

56) **Tong** XK, Hamel E. Regional cholinergic denervation of cortical microvessels and nitric oxide synthase-containing neurons in Alzheimer's disease. Neuroscience. 1999;92(1):163-75. PMID: 10392839

57) **Vaucher** E, Tong XK, Cholet N, Lantin S, Hamel E. GABA neurons provide a rich input to microvessels but not nitric oxide neurons in the rat cerebral cortex: a means for direct regulation of local cerebral blood flow. J Comp Neurol. 2000 May 29;421(2):161-71. PMID: 10813779

58) **Kobayashi** H, Magnoni MS, Govoni S, Izumi F, Wada A, Trabucchi M. Neuronal control of brain microvessel function. Experientia. 1985 Apr 15;41(4):427-34. Review. PMID: 2580734

59) **Amiry-Moghaddam** M, Xue R, Haug FM, Neely JD, Bhardwaj A, Agre P, Adams ME, Froehner SC, Mori S, Ottersen OP. Alpha-syntrophin deletion removes the perivascular but not endothelial pool of aquaporin-4 at the blood-brain barrier and delays the development of brain edema in an experimental model of acute hyponatremia. FASEB J. 2004 Mar;18(3):542-4. Epub 2004 Jan 20. PMID: 14734638

60) **Rapoport** SI. A mathematical model for vasogenic brain edema. J Theor Biol. 1978 Oct 7;74(3):439-67. PMID: 723286

61) **Rapoport** SI. Roles of cerebrovascular permeability, brain compliance, and brain hydraulic conductivity in vasogenic edema, in: Popp AJ, Bourke RS, Nelson LR, Kimelberg HK (Eds.), Neural Trauma, Raven Press, New York, 1979, pp. 51-62.

62) **Rapoport** SI. Brain edema and the blood-brain barrier, in: Welch KMA, Caplan LR, Reis DJ, Siesjö BK, Weir B (Eds.), Primer on cerebrovascular diseases, Academic Press, London, 1997, pp. 25-28.

63) **Quigley** R, Mulder J, Baum M. Ontogeny of water transport in the rabbit proximal tubule. Pediatr Nephrol. 2003 Nov;18(11):1089-94. Epub 2003 Sep 5. Review. PMID: 12961084

64) **Zeuthen** T, MacAulay N. Cotransporters as molecular water pumps. Int Rev Cytol. 2002;215:259-84. Review. PMID: 11952231

65)   **Zeuthen** T, MacAulay N. Passive water transport in biological pores. Int Rev Cytol. 2002;215:203-30. Review. PMID: 11952229

66)   **MacAulay** N, Hamann S, Zeuthen T. Water transport in the brain: role of cotransporters. Neuroscience. 2004;129(4):1031-44. Review. PMID: 15561418

67)   **Preston** GM, Carroll TP, Guggino WB, Agre P. Appearance of water channels in Xenopus oocytes expressing red cell CHIP28 protein. Science. 1992 Apr 17;256(5055):385-7. PMID: 1373524

68)   **Guerin** CF, Regli L, Badaut J. [Roles of aquaporins in the brain] Med Sci (Paris). 2005 Aug-Sep;21(8-9):747-52. Review. French. PMID: 16115461.

69)   **de Groot** BL, Grubmuller H. Water permeation across biological membranes: mechanism and dynamics of aquaporin-1 and GlpF. Science. 2001 Dec 14;294(5550):2353-7. PMID: 11743202

70)   **Agre** P, King LS, Yasui M, Guggino WB, Ottersen OP, Fujiyoshi Y, Engel A, Nielsen S. Aquaporin water channels--from atomic structure to clinical medicine. J Physiol. 2002 Jul 1;542(Pt 1):3-16. Review. PMID: 12096044

71)   **Jung** JS, Bhat RV, Preston GM, Guggino WB, Baraban JM, Agre P. Molecular characterization of an aquaporin cDNA from brain: candidate osmoreceptor and regulator of water balance. Proc Natl Acad Sci U S A. 1994 Dec 20;91(26):13052-6. PMID: 7528931

72)   **Amiry-Moghaddam** M, Ottersen OP. The molecular basis of water transport in the brain. Nat Rev Neurosci. 2003 Dec;4(12):991-1001. Review. PMID: 14682361

73) **Badaut** J, Lasbennes F, Magistretti PJ, Regli L. Aquaporins in brain: distribution, physiology, and pathophysiology. J Cereb Blood Flow Metab. 2002 Apr;22(4):367-78. Review. PMID: 11919508

74) **Amiry-Moghaddam** M, Williamson A, Palomba M, Eid T, de Lanerolle NC, Nagelhus EA, Adams ME, Froehner SC, Agre P, Ottersen OP. Delayed K+ clearance associated with aquaporin-4 mislocalization: phenotypic defects in brains of alpha-syntrophin-null mice. Proc Natl Acad Sci U S A. 2003 Nov 11;100(23):13615-20. Epub 2003 Nov 3. PMID: 14597704

75) **Nielsen** S, King LS, Christensen BM, Agre P. Aquaporins in complex tissues. II. Subcellular distribution in respiratory and glandular tissues of rat. Am J Physiol. 1997 Nov;273(5 Pt 1):C1549-61. PMID: 9374640

76) **Venero** JL, Vizuete ML, Ilundain AA, Machado A, Echevarria M, Cano J. Detailed localization of aquaporin-4 messenger RNA in the CNS: preferential expression in periventricular organs. Neuroscience. 1999;94(1):239-50. PMID: 10613514

77) **Badaut** J, Lasbennes F, Magistretti PJ, Regli L. Aquaporins in brain: distribution, physiology, and pathophysiology. J Cereb Blood Flow Metab. 2002 Apr;22(4):367-78. Review. PMID: 11919508

78) **Amiry-Moghaddam** M, Frydenlund DS, Ottersen OP. Anchoring of aquaporin-4 in brain: molecular mechanisms and implications for the physiology and pathophysiology of water transport. Neuroscience. 2004;129(4):999-1010. PMID: 15561415

79) **Nico** B, Frigeri A, Nicchia GP, Corsi P, Ribatti D, Quondamatteo F, Herken R, Girolamo F, Marzullo A, Svelto M, Roncali L. Severe alterations of endothelial and glial cells in the blood-brain barrier of dystrophic mdx mice. Glia. 2003 May;42(3):235-51. PMID: 12673830

80) **Hof** PR, Pascale E, Magistretti PJ. K+ at concentrations reached in the extracellular space during neuronal activity promotes a Ca2+-dependent glycogen hydrolysis in mouse cerebral cortex. J Neurosci. 1988 Jun;8(6):1922-8. PMID: 3385482

81) **Magistretti** PJ, Pellerin L, Rothman DL, Shulman RG. Energy on demand. Science. 1999 Jan 22;283(5401):496-7. No abstract available. PMID: 9988650

82) **Somjen** GG. Glial cells, function, in: Adelman G (Ed.), Encyclopedia of neuroscience, Birkhauser, Boston, 1987, pp. 465-466.

83) **Brooks** HL, Regan JW, Yool AJ. Inhibition of aquaporin-1 water permeability by tetraethylammonium: involvement of the loop E pore region. Mol Pharmacol. 2000 May;57(5):1021-6. PMID: 10779387

84) **Yool** AJ, Brokl OH, Pannabecker TL, Dantzler WH, Stamer WD. Tetraethylammonium block of water flux in Aquaporin-1 channels expressed in kidney thin limbs of Henle's loop and a kidney-derived cell line. BMC Physiol. 2002;2:4. Epub 2002 Mar 15. PMID: 11914159

85) **Yool** AJ, Weinstein AM. New roles for old holes: ion channel function in aquaporin-1. News Physiol Sci. 2002 Apr;17:68-72. Review. PMID: 11909995

86)   **del Zoppo** GJ, Hallenbeck JM. Advances in the vascular pathophysiology of ischemic stroke. Thromb Res. 2000 May 1;98(3):73-81. Review. PMID: 10812160

87)   **Kempski** O. Cerebral edema. Semin Nephrol. 2001 May;21(3):303-7. Review. PMID: 11320499

88)   **Petty** MA, Wettstein JG. Elements of cerebral microvascular ischaemia. Brain Res Brain Res Rev. 2001 Aug;36(1):23-34. Review. PMID: 11516770

89)   **Astrup** J, Siesjo BK, Symon L. Thresholds in cerebral ischemia - the ischemic penumbra. Stroke. 1981 Nov-Dec;12(6):723-5. PMID: 6272455

90)   **Mergenthaler** P, Dirnagl U, Meisel A. Pathophysiology of stroke: lessons from animal models. Metab Brain Dis. 2004 Dec;19(3-4):151-67. Review. PMID: 15554412

91)   **Back** T, Hoehn-Berlage M, Kohno K, Hossmann KA. Diffusion nuclear magnetic resonance imaging in experimental stroke. Correlation with cerebral metabolites. Stroke. 1994 Feb;25(2):494-500. PMID: 8303762

92)   **Back** T, Ginsberg MD, Dietrich WD, Watson BD. Induction of spreading depression in the ischemic hemisphere following experimental middle cerebral artery occlusion: effect on infarct morphology. J Cereb Blood Flow Metab. 1996 Mar;16(2):202-13. PMID: 8594051

93)   **Wolf** T, Lindauer U, Reuter U, Back T, Villringer A, Einhaupl K, Dirnagl U. Noninvasive near infrared spectroscopy monitoring of regional cerebral blood oxygenation changes during peri-infarct depolarizations in focal cerebral ischemia in the rat. J Cereb Blood Flow Metab. 1997 Sep;17(9):950-4. PMID: 9307608

94) **Iijima** T, Mies G, Hossmann KA. Repeated negative DC deflections in rat cortex following middle cerebral artery occlusion are abolished by MK-801: effect on volume of ischemic injury. J Cereb Blood Flow Metab. 1992 Sep;12(5):727-33. PMID: 1506440

95) **Mies** G, Iijima T, Hossmann KA. Correlation between peri-infarct DC shifts and ischaemic neuronal damage in rat. Neuroreport. 1993 Jun;4(6):709-11. PMID: 8347812

96) **Chen** H, Chopp M, Zhang RL, Bodzin G, Chen Q, Rusche JR, Todd RF 3rd. Anti-CD11b monoclonal antibody reduces ischemic cell damage after transient focal cerebral ischemia in rat. Ann Neurol. 1994 Apr;35(4):458-63. PMID: 8154873

97) **Mori** E, del Zoppo GJ, Chambers JD, Copeland BR, Arfors KE. Inhibition of polymorphonuclear leukocyte adherence suppresses no-reflow after focal cerebral ischemia in baboons. Stroke. 1992 May;23(5):712-8. PMID: 1579969

98) **Zhang** RL, Chopp M, Jiang N, Tang WX, Prostak J, Manning AM, Anderson DC. Anti-intercellular adhesion molecule-1 antibody reduces ischemic cell damage after transient but not permanent middle cerebral artery occlusion in the Wistar rat. Stroke. 1995 Aug;26(8):1438-42; discussion 1443. PMID: 7631350

99) **Becker** K, Kindrick D, Relton J, Harlan J, Winn R. Antibody to the alpha4 integrin decreases infarct size in transient focal cerebral ischemia in rats. Stroke. 2001 Jan;32(1):206-11. PMID: 11136938

100) **Wang** L, McComb JG, Weiss MH, McDonough AA, Zlokovic BV. Nicotine downregulates alpha 2 isoform of Na,K-ATPase at the blood-brain barrier and brain

in rats. Biochem Biophys Res Commun. 1994 Mar 30;199(3):1422-7. PMID: 8147886

101) **Becker** K, Kindrick D, Relton J, Harlan J, Winn R. Antibody to the alpha4 integrin decreases infarct size in transient focal cerebral ischemia in rats. Stroke. 2001 Jan;32(1):206-11. PMID: 11136938

102) **Ritter** LS, Orozco JA, Coull BM, McDonagh PF, Rosenblum WI. Leukocyte accumulation and hemodynamic changes in the cerebral microcirculation during early reperfusion after stroke. Stroke. 2000 May;31(5):1153-61. PMID: 10797180

103) **Ruehl** ML, Orozco JA, Stoker MB, McDonagh PF, Coull BM, Ritter LS. Protective effects of inhibiting both blood and vascular selectins after stroke and reperfusion. Neurol Res. 2002 Apr;24(3):226-32. PMID: 11958413

104) **Gasche** Y, Fujimura M, Morita-Fujimura Y, Copin JC, Kawase M, Massengale J, Chan PH. Early appearance of activated matrix metalloproteinase-9 after focal cerebral ischemia in mice: a possible role in blood-brain barrier dysfunction. J Cereb Blood Flow Metab. 1999 Sep;19(9):1020-8. PMID: 10478654

105) **Heo** JH, Lucero J, Abumiya T, Koziol JA, Copeland BR, del Zoppo GJ. Matrix metalloproteinases increase very early during experimental focal cerebral ischemia. J Cereb Blood Flow Metab. 1999 Jun;19(6):624-33. PMID: 10366192

106) **Lapchak** PA, Chapman DF, Zivin JA. Metalloproteinase inhibition reduces thrombolytic (tissue plasminogen activator)-induced hemorrhage after thromboembolic stroke. Stroke. 2000 Dec;31(12):3034-40. PMID: 11108768

107) **Asahi** M, Asahi K, Jung JC, del Zoppo GJ, Fini ME, Lo EH. Role for matrix metalloproteinase 9 after focal cerebral ischemia: effects of gene knockout and enzyme inhibition with BB-94. J Cereb Blood Flow Metab. 2000 Dec;20(12):1681-9. PMID: 11129784

108) **Rosenberg** GA, Estrada EY, Dencoff JE. Matrix metalloproteinases and TIMPs are associated with blood-brain barrier opening after reperfusion in rat brain. Stroke. 1998 Oct;29(10):2189-95. PMID: 9756602

109) **Kimelberg** HK. Current concepts of brain edema. Review of laboratory investigations. J Neurosurg. 1995 Dec;83(6):1051-9. Review. PMID: 7490620

110) **Kimelberg** HK, Ransom BR. Physiological and pathological aspects of Astrocytic swelling, in: Fedoroff S, Vernadakis A (Eds.), I: Astrocytes, Vol. 3, Academic Press, Florida, 1986, pp. 129-166.

111) **Mongin** AA, Kimelberg HK. Astrocytic swelling in neuropathology, in: Kettenmann HO, Ranson BR (Eds.), Neuroglia, Oxforf University Press, New York, 2004, pp. 550-562.

112) **Klatzo** I. Presidental address. Neuropathological aspects of brain edema. J Neuropathol Exp Neurol. 1967 Jan;26(1):1-14. Review. PMID: 5336776

113) **Sykova** E, Svoboda J, Polak J, Chvatal A. Extracellular volume fraction and diffusion characteristics during progressive ischemia and terminal anoxia in the spinal cord of the rat. J Cereb Blood Flow Metab. 1994 Mar;14(2):301-11. PMID: 8113325

114) **Van Harreveld** A. Brain tissue electrolytes. London, 1966: Butterworths.

115) **Popp** AJ, Feustel PJ, Kimelberg HK. Pathophysiology of traumatic brain injury, in: Wilkins RH, Renbachary SS (Eds.), Neurosurgery Vol. II, McGraw-Hill, New York, 1996, pp. 2623-2637.

116) **Mark** KS, Davis TP. Cerebral microvascular changes in permeability and tight junctions induced by hypoxia-reoxygenation. Am J Physiol Heart Circ Physiol. 2002 Apr;282(4):H1485-94. PMID: 11893586

117) **Abbruscato** TJ, Davis TP. Combination of hypoxia/aglycemia compromises in vitro blood-brain barrier integrity. J Pharmacol Exp Ther. 1999 May;289(2):668-75. PMID: 10215638

118) **Fischer** S, Clauss M, Wiesnet M, Renz D, Schaper W, Karliczek GF. Hypoxia induces permeability in brain microvessel endothelial cells via VEGF and NO. Am J Physiol. 1999 Apr;276(4 Pt 1):C812-20. PMID: 10199811

119) **Trachtenberg** MC. Brain cell responses to extracellular protein, in: Grossman RG, Gildenberg PL (Eds.), Head injury: basic and clinical aspects, Raven Press, New York, 1982, pp. 169-178.

120) **Plateel** M, Teissier E, Cecchelli R. Hypoxia dramatically increases the nonspecific transport of blood-borne proteins to the brain. J Neurochem. 1997 Feb;68(2):874-7. PMID: 9003080

121) **Cipolla** MJ, Crete R, Vitullo L, Rix RD. Transcellular transport as a mechanism of blood-brain barrier disruption during stroke. Front Biosci. 2004 Jan 1;9:777-85. PMID: 14766407

122) **Kondo** T, Kinouchi H, Kawase M, Yoshimoto T. Astroglial cells inhibit the increasing permeability of brain endothelial cell monolayer following hypoxia/reoxygenation. Neurosci Lett. 1996 Apr 19;208(2):101-4. PMID: 8859900

123) **Huber** JD, Witt KA, Hom S, Egleton RD, Mark KS, Davis TP. Inflammatory pain alters blood-brain barrier permeability and tight junctional protein expression. Am J Physiol Heart Circ Physiol. 2001 Mar;280(3):H1241-8. PMID: 11179069

124) **Hayashi** Y, Nomura M, Yamagishi S, Harada S, Yamashita J, Yamamoto H. Induction of various blood-brain barrier properties in non-neural endothelial cells by close apposition to co-cultured astrocytes.Glia. 1997 Jan;19(1):13-26. PMID: 8989564

125) **Mun-Bryce** S, Rosenberg GA. Matrix metalloproteinases in cerebrovascular disease. J Cereb Blood Flow Metab. 1998 Nov;18(11):1163-72. Review. PMID: 9809504

126) **Rosenberg** GA, Estrada EY, Dencoff JE. Matrix metalloproteinases and TIMPs are associated with blood-brain barrier opening after reperfusion in rat brain. Stroke. 1998 Oct;29(10):2189-95. PMID: 9756602

127) **Venero** JL, Vizuete ML, Machado A, Cano J. Aquaporins in the central nervous system. Prog Neurobiol. 2001 Feb;63(3):321-36. Review. PMID: 11115728

128) **Price** DL, Ludwig JW, Mi H, Schwarz TL, Ellisman MH. Distribution of rSlo Ca2+-activated K+ channels in rat astrocyte perivascular endfeet. Brain Res. 2002 Nov 29;956(2):183-93. PMID: 12445685

129) **Yamamoto** N, Sobue K, Miyachi T, Inagaki M, Miura Y, Katsuya H, Asai K. Differential regulation of aquaporin expression in astrocytes by protein kinase C. Brain Res Mol Brain Res. 2001 Nov 1;95(1-2):110-6. PMID: 11687282

130) **Vajda** Z, Pedersen M, Fuchtbauer EM, Wertz K, Stodkilde-Jorgensen H, Sulyok E, Doczi T, Neely JD, Agre P, Frokiaer J, Nielsen S. Delayed onset of brain edema and mislocalization of aquaporin-4 in dystrophin-null transgenic mice. Proc Natl Acad Sci U S A. 2002 Oct 1;99(20):13131-6. Epub 2002 Sep 13. PMID: 12232046

131) **Papadopoulos** MC, Saadoun S, Binder DK, Manley GT, Krishna S, Verkman AS. Molecular mechanisms of brain tumor edema. Neuroscience. 2004;129(4):1011-20. Review. PMID: 15561416

132) **Han** Z, Wax MB, Patil RV. Regulation of aquaporin-4 water channels by phorbol ester-dependent protein phosphorylation. J Biol Chem. 1998 Mar 13;273(11):6001-4. PMID: 9497312

133) **Amiry-Moghaddam** M, Ottersen OP. The molecular basis of water transport in the brain. Nat Rev Neurosci. 2003 Dec;4(12):991-1001. Review. PMID: 14682361

134) **Papadopoulos** MC, Krishna S, Verkman AS. Aquaporin water channels and brain edema. Mt Sinai J Med. 2002 Sep;69(4):242-8. Review. PMID: 12357265

135) **Agre** P, Kozono D. Aquaporin water channels: molecular mechanisms for human diseases. FEBS Lett. 2003 Nov 27;555(1):72-8. Review. PMID: 14630322

136) **Badaut** J, Hirt L, Granziera C, Bogousslavsky J, Magistretti PJ, Regli L. Astrocyte-specific expression of aquaporin-9 in mouse brain is increased after

transient focal cerebral ischemia. J Cereb Blood Flow Metab. 2001 May;21(5):477-82. PMID: 11333357

137) **Goldin** AL. Maintenance of Xenopus laevis and oocyte injection.Methods Enzymol. 1992;207:266- 79. PMID: 1528120

138) **Clark** WM, Lessov NS, Dixon MP, Eckenstein F. Monofilament intraluminal middle cerebral artery occlusion in the mouse. Neurol Res. 1997 Dec;19(6):641-8. PMID: 9427967

139) **Hattori** K, Lee H, Hurn PD, Crain BJ, Traystman RJ, DeVries AC. Cognitive deficits after focal cerebral ischemia in mice. Stroke. 2000 Aug;31(8):1939-44. PMID: 10926961

140) **O'Donnell** ME, Tran L, Lam TI, Liu XB, Anderson SE. Bumetanide inhibition of the blood-brain barrier Na-K-Cl cotransporter reduces edema formation in the rat middle cerebral artery occlusion model of stroke. J Cereb Blood Flow Metab. 2004 Sep;24(9):1046-56. PMID: 15356425

141) **Haas** M and McManus TJ. Bumetanide inhibits (Na + K + 2Cl) co-transport at a chloride site. *Am J Physiol* 1983 **245**(3):C235-240.

142) Kusuhara et al.1999

143) **Yan** Y, Dempsey RJ and Sun D. Na+-K+-Cl- cotransporter in rat focal cerebral ischemia. *J Cereb Blood Flow Metab* 2001 **21**(6):711-721.

144) **de Groot** BL and Grubmuller H. The dynamics and energetics of water permeation and proton exclusion in aquaporins. *Curr Opin Struct Biol* 2005**15**(2):176-183.

145) **Hasegawa** H, Ma T, Skach W, Matthay MA, Verkman AS. Molecular cloning of a mercurial-insensitive water channel expressed in selected water-transporting tissues. J Biol Chem. 1994 Feb 25;269(8):5497-500. PMID: 7509789

146) **Nagelhus** EA, Veruki ML, Torp R, Haug FM, Laake JH, Nielsen S, Agre P, Ottersen OP. Aquaporin-4 water channel protein in the rat retina and optic nerve: polarized expression in Muller cells and fibrous astrocytes. J Neurosci. 1998 Apr 1;18(7):2506-19. PMID: 9502811

147) **Nagelhus** EA, Horio Y, Inanobe A, Fujita A, Haug FM, Nielsen S, Kurachi Y, Ottersen OP. Immunogold evidence suggests that coupling of K+ siphoning and water transport in rat retinal Muller cells is mediated by a coenrichment of Kir4.1 and AQP4 in specific membrane domains. Glia. 1999 Mar;26(1):47-54. PMID: 10088671

148) **Dalloz** C, Sarig R, Fort P, Yaffe D, Bordais A, Pannicke T, Grosche J, Mornet D, Reichenbach A, Sahel J, Nudel U, Rendon A. Targeted inactivation of dystrophin gene product Dp71: phenotypic impact in mouse retina. Hum Mol Genet. 2003 Jul 1;12(13):1543-54. PMID: 12812982

149) **Neely** JD, Amiry-Moghaddam M, Ottersen OP, Froehner SC, Agre P, Adams ME. Syntrophin-dependent expression and localization of Aquaporin-4 water channel protein. Proc Natl Acad Sci U S A. 2001 Nov 20;98(24):14108-13. PMID: 11717465

150) **Frigeri** A, Nicchia GP, Nico B, Quondamatteo F, Herken R, Roncali L, Svelto M. Aquaporin-4 deficiency in skeletal muscle and brain of dystrophic mdx mice. FASEB J. 2001 Jan;15(1):90-98. PMID: 11149896

151) **Manley** GT, Binder DK, Papadopoulos MC, Verkman AS. New insights into water transport and edema in the central nervous system from phenotype analysis of aquaporin-4 null mice. Neuroscience. 2004;129(4):983-91. Review. PMID: 15561413

152) **Yoshida** M, Yonetani A, Shirasaki T, Wada K. Dietary NaCl supplementation prevents muscle necrosis in a mouse model of Duchenne muscular dystrophy. Am J Physiol Regul Integr Comp Physiol. 2006 Feb;290(2):R449-55. Epub 2005 Sep 22. PMID: 16179484

153) **Naik** DV, Valtin H. Hereditary vasopressin-resistant urinary concentrating defects in mice. Am J Physiol. 1969 Oct;217(4):1183-90. PMID: 5824320

154) **Johnson** RF, Beltz TG, Thunhorst RL, Johnson AK. Investigations on the physiological controls of water and saline intake in C57BL/6 mice. Am J Physiol Regul Integr Comp Physiol. 2003 Aug;285(2):R394-403. Epub 2003 Apr 24. PMID: 12714354

155) **Van Loo** PL, Mol JA, Koolhaas JM, Van Zutphen BF, Baumans V. Modulation of aggression in male mice: influence of group size and cage size. Physiol Behav. 2001 Apr;72(5):675-83. PMID: 11336999

156) **Stewart** AD, Stewart J. Studies on syndrome of diabetes insipidus associated with oligosyndactyly in mice. Am J Physiol. 1969 Oct;217(4):1191-8. PMID: 4309975

157) **Rocha** MJ, Chen Y, Oliveira GR, Morris M. Physiological regulation of brain angiotensin receptor mRNA in AT1a deficient mice. Exp Neurol. 2005 Sep;195(1):229-35. PMID: 16023638

158) **Ma** T, Yang B, Gillespie A, Carlson EJ, Epstein CJ, Verkman AS. Generation and phenotype of a transgenic knockout mouse lacking the mercurial-insensitive water channel aquaporin-4. J Clin Invest. 1997 Sep 1;100(5):957-62. PMID: 9276712

159) **Chou** CL, Knepper MA, Hoek AN, Brown D, Yang B, Ma T, Verkman AS. Reduced water permeability and altered ultrastructure in thin descending limb of Henle in aquaporin-1 null mice. J Clin Invest. 1999 Feb;103(4):491-6. PMID: 10021457